UNIVERSIDAD DE LA RIOJA

TESIS DOCTORAL

Título
Impact of integrase inhibitors on gut and oral microbiome

Autor/es
Pablo Villoslada Blanco

Director/es
José Antonio Oteo Revuelta y Carmen Patricia Pérez Matute

Facultad
Facultad de Ciencia y Tecnología

Titulación

Departamento
Agricultura y Alimentación

Curso Académico

UNIVERSIDAD DE LA RIOJA

TESIS DOCTORAL

2022

Programa de Doctorado en Ciencias Biomédicas y Biotecnológicas

IMPACT OF INTEGRASE INHIBITORS ON GUT AND ORAL MICROBIOME

IMPACTO DE LOS INHIBIDORES DE LA INTEGRASA SOBRE EL MICROBIOMA INTESTINAL Y ORAL

Pablo Villoslada Blanco

Director/a: José Antonio Oteo Revuelta

Director/a: Patricia Pérez Matute

Don José Antonio Oteo Revuelta, Doctor en Medicina y Cirugía, Jefe del Departamento de Enfermedades Infecciosas del Hospital Universitario San Pedro – Centro de Investigación Biomédica de La Rioja (CIBIR),

Doña Patricia Pérez-Matute, Doctora en Bioquímica, Responsable del Laboratorio de Enfermedades Infecciosas, Microbiota y Metabolismo del Departamento de Enfermedades Infecciosas del Centro de Investigación Biomédica de La Rioja (CIBIR), por la presente

DECLARAN

QUE la memoria titulada **"Impacto de los inhibidores de la integrasa sobre el microbioma intestinal y oral"** (**"*Impact of integrase inhibitors on gut and oral microbiome*"**), que presenta Don Pablo Villoslada-Blanco, graduado en Bioquímica, ha sido realizada en el Centro de Investigación Biomédica de La Rioja (CIBIR) bajo su dirección y reúne las condiciones específicas para optar al grado de Doctor con la mención de "Doctor Internacional".

Y para que conste y surta los efectos oportunos, firman la presente en Logroño a 13 de octubre de 2022.

Fdo.: Dr. José A. Oteo Revuelta   Fdo.: Dra. Patricia Pérez-Matute

A toda mi familia

y a los que ya no están aquí

Por último, me gustaría dar las gracias a toda mi familia y amigos, los cuales me han apoyado durante estos cuatro años y, en especial, a mi madre y a mi padre, que han puesto todo lo que ha estado en su mano y más para que yo pueda alcanzar mis sueños.

'I do not fear computers. I fear the lack of them.'

- Isaac Asimov

TABLE OF CONTENTS

ABBREVIATIONS

#

3TC: lamivudine

A

ABC: abacavir

AIDS: acquired immunodeficiency syndrome

ART: antiretroviral treatment

ASV: amplicon sequence variant

AZT: atazanavir

B

BIC: bictegravir

bp: base pairs

BT: bacterial translocation

C

CA: capsid protein

CAB: cabotegravir

CCL20: C-C motif chemokine ligand 20

CCR5: chemokine receptor 5

CD: Crohn's disease

CD163: cluster of differentiation 163

CD4: cluster of differentiation 4

CD8: cluster of differentiation 8

CDCs: Centers for Disease Control and Prevention from USA

cDNA: complementary deoxyribonucleic acid

CEImLAR: Committee for Ethics in Drug Research in La Rioja

CIBIR: Center for Biomedical Research of La Rioja

CMV: cytomegalovirus

CNS: central nervous system

COBI: cobicistat

CORE: Core Oral Microbiome

CRC: colorectal cancer

CSC: cleaved synaptic complex

CVD: cardiovascular disease

CXCR4: chemokine receptor 4

D

DC: dendritic cells

DGGE: denaturing gradient gel electrophoresis

DKA-β: β-diketo acid

DNA: deoxyribonucleic acid

DOR: doravirine

DRV: darunavir

DRV/c: darunavir boosted with cobicistat

DRV/r: darunavir boosted with ritonavir

DTG: dolutegravir

E

EDTA: ethylenediamine tetraacetic acid

EFV: efavirenz

ELISA: enzyme-linked immunosorbent assay

EMA: European Medicines Agency

env: envelope

ESI: electrospray interface

ETR: etravirine

EVG: elvitegravir

F

FDA: Food and Drug Administration

FPV: fosamprenavir

FTC: emtricitabine

G

gag: group-specific antigen

GALT: gut-associated lymphoid tissue

GBV-C: GB virus C

GC-MS: gas chromatography coupled to mass spectrometry

GF: germ-free

GIT: gastrointestinal tract

GM: gut microbiota

GOT/AST: glutamic oxalacetic transaminase or aspartate aminotransferase

GPT/ALT: pyruvic glutamic transaminase or alanine aminotransferase

H

HBV: hepatitis B virus

HCV: hepatitis C virus

HDL: high density lipoprotein

HERV: human endogenous retrovirus

HIV: human immunodeficiency virus

HIV-1: human immunodeficiency virus type 1

HIV-2: human immunodeficiency virus type 2

HOMA-IR: homeostasis model assessment insulin resistance index

HOMD: Human Oral Microbiome database

HPV: human papillomavirus

HRP: horseradish peroxidase

HUSP: Hospital Universitario San Pedro

I

IBD: inflammatory bowel disease

IBS: irritable bowel syndrome

ICAM-1: intracellular adhesion molecule 1

ICVV: Institute of Grapevine and Wine Sciences

iFABP: intestinal fatty acid binding protein

IFN-α: interferon α

IL-1: interleukin 1

IL-10: interleukin 10

IL-17: interleukin 17

IL-18: interleukin 18

IL-1β: interleukin 1β

IL-22: interleukin 22

IL-6: interleukin 6

IL-8: interleukin 8

IN: integrase

INI: integrase inhibitor

IN_n: multimers of integrase

INSTI: integrase strand transfer inhibitor

K

KPa: kilopascal

L

LBP: lipopolysaccharide binding protein

LDL: low density lipoprotein

LPS: lipopolysaccharide

LTR: long terminal repeat

M

MA: outer capsid membrane

mCD14: membrane cluster of differentiation 14

mCD163: membrane cluster of differentiation 163

MCP-1: macrophage chemoattractant protein 1

MetaHIT: Metagenomics of the Human Intestinal Tract

MPS: multi-purpose sampler

mRNA: messenger ribonucleic acid

MS: mass spectrometry

MSM: men who have sex with men

N

NAFLD: non-alcoholic fatty liver disease

NC: nucleocapsid

NCBI: National Center for Biotechnology Information

NEC: necrotizing enterocolitis

Nef: negative regulating factor

NGS: next-generation sequencing

NK: natural killer

NMR: nuclear magnetic resonance

NNRTI: non-nucleoside reverse transcriptase inhibitor

NRTI: nucleoside and nucleotide reverse transcriptase inhibitor

NVP: nevirapine

P

PAI-1: plasminogen activator protein 1

PCoA: Principal Coordinate Analysis

PCR: polymerase chain reaction

PE: phycoerythrin

PES: polyethersulfone

PI: protease inhibitor

pol: polymerase

PR: protease

PTFE: polytetrafluoroethylene

PVDV: polyvinylidene fluoride

Q

QQQ: tiple quadrupole

R

RaFAH: Random Forest Assignments of Hosts

RAL: raltegravir

Rev: RNA splicing-regulator

RNA: ribonucleic acid

RPV: rilpivirine

rRNA: ribosomal ribonucleic acid

RT: reverse transcriptase

RTV: ritonavir

S

sCD14: soluble cluster of differentiation 14

sCD163: soluble cluster of differentiation 163

SCFA: short chain fatty acid

SEM: standard error of the mean

SIV: simian immunodeficiency virus

SIVcpz: simian immunodeficiency virus from Central African chimpanzees

SIVgor: simian immunodeficiency virus from gorillas

SIVsm: simian immunodeficiency virus from West African sooty mangabeys

SQV: saquinavir

SSC: stable synaptic complex

STC: strand transfer complex

SU: surface protein

T

T2D: type 2 diabetes

TAF: tenofovir alafenamide

Tat: transactivator protein

tBuEtO: *terc*-butylethylether

TCC: targe capture complex

TDF: tenofovir

tDNA: target deoxyribonucleic acid

TGGE: temperature gradient gel electrophoresis

Th17: T helper 17

TLR: toll-like receptor

TLR-4/MD-2: toll-like receptor 4/MD-2

TM: transmembrane protein

TMA: trimethylamine

TMAO: trimethylamine N-oxide

TNF-α: tumor necrosis factor α

TPV: tripranavir

Treg: regulatory T cell

T-RFLP: terminal-restriction fragment length polymorphism

TTMDV: Torque teno midi virus

TTV: Torque teno virus

U

UC: ulcerative colitis

UPLC: ultra performance liquid chromatography

V

VCAM-1: vascular cell adhesion molecule 1

vDNA: viral deoxyribonucleic acid

Vif: viral infectivity factor

VLP: viral like particle

Vpr: virus protein r

Vpu: virus protein unique

W

WGA: whole genome amplification

WHO: World Health Organization

GLOSSARY OF TERMS

Microbiota: the community of microorganisms inhabiting a specific environment.

Microbiome: the genomic content of the microbiota.

Bacteriome: the bacteria inhabiting a specific environment and their genomic content.

Virome: the viruses inhabiting a specific environment and their genomic content.

Omics: the set of technologies aim to collectively characterize and quantify pools of biological molecules.

Metagenomic: the study of the genetic material of the microbes inhabiting a specific environment.

Metatranscriptomic: the study of the gene expression of the microbes inhabiting a specific environment.

Metabolomic: the study of the metabolites.

LIST OF TABLES

LIST OF FIGURES

Figure 32. PCoAs from phages in faecal samples of the studied population.

Figure 33. Relative abundance of the lysogenic phages comparing control group *vs.* HIV-infected patients and control group *vs.* naive patients *vs.* INSTIs-treated patients taking into account all viral classes (**A** and **B**) and only *Caudoviricetes* class (**C** and **D**).

Figure 34. Host prediction of the different phages. **A)** Prediction of which bacteria is infected by phage grouped based on class-level taxonomy. **B)** Differences between control and HIV in the relative abundance of the phages infecting bacterial phyla. **C)** Differences between control, naive, and INSTIs in the relative abundance of the phages infecting bacterial phyla.

Figure 35. Correlation plot between α-diversity indexes from bacteria and phages.

Figure 36. Different indexes of α-diversity from bacteria in salivary samples of the studied population.

Figure 37. PCoAs from bacteria in salivary samples from the studied population.

ABSTRACT

Human immunodeficiency virus (HIV) infection is now considered a chronic disease thanks to the extended use of antiretroviral treatment (ART). However, chronic immune activation, inflammation, and increased bacterial translocation (BT) could persist in these patients despite ART. These facts have been described as predictors for clinical events and mortality in these patients. Gut microbiota (GM) changes induced by HIV infection and ART seem to be related to such inflammatory state. The role of integrase strand transfer inhibitors (INSTIs), the preferred choice for the treatment of naive patients, on GM (bacteriome) has not been deeply investigated. There are also no studies focused on the effects of HIV infection and/or ART on gut virome, despite the fact that viruses are the most abundant components of human GM. The main objective of this Doctoral Thesis was to deeply characterize GM composition (both bacteriome and virome) and oral bacteriome of HIV-infected patients in comparison with non-HIV-infected subjects, and to analyse the impact of INSTIs-based treatments. To accomplish this objective, 26 non-HIV-infected volunteers and 30 HIV-infected patients (15 naive and 15 under INSTI-regimen) were recruited. Blood samples were extracted to analyse biochemical parameters and markers of BT, inflammation, cardiovascular risk, gut permeability, and bacterial metabolism. Gut bacteriome composition and oral bacteriome composition was analysed using 16S rRNA gene sequencing and gut virome composition was studied using shotgun sequencing.

Our results showed that HIV-infection increased BT, inflammation, cardiovascular risk, and gut permeability, whereas INSTIs counteracted these effects. Regarding gut bacteriome, the reduction in bacterial richness induced by HIV infection was restored by INSTIs ($p < 0.05$ naive *vs.* control *Observed features* and *Chao1 estimator* indexes). β-diversity revealed that HIV-infected people were separated from the control group independently of treatment ($p < 0.05$ naive *vs.* control and $p < 0,05$ INSTIs *vs.* control). Considering gut virome, the results showed that bacteriophages are the most abundant and diverse viruses in the

gut independent from the HIV status and the use of treatment. Neither HIV infection nor INSTIs-based treatment had an effect on eukaryotic viruses composition. On the other hand, HIV infection was accompanied by a decrease in phage richness which was reverted after INSTIs-based treatment ($p<0.01$ naive *vs.* control *Observed features* index and $p<0.05$ naive *vs.* control *Fisher's alpha* index). β-diversity of phages revealed that samples from HIV-infected patients clustered separately from those belonging to the control group (padj<0.01 naive *vs.* control and padj<0.05 INSTIs *vs.* control). However, it is worth mentioning that samples coming from INSTIs-treated patients grouped more closely together compared to naive patients. Differential abundant analysis showed an increase in phages belonging to the *Caudoviricetes* class in the naive group compared to the control group (padj<0.05) and a decrease of *Malgrandaviricetes* class phages in the INSTIs-treated group compared to the control group (padj<0.001). Besides, it was observed that INSTIs-based treatment was not able to reverse the increase of lysogenic phages associated with HIV infection ($p<0.05$ *vs.* control) or to modify the decrease observed on the relative abundance of Proteobacteria-infecting phages ($p<0.05$ *vs.* control). Finally, with respect to oral bacteriome, our study was unable to detect differences neither in α-diversity nor in β-diversity between the three groups analysed, although some taxa were revealed to be increased in the naive group and in the INSTIs-treated group compared to controls.

In conclusion, this Doctoral Thesis shows that current antiretroviral regimens based on INSTIs are able to reverse the impact of HIV infection on BT, systemic inflammation, gut permeability, and gut bacterial diversity/richness reaching similar levels than those observed in an uninfected/control population. Besides, our study describes for the first time the impact of HIV and INSTIs on the gut virome and demonstrates that INSTIs-based treatments are able to partially restore gut dysbiosis, not only at the bacterial, but also at the viral level. These results suggest a protective role of INSTIs in disease progression, in subsequent immune activation, and in the development of future age-related complications such as cardiovascular events and opens several opportunities for new studies focused on microbiota-based therapies.

RESUMEN

La infección por el virus de la inmunodeficiencia humana (VIH) es considerada actualmente como una enfermedad crónica gracias al uso del tratamiento antirretroviral (TAR). Sin embargo, a pesar del TAR, estos pacientes pueden presentar un estado de inmunoactivación e inflamación crónica, así como un incremento de la translocación bacteriana (TB). La presencia de estos hechos es considerada un predictor de futuros eventos clínicos y de mortalidad en estos pacientes. Además, los cambios en la microbiota intestinal (MI) inducidos por la infección por el VIH y por el ART podrían estar relacionados con este estado inflamatorio crónico. En este sentido, el papel de los inhibidores de la integrasa (IINs), terapia preferente en los pacientes naïve, sobre la MI (bacterioma) no ha sido analizado en profundidad. Tampoco se han desarrollado estudios concluyentes sobre el impacto de la infección por VIH y/o el TAR en el viroma, a pesar de que los virus son el componente más abundante de la MI en los seres humanos. El objetivo de esta tesis fue caracterizar en profundidad la composición de la MI (incluyendo bacterioma y viroma) y el bacterioma oral en pacientes infectados por el VIH en comparación con una población no infectada y analizar el impacto de los IINs. Para lograr este objetivo se reclutaron 26 voluntarios no infectados por el VIH y 30 pacientes infectados por el VIH (15 naïve y 15 bajo tratamiento con IINs). Se extrajeron muestras de sangre para analizar parámetros bioquímicos y marcadores de TB, inflamación, riesgo cardiovascular, permeabilidad intestinal y metabolismo bacteriano. La composición del bacterioma intestinal y oral fue analizado mediante secuenciación del gen del ARNr 16S y la composición del viroma intestinal se estudió mediante secuenciación "shotgun".

Nuestros resultados mostraron que la infección por el VIH incrementó la TB, la inflamación, el riesgo cardiovascular y la permeabilidad intestinal, mientras que los IINs contrarrestaron estos efectos. En cuanto al bacterioma intestinal, la reducción en la riqueza bacteriana inducida por la infección por el VIH fue restaurada por los IINs (p<0,05 naïve *vs.* control en los índices *Observed features* y *Chao1 index*). La β-diversidad reveló que los pacientes infectados por

el VIH estaban separados del grupo control independientemente del tratamiento (p<0,05 naïve *vs.* control and p<0,05 IINs *vs.* control). Considerando el viroma intestinal, los resultados mostraron que los bacteriófagos son los virus más abundantes y diversos en el intestino independientemente de la infección por VIH y del tratamiento. Ni la infección por el VIH ni el tratamiento con IINs tuvo un efecto sobre la composición de los virus eucariotas. Por otro lado, la infección por VIH se vio acompañada de una disminución en la riqueza de fagos que fue revertida tras el tratamiento (p<0,01 naïve *vs.* control en el índice de *Observed features* y p<0,05 naïve *vs.* control en el índice *Fisher's alpha*). La β-diversidad de los fagos reveló que las muestras de pacientes infectados por el VIH agrupaban de manera separada con respecto a las pertenecientes al grupo control (padj<0,01 naïve *vs.* control y padj<0,05 IINs *vs.* control). Sin embargo, cabe mencionar que las muestras procedentes de pacientes tratados se encontraban más agrupadas entre sí que aquellas procedentes de pacientes naïve. El análisis de la abundancia diferencial de los fagos mostró un incremento de la clase *Caudoviricetes* en el grupo naïve con respecto al grupo control (padj<0,05) y una disminución de la clase *Malgrandaviricetes* en el grupo tratado con respecto al grupo control (padj<0,001). Además, se observó que el tratamiento con IINs no fue capaz de revertir el incremento en los fagos lisogénicos asociados a la infección por VIH (p<0,05 *vs.* control) ni modificar la disminución observada en la abundancia relativa de los fagos que infectan al filo Proteobacteria (p<0,05 *vs.* control). Finalmente, con respecto al bacterioma oral, nuestro estudio fue incapaz de detectar diferencias en la α-diversidad y en la β-diversidad, aunque sí que se observaron algunos taxones bacterianos incrementados en el grupo naïve y en el grupo tratado en comparación al grupo control.

En conclusión, esta Tesis Doctoral muestra que los TARs actuales basados en IINs son capaces de revertir el impacto de la infección por el VIH en la TB, la inflamación sistémica, la permeabilidad intestinal y la riqueza bacteriana, alcanzando niveles similares a los observados en una población control no infectada. Además, nuestro estudio describe por primera vez el impacto del VIH y los IINs en el viroma intestinal y demuestra que los tratamientos basados en

IINs son capaces de restaurar la disbiosis intestinal tanto a nivel bacteriano como vírico. Estos resultados sugieren un efecto protector de los IINs en la progresión de la enfermedad, en la subsecuente activación inmune y en el desarrollo de futuras complicaciones relacionadas con la edad como los eventos cardiovasculares y, por tanto, abre numerosas oportunidades para desarrollar nuevos estudios focalizados en terapias coadyuvantes basadas en la microbiota.

1. INTRODUCTION

1.1. Human immunodeficiency virus

1.1.1. Origin and epidemiology

One of the major public health problems reported in our history (despite the actual COVID-19 pandemic) occurred in 1981, when a large number of homosexual men suffered from unusual opportunistic infections and rare malignancies. This "new disease" was recognized in 1982 by the Centers for Disease Control and Prevention (CDCs) from USA as "acquired immunodeficiency syndrome" (AIDS), because the immune system of these patients were weakened (1–3). In one year, the team of Luc Montagnier at the Pasteur Institute in Paris and the American team of Roberto Gallo identified the causal agent of such disease (4,5), which was later named as "human immunodeficiency virus" (HIV) (6). There was a great controversy about who were the first to isolate the virus, but in 1994 the French team was recognised as the first team able to identify and characterize the virus and, because of that, Montagnier and his colleague Françoise Barré-Sinoussi were awarded with the Nobel Prize in Medicine in 2008 (7). Nevertheless, in 1986, a second type of the virus was discovered in AIDS patients in West Africa: HIV-2 (8). In fact, AIDS syndrome can be caused by both HIV types 1 (HIV-1) and 2 (HIV-2). HIV-1 evolved from simian immunodeficiency viruses (SIVs) from Central African chimpanzees (SIVcpz) and gorillas (SIVgor) and HIV-2 from SIV from West African sooty mangabeys (SIVsm), and through cross-species infection they were transferred to humans (9–11). Thus, HIV infection can be considered a remote zoonotic disease. Both HIV-1 and HIV-2 are grouped to the genus *Lentivirus* within the family of Retroviridae, subfamily Orthoretrovirinae (12), and are very similar in modes of transmission and in intracellular replication pathways (13). However, HIV-2 is far less frequent and patients with HIV-2 have lower plasma viral load than patients infected by HIV-1 and, consequently, HIV-2 has a lower transmissibility and a reduced probability of progression to AIDS, being less pathogenic (14,15). Thus, taking into account the higher pathogenicity, the global

distribution and the type of patients of our environment, this Doctoral Thesis is focused on HIV-1-infected patients.

HIV-1 is subdivided into four phylogenetical groups (M, N, O and P) (16–18). Groups M, N, and O are related to SIVcpz while group P is closed to SIVgor from Cameroon (9,10,18,19). HIV-1 group M is the cause of the global pandemic (20) and a study placed its origin around the early 1920s in Kinshasa (Democratic Republic of the Congo) as zoonotic events. Considering that hunting apes is usual in Africa, it is possible that virus jumped from ape to human through a bit, a scratch, or a contact between the blood of a dead ape and an open wound. Then, the virus was spread mainly by sex practice and trade (11).

Since the beginning of the AIDS epidemic (in the early 80's), more than 80 million people have been infected by HIV and approximately 40 million people have died because of this infection. The most recent data published by the World Health Organization (WHO) estimate that a mean of 38.4 million people (33.9-43.8) were living with HIV at the end of 2021, of whom, 1.5 million (1.1-2.0) were diagnosed in that year (21). In 2000, AIDS was the eight cause of death in the world and, although deaths from AIDS have decreased by 51%, it stands in the nineteenth place (22) (last search in August 2022). Concerning Spain, 150000 people were living with HIV in 2019 (21).

1.1.2. Genome structure

The genome structure of HIV was perfectly reviewed by The German Advisory Committee Blood in 2016 (13). The HIV genome consists of two identical single-stranded ribonucleotide acid (RNA) molecules that are enclosed within the core of the virus particle. The proviral deoxyribonucleotide acid (DNA) is generated by the reverse transcription of the viral RNA genome into DNA, degradation of the RNA and integration of the double-stranded DNA (dsDNA) into the human genome. This proviral DNA is flanked at both ends by LTR (long terminal repeat) sequences. The 5'LTR region codes for the promotor followed by the open reading frames of the genes *gag* (group-specific antigen), *pol*

(polymerase), and *env* (envelope). The *gag* gene encodes the protein of the outer capsid membrane (MA, p17), the capsid protein (CA, p24), the nucleocapsid (NC, p7), and a smaller, nucleic acid-stabilising protein. The *pol* gene codes the enzymes protease (PR, p12), reverse transcriptase (RT, p51), RNase H (p15), and integrase (IN, p32). The *env* gene encodes the two envelope glycoproteins gp120 (surface protein, SU) and gp41 (transmembrane protein, TM). In addition to the structural proteins, the HIV genome codes for several regulatory proteins such as Tat (transactivator protein, p14) and Rev (RNA splicing-regulator, p19), necessary for the initiation of HIV replication, and Nef (negative regulating factor, p27), Vif (viral infectivity factor, p23), Vpr (virus protein r, p15), and Vpu (virus protein unique, p16), having an impact on viral replication, virus budding, and pathogenesis.

1.1.3. Virion structure

The virion is round, measures approximately 100 nm of diameter and have a lipid bilayer as its envelope. This lipid bilayer contains 72 knobs composed of trimers of the Env proteins. Specifically, the transmembrane glycoprotein gp41 forms trimmers embedded to the membrane which allows the anchoring of trimmers of the glycoprotein gp120 (23). Below the envelope is the outer capsid membrane formed by the MA, which is assembled to the capsid formed by the CA (24). Inside the capsid, two identical molecules of viral genomic RNA are located alongside several molecules of RT, RNase H, and IN composing the nucleocapsid (12). Besides, inside the capsid there are some copies of the proteins PR, Nef, Vif, Vpr, and NC (**Figure 1**).
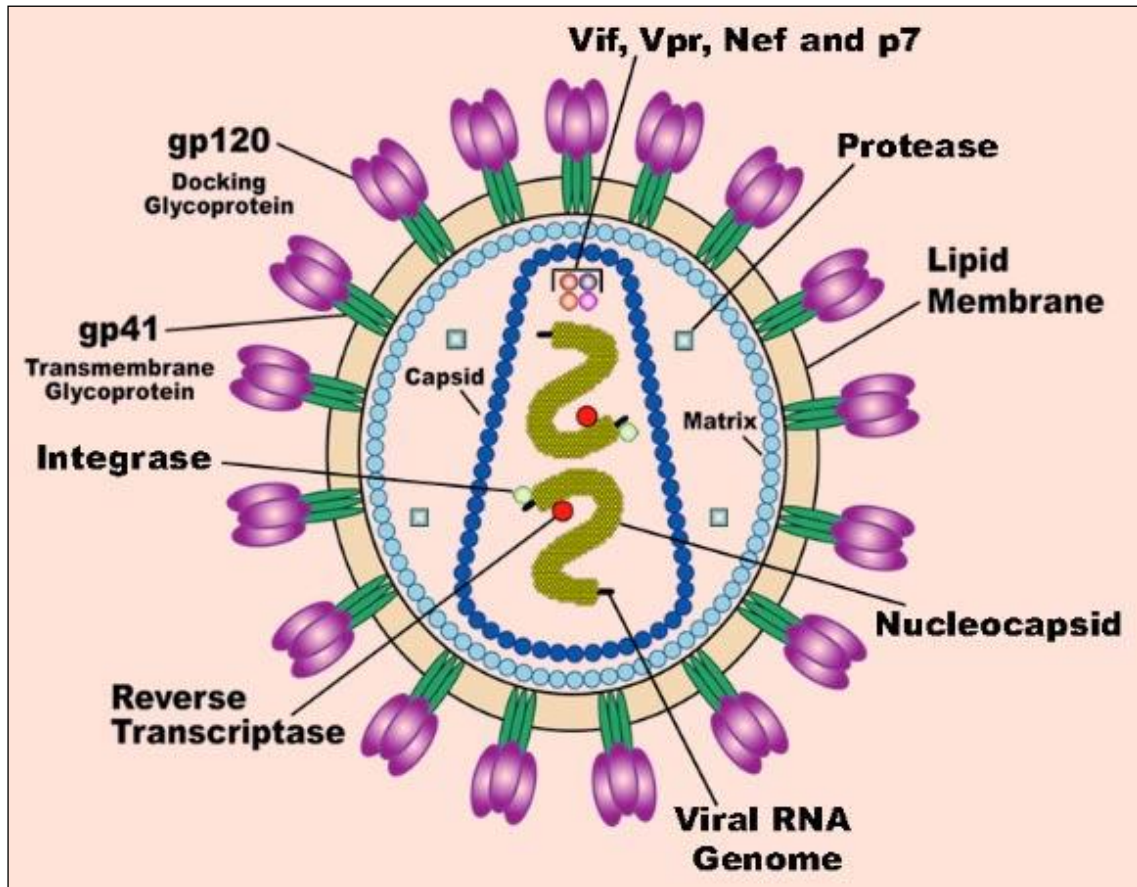
Figure 1. Structure of the HIV-1 virion. From US National Institute of Health (25). HIV-1 (human immunodeficiency virus type 1), Nef (negative regulating factor), p7 (nucleocapsid protein), Vif (viral infectivity factor), Vpr (virus protein).

1.1.4. Infection of human cells

The surface glycoprotein gp120 of the mature HIV has tropism for the cluster of differentiation 4 (CD4) receptor present in the host cell, therefore, all CD4-positive cells such as lymphocytes T helper, macrophages, dendritic cells (DCs), and astrocytes are susceptible to be infected by HIV. Once this initial contact occurred, gp120 shows a conformational change which allows the interaction with the coreceptor chemokine receptor 5 (CCR5) or chemokine receptor 4 (CXCR4 or fusin) (26,27). This second contact triggers an additional conformational change in gp120 and, subsequently, in gp41, which presents its N-terminus to the viral membrane and due to the high hydrophobicity inserts into the membrane of the target cell completing the fusion between the cell membrane and the viral envelope (12,28). After the fusion, the viral capsid is translocated to

the cytoplasm where is taken up by an endosome which allows the release of the capsid contents into the cytoplasm by a change in the pH value (29). Inside the infected cell, the reverse transcriptase transcribes the single-stranded RNA into complementary deoxyribonucleic acid (cDNA), at the same time that the RNase H degrades the RNA and, following, the single-stranded cDNA is converted into dsDNA, known as proviral DNA. by the polymerase activity of the reverse transcriptase (30). The next step is the transport of a complex consisting of the proviral DNA and the IN into the nucleus where the integration into the human host cell genome takes place finalising the HIV infection of the cell and the establishment of a persistent infection (13). In this point, the proviral genome can be replicated as part of the host cell genome during cell division. However, latent infection is rare, and it is more frequent that after the activation of infected cells the synthesis of viral messenger ribonucleic acid (mRNA) starts (31). The attachment of HIV to a host cell requires between 20 min to 2 h, the transcription of the viral RNA genome into the proviral DNA last around 6 h, the integration into the host takes an additional 6 h and, after the integration, the first virus particles are detectable after approximately 12 h. In summary, 24 h after infection the first progeny viruses are released (32–34) (**Figure 2**).
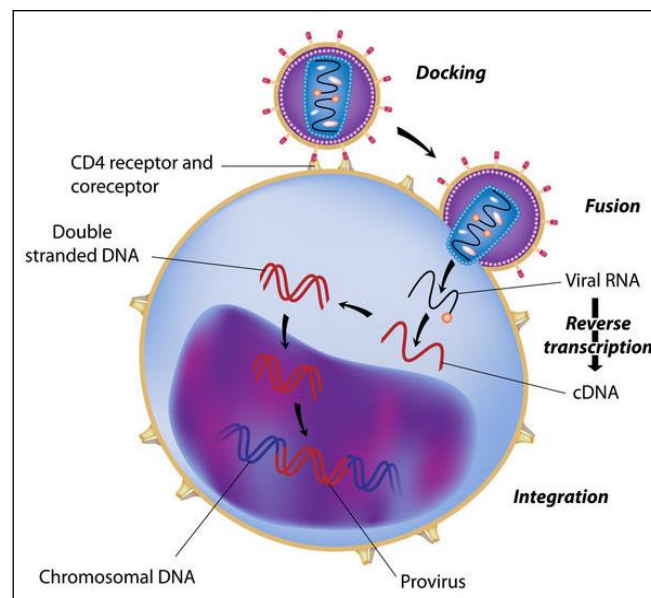
Figure 2. HIV infection of human cells. From HIV.gov (35). CD4 (cluster of differentiation 4), cDNA (complementary deoxyribonucleic acid), DNA (deoxyribonucleic acid), HIV (human immunodeficiency virus), RNA (ribonucleic acid).

1.1.5. Natural history of HIV infection

The first period after HIV infection, which starts 3-4 weeks after exposition, is defined as acute HIV infection (**acute phase**) and, generally, lasts 6-12 weeks. It is characterized by the first detection of HIV RNA in plasma and the formation of HIV-specific antibodies. Depending on the mode of transmission, the virus gets into the bloodstream directly (parenterally transmission) or must break through mucous membranes (sexual transmission). In the second case, the virus traffics between the DCs and macrophages presented in the mucous membranes after being transferred to lymphocytes T CD4+ (36–38). Then, the virus or infected cells reaches the lymph nodes where activated lymphocytes T CD4+ CCR5+ are found and this facilitates the replication and the dissemination to secondary lymphoid tissues, mainly the gut-associated lymphoid tissue (GALT). GALT is the largest immune organ in the body and it stores a large amount of effector memory T cells (36), which are cells in a continuous state of activation, making them very susceptible to HIV infection (39). Besides, during the earliest stage of HIV infection, some HIV-infected cells located in the GALT go into a latent state remaining without producing new HIV particles for years. However, suddenly, they can be activated and start producing more HIV virions (40,41). HIV infection also depletes T helper 17 (Th17) cells, which play a key role in antimicrobial defence (42,43). On the other hand, the infection of macrophages involves the secretion of cytokines that induce a significant increase in the recruitment of more activated lymphocytes T CD4+ triggering the transmission of the virus "cell by cell" and enhancing the intestinal infection (37). At this time, 10-14 days post infection, HIV can be detected reaching a peak of plasma viremia and a decline in peripheral lymphocytes T CD4+ after 3-4 weeks of infection (13,36,44). This situation can be accompanied by symptoms such as fever, fatigue, lymphadenopathy, sore throat, and exanthema (45). After that, viral replication is reduced, probably due to virus-specific immune responses getting at a steady state that defines the initiation of the **chronic phase**, characterised by a low but constant replication and which could generally last up to 7-10 years. In this phase, the immune response increases the circulating lymphocytes T CD4+ reaching

"normal" levels (over 500 cells/mm³) and the previous symptoms disappeared. Nevertheless, the depleted lymphocytes T CD4+ in GALT are not completely restored (13,36,46). Subsequently, the number of lymphocytes T CD4+ continues falling at a very low levels (below 200 cells/mm³) and this marks the beginning of **AIDS** (36,44,47)**.** The time to develop AIDS without therapy can vary between 2 and 25 years or even more since the infection (13,36). However, patients under antiretroviral treatment (ART) show a reduction in viral load to undetectable levels and a recovery of lymphocytes T CD4+ (48) (**Figure 3**). In fact, thanks to ART, HIV infection is now considered as a chronic disease with no fatal outcome (49).
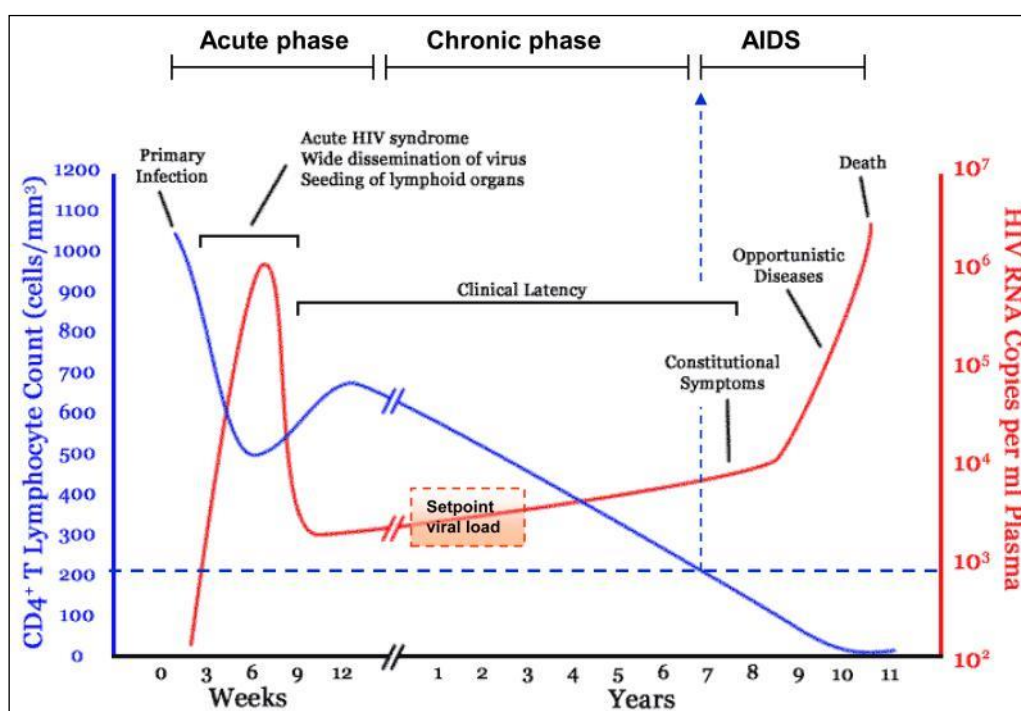
Figure 3. Typical natural course of HIV infection. From An and Winkler, 2010 (44). AIDS (acquired immunodeficiency syndrome), CD4 (cluster of differentiation 4), HIV (human immunodeficiency virus), RNA (ribonucleic acid).

1.1.6. Antiretroviral treatment

The highly effective antiretroviral therapy in the mid-1990s transformed the HIV infection into a chronic disease (49). HIV-infected people under ART significantly reduce their mortality and the associated morbidity (50–52) in addition to a lower risk of transmitting the virus to others (53–55). Throughout the years of fighting against HIV pandemic, different treatments have been

dynamically developed. There are different families of drugs that interfere with the replication cycle of the virus at different stages/points: i) binding with the host cell (co-receptor antagonists); ii) fusion with the host cell (fusion inhibitors); iii) reverse transcription of the RNA (nucleoside and nucleotide reverse transcriptase inhibitors (NRTIs) and non-nucleoside reverse transcriptase inhibitors (NNRTIs)); iv) integration with the host genome (integrase inhibitors (INIs)); and v) proteolytic cleavage and virion release (protease inhibitors (PIs)) (56–58) (**Figure 4**).
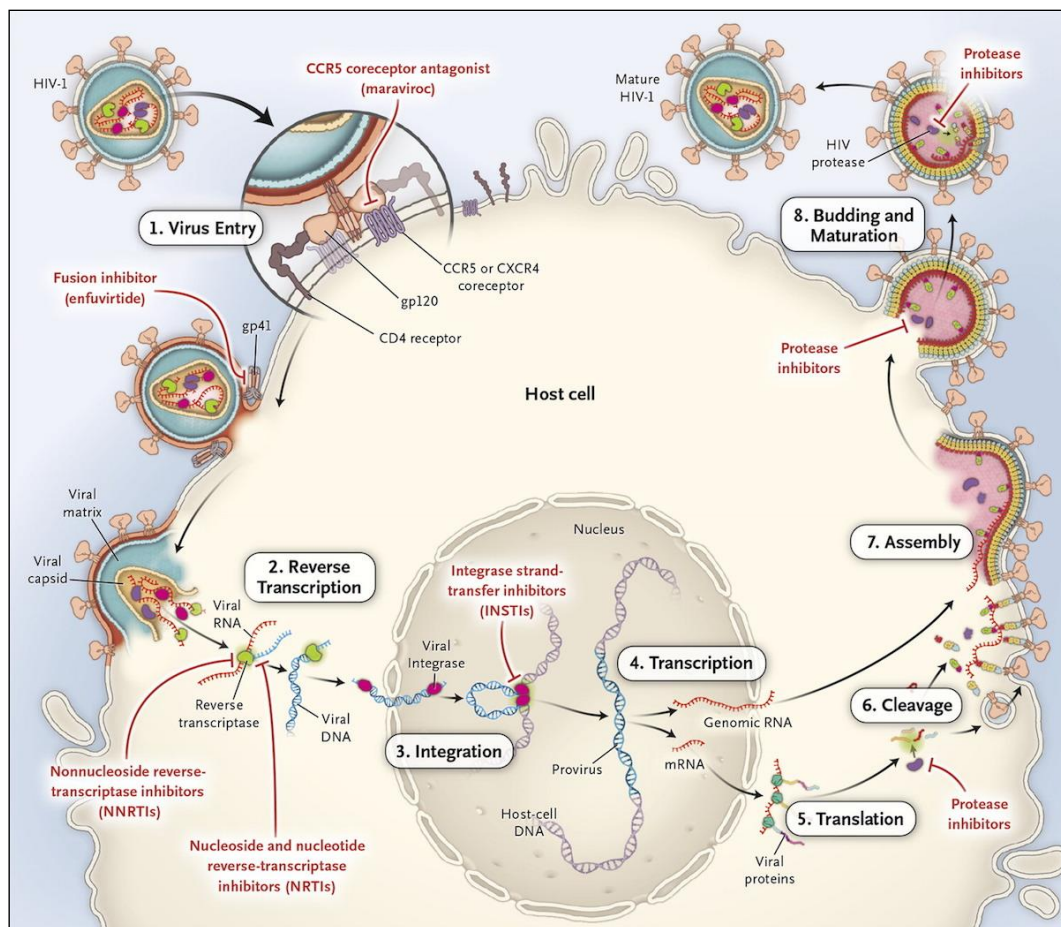
Figure 4. Reproductive cycle of HIV-1 and sites of action of ARTs. From Gandhi and Gandhi, 2014 (59). ARTs (antiretroviral treatments), CCR5 (chemokine receptor 5), CD4 (cluster of differentiation 4), CXCR4 (chemokine receptor 4), DNA (deoxyribonucleic acid), HIV-1 (human immunodeficiency virus type 1), mRNA (messenger ribonucleic acid), RNA (ribonucleic acid).

Nowadays, the recommended guidelines for the initial treatment of HIV-infected people in Spain consist of the combination of two or three drugs. Guidelines consisted in three drugs include two NRTIs alongside with an INI, an NNRTIs or a boosted PI. The NRTIs used as backbone are emtricitabine (FTC), tenofovir alafenamide (TAF), abacavir (ABC), and lamivudine (3TC), whereas the NNRTIs are doravirine (DOR) and rilpivirine (RPV). Finally, the unique boosted PI recommended is dorunavir (DRV) either with cobicistat (COBI) (DRV/c) or ritonavir (RTV) (DRV/r). It is important to highlight that **all the preferred regimens include an INI** in the Spanish guidelines (GESIDA) as follows: a) bictegravir (BIC)/FTC/TAF (a.k.a. Biktarvy®), b) dolutegravir (DTG)/ABC/3TC (a.k.a. Triumeq®) and c) DGT+FTC/TAF (a.k.a. Trivicay®+Descovy®). On the other hand, the alternative guidelines are as follows: a) raltegravir (RAL)+FTC/TAF (a.k.a. Isentress®+Descovy®), b) DRV/c/FTC/TAF (a.k.a. Symtuza®) or DRV/r+FTC/TAF (a.k.a. Prezista®+Norvir®+Descovy® and c) DOR+FTC/TAF (a.k.a. Pifeltro®+Descovy®) and d) RPV/FTC/TAF (Odefsey®). Finally, the only two-drug combination which is approved by GESIDA include one NRTI (3TC) and one INI (DTG) (DTG/3TC, a.k.a. Dovato®) (**Table 1**). With these combinations, it is possible to achieve a viral load below 50 copies/ml after 48 weeks of treatment in 85% of cases. However, these recommendations are not valid in pregnant women and people with tuberculosis (60).

Table 1. Recommended Spanish guidelines for the initial treatment of HIV-infected people. Adapted from *Documento de consenso de GeSIDA*, 2022 (60).

3rd drug	Combination
Preferred ones	
INI	BIC/FTC/TAF (Biktarvy®)
	DTG/ABC/3TC (Triumeq®)
	DTG+FTC/TAF (Trivicay®+Descovy®)
	DTG/3TC (Dovato®)
Alternative ones	
INI	RAL+FTC/TAF (Isentress®+Descovy®)
Boosted PI	DRV/c/FTC/TAF (Symtuza®)
	DRV/r+FTC/TAF (Prezista®+Norvir®+Descovy®)
NNRTI	DOR+FTC/TAF (Pifeltro®+Descovy®)
	RPV/FTC/TAF (Odefsey®)

3TC (lamivudine), ABC (abacavir), BIC (bictegravir), DRV/c (darunavir boosted with cobicistat), DRV/r (darunavir boosted with ritonavir), DOR (doravirine), DTG (dolutegravir), FTC (emtricitabine), INI (integrase inhibitor), NNRTI (non-nucleoside reverse transcriptase inhibitor), PI (protease inhibitor), RAL (raltegravir), RPV (rilpivirine), TAF (tenofovir alafenamide).

Next, the characteristics of each of the families of anti-HIV drugs are briefly detailed, going into depth in the INIs, as they are the focus of this Doctoral Thesis.

A. Co-receptor antagonists or CCR5 antagonists

The appropriate use of CCR5 receptor antagonists depends on the knowledge of the existence of three strains of HIV-1: R5 HIV-1 (which binds to the CCR5 co-receptor), X4 HIV-1 (which binds to the CXCR4 co-receptor), and dual-tropic HIV (which binds either CCR5 or CXCR4 co-receptor) (61,62). Thus, this therapy is only effective in people infected by the R5 strain. CCR5 receptor antagonists bind to the CCR5 co-receptor inducing a conformational change that prevents the binding of gp120 (61,63). Maraviroc is the only CCR5 antagonist approved by the Food and Drug Administration (FDA) (64), but in Spain, the GESIDA guidelines do not recommend its use as initial therapy in naive patients (60).

B. Fusion inhibitors

Enfuvirtide is the only fusion inhibitor approved by the FDA (64) and the European Medicines Agency (EMA) (65), but it is not recommended in the GESIDA guidelines nowadays (60). This drug is a 36-amino-acid synthetic peptide that correspond to a 36-amino-acid segment in the gp41 heptad repeat region 2, so it binds to the heptad repeat region 1 preventing the folding of the gp41 and, consequently, blocking the fusion (62,66,67).

C. Nucleoside and nucleotide reverse transcriptase inhibitors

NRTIs act as host nucleotide decoys and cause termination of elongating of the HIV DNA chain since unlike human nucleotides they lack the 3'-hydroxyl group and additional nucleotides cannot be added. They also require intracellular phosphorylation to obtain an active state (56,58). Nowadays, in Spain, three nucleoside reverse transcriptase inhibitors (3TC, FTC, and ABC) and one nucleotide reverse transcriptase inhibitor (TAF) are used (60).

D. Non-nucleoside reverse transcriptase inhibitors

NNRTIs bind directly to the RT and inhibit its function. Specifically, they bind to a hydrophobic pocket in the p66 subunit, which is close to the active site (68,69). This cause a conformational change in the polymerase domain blocking the DNA polymerization (68,70). In Spain, there are five NNRTIs used nowadays (nevirapine (NVP), efavirenz (EFV), etravirine (ETR), RPV, and DOR) (60).

E. Integrase inhibitors

The currently available INI drugs specifically block the integrase strand transfer step and because of that they are known as integrase strand transfer inhibitors (INSTIs) (71,72). INSTIs bind to the IN when this is attached to the viral deoxyribonucleic acid (vDNA) (41) inhibiting the active site through the union of the diketo acid group of the INSTIs to the magnesium ions in the active site of the IN (73). Besides, INSTIs displace the HIV DNA 3'-hydroxil ends interrupting the integration process (74). Finally, when the integration is blocked, the HIV DNA

becomes a substrate for host repair enzymes that convert this complex into a by-product (75). The first INI that was approved by the FDA in 2007 was RAL (76). Since then, other three INIs have been also approved: elvitegravir (EVG) in 2012, DGT in 2013, and BIC in 2018 (10-12) (**Figure 5**). Besides, another INI was approved in Canada in March 2020 called cabotegravir (CAB) (77) (**Figure 6**) but it does not appear in GESIDA (78) or EMA (65) guidelines up to now.
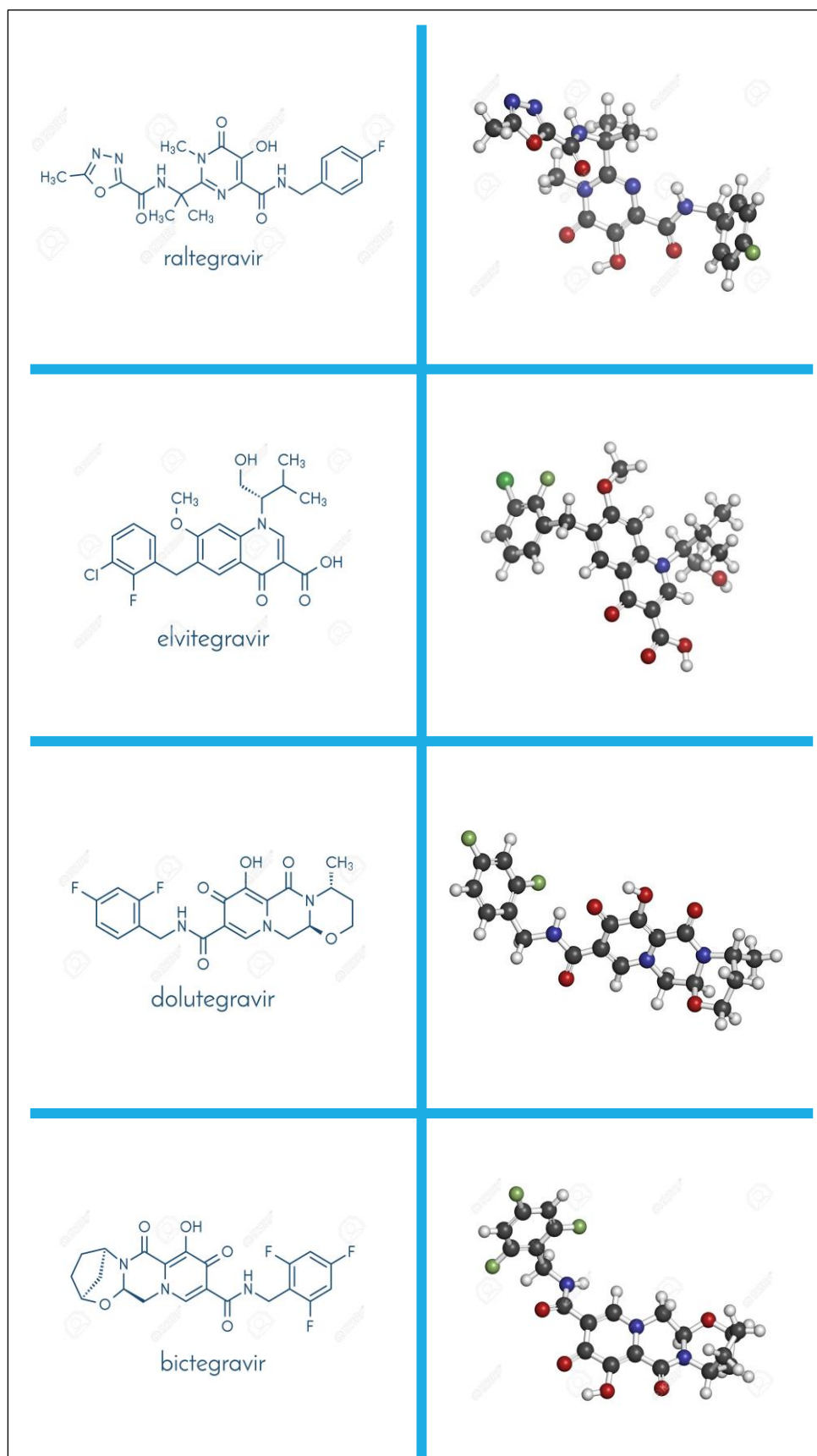
Figure 5. Structure of the integrase inhibitors approved in Spain. From 123rf.com (79).
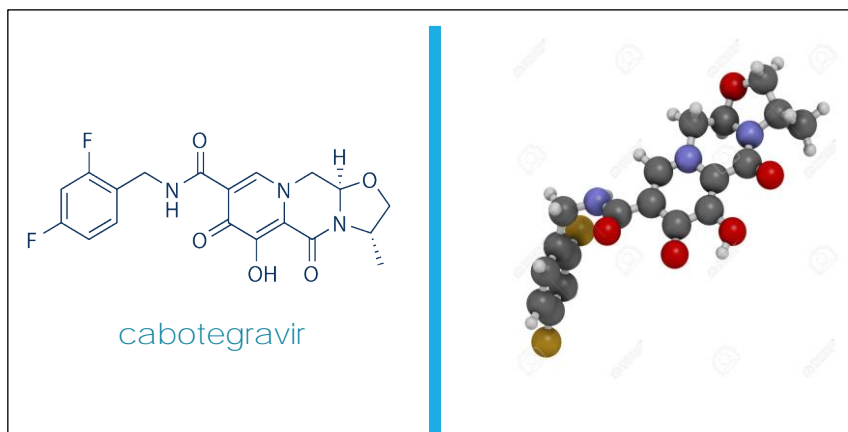
Figure 6. Structure of cabotegravir. From Selleckchem.com (80) and 123rf.com (79).

The discovery and development of these inhibitors were possible thanks to the demonstration of the existence of a nucleoprotein complex named intasome required for catalysis (81–83) and two independent IN enzymatic activities: 3-processing and strand transfer (84,85). This intasome consists of multimers of IN (IN_n) bound to the vDNA forming the stable synaptic complex (SSC). Within this complex two or three nucleotides are removed from the 3' ends of the vDNA exposing the reactive 3'-hydroxyl groups and forming the cleaved synaptic complex (CSC). Then, intasome captures target deoxyribonucleic acid (tDNA) forming the target capture complex (TCC) and IN joins these processed groups with the phosphates on the opposing tDNA strands forming the strand transfer complex (STC) (86) Finally, the host cell DNA repair enzymes complete the process (87) (**Figure 7**). The INI developed up to now inhibit this second process through a β-diketo acid (DKA-β) in their pharmacophore which ligate the two catalytic Mg^{2+} ions in the enzyme (88).
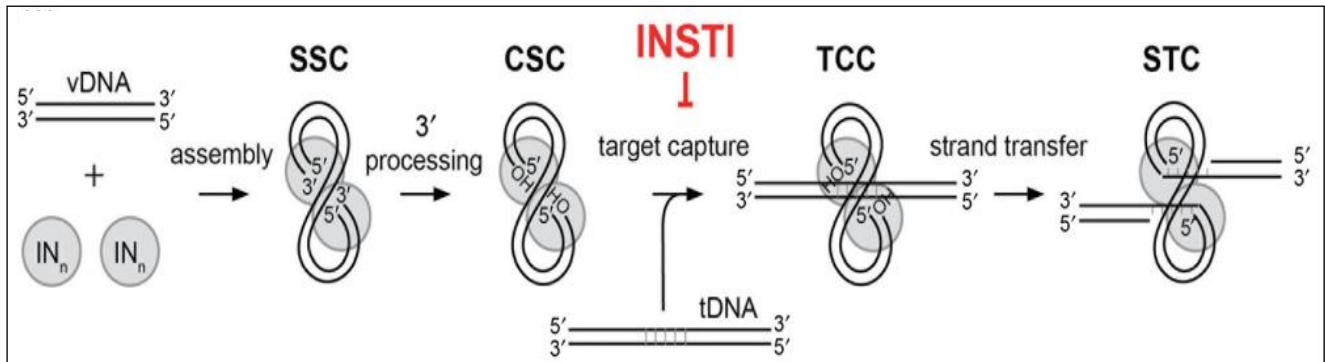
Figure 7. Mechanism of action of INSTIs. From Jóźwik *et al.*, 2020 (87). CSC (cleaved synaptic complex), IN_n (multimers of IN), INSTIs (integrase strand transfer inhibitors), SSC (stable synaptic complex), STC (strand transfer complex), tDNA (target DNA), TCC (target capture complex), vDNA (viral DNA).

INSTIs are generally well tolerated. Besides, INSTIs have shown to be more efficient and also to trigger less resistance compared to other ARTs. This has been excellently reviewed by Yang *et al.*, 2019 (89). However, some toxicity profiles such as neurological, weight gain, and gastrointestinal symptoms have been detected for this class of drugs (90–92). Finally, it is known that, despite therapeutic efficacy, some latent-infected cells keep the provirus integrated into their DNA, but without expressing viral proteins. These cells are known as "reservoirs" (93) and they contribute to low levels virus replication (94) and immune activation (95). Due to the mechanisms of action of INSTIs, it has been speculated that INSTIs could also reduce these reservoirs more than other ARTs (96–100). Thus, to sum up, INSTIs arise as the first regimen of choice in naive HIV-infected people, but they have also showed good results as "switch therapies" (89).

F. Protease inhibitors

PIs are complex molecules which inhibit HIV PR by binding to its active site (101,102) and, therefore, preventing the infection of new cells. In Spain, five PIs are available nowadays: atazanavir (AZT), darunavir (DRV), fosamprenavir (FPV), saquinavir (SQV), and tripranavir (TPV)) (60). These drugs are usually accompanied by a booster, either RTV or COBI. RTV is a potent inhibitor of the CYP3A4 isozyme, the primary enzyme involved in the metabolism of most PIs. On the other hand, COBI is an inhibitor of another isozyme of the CYP3A, and it

is only used to boost AZT or DRV. Thus, these drugs increases the absorption and the half-life of PIs (103).

1.2. Microbiome
1.2.1. Definition

More than 100 trillion microorganisms coexist and interact within the human body (104). This group of microorganisms is known with the term of "microbiota", defined as the community of microorganisms inhabiting a specific environment, including bacteria (bacteriome), archaea, viruses (virome), and some other unicellular eukaryotes (105,106). On the other hand, the term "microbiome" refers to the genomic content of the microbiota (107). The human gut microbiome is about 200 times the number of genes in the human body (104) and, for this reason, humans are also referred to as "superorganisms" (52). There are lots of studies that have demonstrated that alterations in microbiota (mainly gut microbiota (GM)) play an important role in health and disease (108–110). Thus, GM has been considered an "essential organ" (111). Because of that, this Doctoral Thesis is focused on GM, although oral microbiota is also important in health and disease (112) and we will also address its study briefly.

1.2.2. Composition, development, and establishment

The human bacteriome is mainly composed of four bacterial phyla: Firmicutes, Bacteroidetes, Proteobacteria, and Actinobacteria (113) distributed unequally along the human body. The gastrointestinal tract (GIT) harbours the vast majority of these bacteria in number and also in diversity, with about 25 phyla inside the stomach and 195 phyla inside the colon. Below is the mouth (about 56 phyla), the skin (about 48 phyla), and the oesophagus (about 42 phyla). Finally, the vaginal bacteriome in women is composed of 5 different phyla (114) (**Figure 8**).
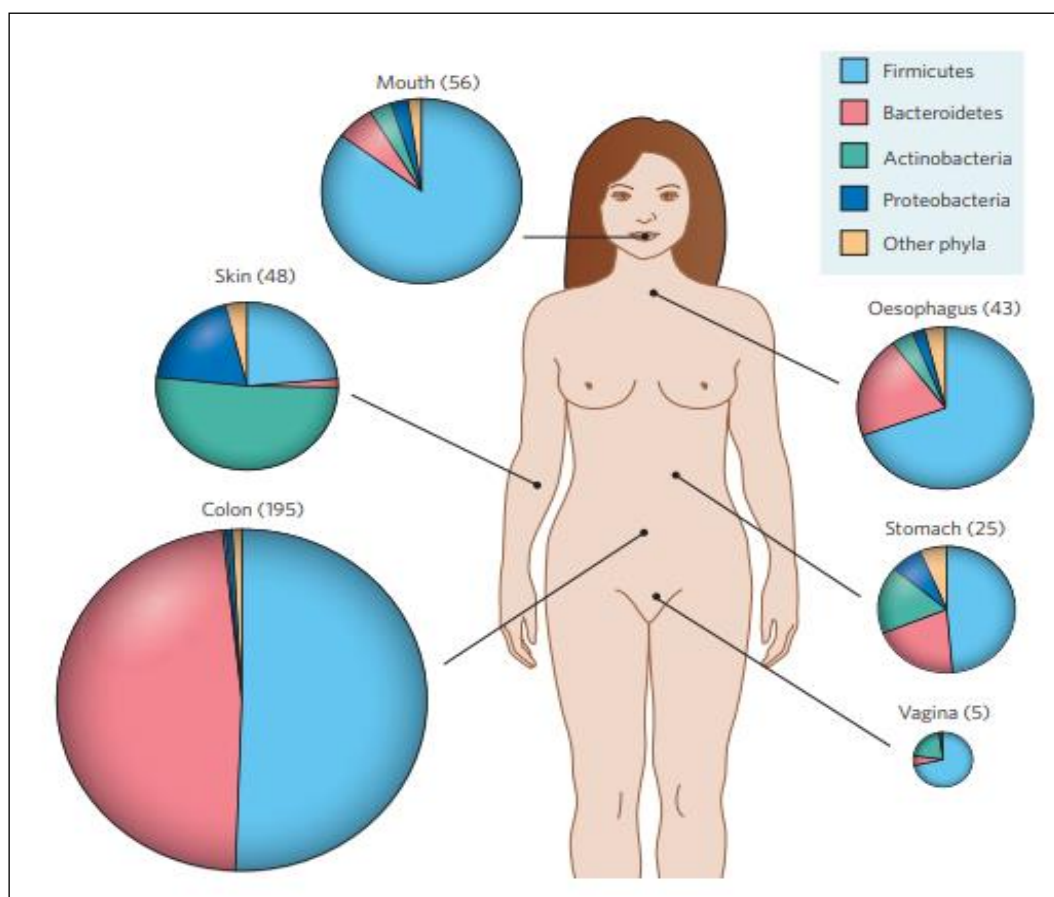
Figure 8. Site-specific distribution of bacterial phyla in healthy humans. The area of the chart for each site represents the average number of distinct phylotypes per individual and the mean number of phylotypes per individual is shown in parentheses. From Dethlefsen *et al.*, 2007 (114).

Thanks to the international and collaborative project METAgenomics of the Human Intestinal Tract (MetaHIT) carried out in Europe and Asia, the human intestinal environment has been classified into three large groups or "enterotypes" according to the relative abundance of three genera: *Bacteroidetes* (enterotype 1), *Prevotella* (enterotype 2), and *Ruminicocuss* (enterotype 3) (115). However, others compositional models have been suggested recetly (116–118) and a debate still exists concerning this issue.

Microbiota development starts in early life, since during fetal life, the GIT is sterile due to the sterile uterine environment. However, some authors have shown that the fetal intestine may be in contact with microbes present in the swallowed amniotic fluid (119). After birth, the infant gut is influenced by different factors such as the type of birth (vaginal birth *vs*. caesarean), diet (breast milk *vs*.

formula milk and the passage from liquid to solid feed), sanitary conditions, the usage of antibiotics, and supplementation with prebiotics and/or probiotics (120–122). Around 2.5-3 years of age, the microbiota presents an adult-like profile with a dense microbial population (123). However, this microbiota is not completely stable and can be influenced during life by genetic, epigenetic and environmental factors such as diet (dietary patterns based on the country of origin), use of antibiotics, and other life events (puberty, ovarian cycle, pregnancy, and menopause) (124,125). Because of that, microbiota presents a high interindividual variability (126). Finally, in older ages, microbiota becomes less diverse and is characterized by a higher Bacteroides to Firmicutes ratio, increases in Proteobacteria, and decreases in *Bifidobacterium* (123) (**Figure 9**).
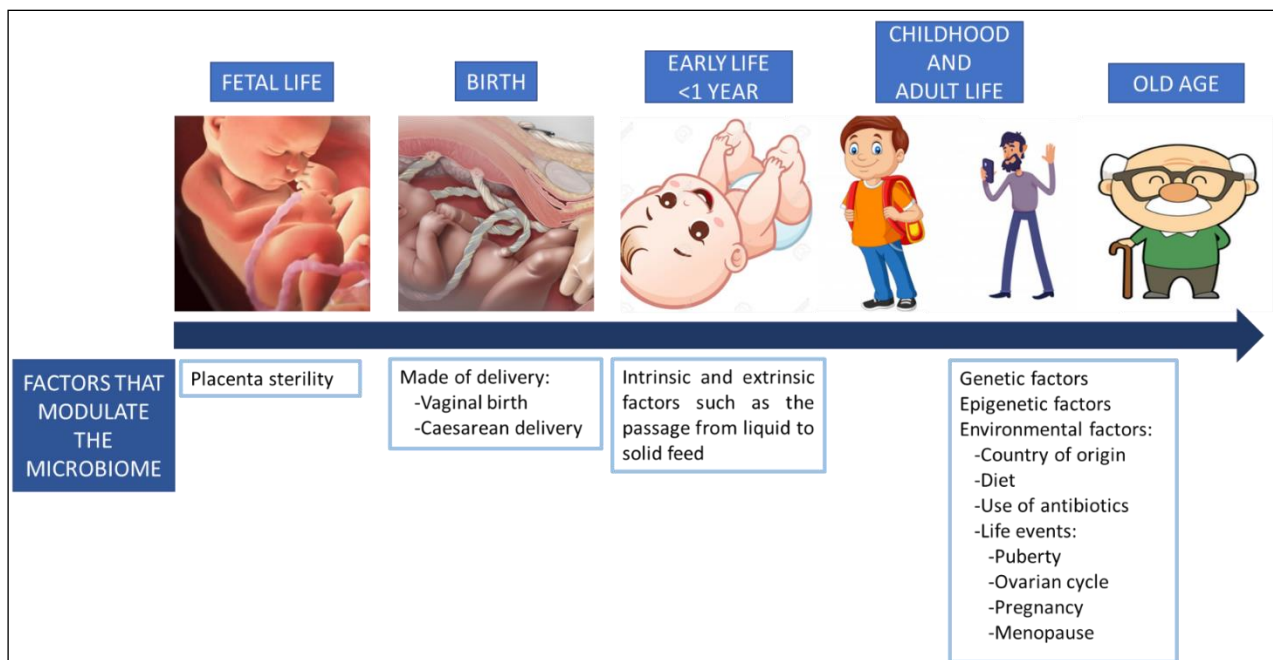
Figure 9. Development of the human microbiota and factors that modulate it in the different phases of the life. Original contribution made with PowerPoint.

1.2.3. Functions of gut microbiota

1.2.3.1. Metabolism

GM affects energy harvest from diet and energy storage. This is due to the ability of some GM enzymes such as glycoside hydrolases and polysaccharide lyases to cleave glycoside linkages present in plant polysaccharides and dietary fibers (127,128). Specifically, these plant polysaccharides are metabolized to oligosaccharides and monosaccharides and subsequently fermented to short chain fatty acids (SCFAs), particularly acetate, propionate, and butyrate. Butyrate provides energy for cellular metabolism while acetate and propionate serves as substrates for gluconeogenesis and lipogenesis (129). Besides, GM influences lipid and cholesterol metabolism, through the conversion, for example, of bile acids into secondary acids affecting enterohepatic circulation, *de novo* synthesis of bile acids, emulsification, and cholesterol absorption (130). Finally, GM contributes to synthesize essential amino acids and vitamins (131,132), and is able to biotransform lots of xenobiotics -such as drugs- influencing their absorption and bioavailability (133) (**Figure 10**).

1.2.3.2. Protective role

One of the most important functions of GM is to avoid the colonization of gut by exogenous and potentially harmful microorganisms. Some of the mechanisms involved in this protective role are direct competition for limited nutrients and modulation of host immune responses (134). Bacteria from the GM can inhibit the growth of their competitors by producing "bacteriocins" (antimicrobial peptides or proteins) (135). On the other hand, GM can regulate the development and function of different types of immune cells. Some species of Clostridia-related bacteria and *Bacteroides fragilis* are able to induce the development of steady-state Th17 lymphocytes and the activation of regulatory T cells (Tregs) (136). Besides, commensal microbiota can maintain host-intestinal microbial T cell mutualism (137). Other examples of this protective role is showed by *Bifidobacterium longum*, which stimulates the production of

interleukin 10 (IL-10) and other proinflammatory cytokines such as tumor necrosis factor α (TNF-α) (138) (**Figure 10**).

1.2.3.3. Trophic role

GM modulates the proliferation and differentiation of colonic epithelial cell through the production of SCFAs. Specifically, butyrate can influence gene expression and protein synthesis and, consequently, modify the microstructure of the small and large intestine, accelerating the maturation of the intestinal mucosa, inducing the repair of the intestinal mucosa, and reducing the apoptosis of enterocytes inside the small intestine (139) (**Figure 10**).

1.2.3.4. Microbiota-gut-brain axis

The gut houses its own nervous system known as the enteric nervous system, which is in constant communication with the central nervous system (CNS). In this point, GM produce catecholamines, histamine, and other biologically neuroactive substances that can stimulate host neurophysiology either through the interaction with receptors in the enteric nervous system or entering into the portal and systemic circulation and interacting with receptors in the CNS (140,141). Recently, evidences have emerge about this microbiota-gut-brain axis and its implication in several neurological diseases (such as Alzheimer disease (142)), but also in development, learning, memory, and behaviour (143,144) (**Figure 10**).

1.2.3.5. Gut-liver axis

The gut-liver axis refers to the close anatomical and functional relationship between the gut and the liver. Some evidence has arisen indicating that gut-liver axis malfunction and, specifically, pathological bacterial overgrowth, intestinal dysbiosis, and increased intestinal permeability is a leading factor in the development and progression of non-alcoholic fatty liver disease (NAFLD), the most common chronic liver disease. Besides, NAFLD itself contribute also to gut dysbiosis (92) (**Figure 10**).

1.2.3.6. Other functions

In recent years, other gut axis have been proposed, such as "gut-kidney" (145), "gut-heart" (146), and "gut-lung" axis (147). A recent study has also proposed the use of probiotics and prebiotics for the prevention or alleviation of COVID-19 because of the connection between the gut and the lung ("gut-lung axis") (148) (**Figure 10**).
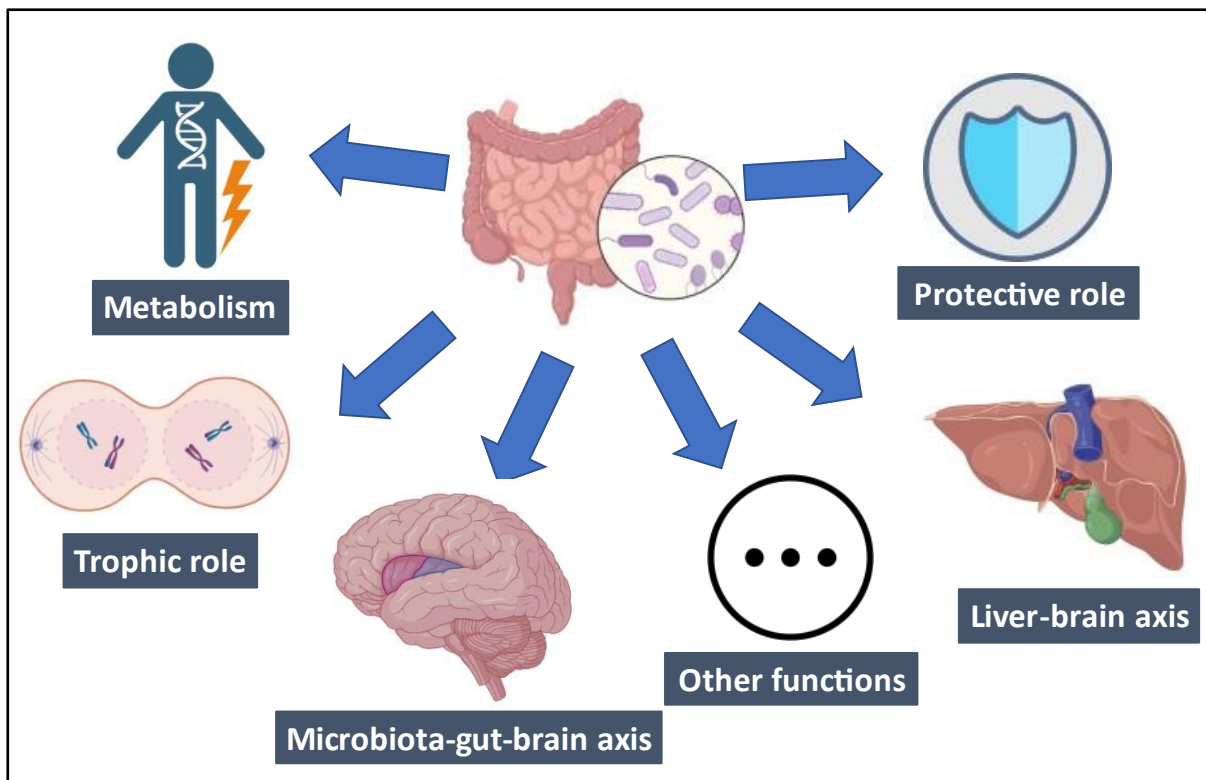
Figure 10. Functions of the gut microbiota. Original contribution made with BioRender.

1.2.4. Approaches for microbiota analyses

Before the development of next-generation sequencing (NGS) the identification of microbiota was challenging since most microbial communities were unculturable (149). Some of the technique used for microbiota studies were microscope visualization, staining, and cultivation (150).

Then, techniques such as terminal-restriction fragment length polymorphism (T-RFLP), denaturing gradient gel electrophoresis (DGGE), and

temperature gradient gel electrophoresis (TGGE) appeared (151). Some examples of the use of these techniques for analysing microbiota are the following. T-RFLP (based on the presence of specific polymerase chain reaction (PCR) fragment lengths for individual genotypes after digestion with a restriction enzyme) was used to identify gut dysbiosis associated with necrotizing enterocolitis (NEC) in animal models suggesting a significant role for *Clostridium* in pathogenesis (152), whereas DGGE (used to separate a mixture of DNA fragments according to their melting point) showed that human gut microbiome was disrupted by antibiotic administration (153). Finally, TGGE (a form of electrophoresis in which temperature gradient is used to denature molecules as they move through either acrylamide or agarose gel) allowed the identification of a direct correlation between *Sphingomonas* with NEC in human infants (154).

Subsequently, the emergence of DNA sequencing technologies allowed a more precise and rapid taxonomic identification of individuals within complex microbial communities although these techniques were slow and expensive (151). The 16S ribosomal ribonucleic acid (rRNA) gene sequencing was originally performed by cloning the full gene into plasmid vectors, transforming it into suitable hosts (usually *Escherichia coli*) and sequencing it (155). These clone libraries were usually used to implement other methods like Southern blotting and *in situ* hybridization due to the high costs of sequencing (156).

Finally, more recent PCR-based massive parallel sequencing technologies (157) along with advancement in bioinformatics tools have allowed the obtainment of high throuput data. Thus, nowadays, one standard method for determination of gut microbiome composition is carried out by isolation of total DNA from samples, PCR amplification of regions universally conserved (16S rRNA gene in bacteria and 18S rRNA gene in fungi), and high-throughput sequencing of those amplicons. This technique eliminates the need for cloning genes, blotting RNA, and cultivation (151). However, is important to normalize sample storage, primer efficiency, PCR amplification conditions, sequences platform, bioinformatics pipeline, and protocols of DNA extractions in order to avoid the introduction of biases that could skew the results (158,159). Whole

genome sequencing (WGS) extends the information provided by shotgun sequencing (16S/18S sequencing) and allows the identification of other components of the microbiota such as viruses (viroma) and the discovery of information about gene content and metabolic pathways. However, viroma data is often omitted from compositional studies (151,160).

Nevertheless, the information provided by these previous techniques (metagenomic) represents only potential functions since genes identified may or may not be expressed. In fact, although scientists were initially focused on compositional studies (metagenomic), they gradually became more interested in functionality studies (metatranscriptomic) and in identifying networks within microbial ecosystems (metabolomic) (151). This is possible thanks to techniques such as chromatography, mass spectrometry (MS), and nuclear magnetic resonance (NMR) (161–163).

1.2.5. Gut microbiota: focus on gut bacteriome

Under normal conditions, there is a homeostatic equilibrium within microbial communities, microorganisms, and host. The appearance of some perturbations can alter this balance producing dysbiosis (changes in composition and/or functionality of microbial communities). Fortunately, there is a threshold of perturbations that can be reversed by the resilience mechanisms of the organism (164). However, when these mechanisms are not enough to counteract the changes induced on GM, dysbiosis occurs and this could be due to a loss of certain microorganisms and/or an excessive growth of others, leading to a loss of microbial diversity and/or richness (165). In fact, alterations in microbiota can result from exposure to environmental factors such as diet, toxins, drugs, and pathogen microorganisms, among others.

The main approach for studying changes in composition of the intestinal microbiota in relation to disease has mainly relied on the phylogenetic characterisation of the microbiota of diseased individuals in comparison with "apparently" healthy individuals. However, as it exists a great inter and intra-

individual variation it is difficult to establish precise relations and it is also important to take into account that it is not clear if this phylogenetic changes are a cause or a consequence of a disease (166).

There is growing evidence that dysbiosis of the GM is associated with the pathogenesis of both intestinal and extra-intestinal disorders (167). Among the intestinal disorders, it is interesting to cite inflammatory bowel disease (IBD), irritable bowel syndrome (IBS), celiac disease, and colorectal cancer (CRC). For example, in IBD, patients show a decrease in microbial diversity alongside a decrease in the relative abundance of Firmicutes and an increase in the relative abundance of Bacteroidetes and Enterobacteriaceae (168). Besides, it has been observed differences in the microbiota of Crohn's disease (CD) and ulcerative colitis (UC), the most prevalent forms of IBD (169,170). On the other hand, changes in microbiota composition have been described in the different subtypes of IBS compared to healthy individuals (171,172). Celiac disease and CRC have been associated with increased diversity and richness of GM compared to control group (173–175). Moreover, among the extra-intestinal disorders are metabolic disorders such as obesity and type 2 diabetes (T2D). In obese humans, an increase in the relative abundance of Firmicutes and a decrease in the relative abundance of Bacteroidetes have been observed (109,176) and it have been also described a decrease in GM diversity (109,177). Besides, considering the role of GM in metabolism, it is reasonable to assume that the high-fat diet and the overconsumption of food responsible for the greater prevalence of obesity and T2D in the West induce alterations in host metabolism and immune homeostasis through changes in GM (166). It could be possible that the GM of obese individuals are more efficient in converting food into useable energy and in storing this energy in fat (109,178–180). Finally, GM dysbiosis has also been observed in CNS-related disorders, what could be related to the microbiota-gut-brain axis. For example, it is known that enteric infections can cause anxiety, depression, and cognitive dysfunction (181). Taking into account that all aforementioned diseases have a direct or indirect relationship with GM dysbiosis, it is perhaps no coincidence that gut disorders including IBD an IBS are common comorbidities of other disorders such as depression and anxiety (182,183).

1.2.6. Gut virome

DNA and RNA viruses that constitute the "intestinal virome" are at least equivalent in number to bacterial cells (184), but on gut mucosal surfaces and within the mucosa layers they may outnumber bacterial cells twenty times (185). The human virome is composed of eukaryotic and prokaryotic viruses, including viruses that infect human cells, viruses that infect microbes (such as bacteria, fungi, and archaea), and plant viruses that are primarily derived from environment and diet (186). Gut virome could play an important role in the pathogenesis of disease, including IBD (187), *Clostridioides difficile* infection (188), obesity (189), diabetes (189), SARS-CoV-2 infection (190,191), liver diseases (192), CRC, as well as malnutrition (193). Besides, gut virome reconstitution has shown great potential as disease therapeutics through faecal microbiota transplantation, faecal virome transplantation, and phage therapy (188,194,195).

1.2.6.1. Eukaryotic viruses

Eukaryotic viruses present in gut virome cover *Picobimaviridae*, *Adenoviridae*, *Anelloviridae,* and *Astroviridae* family members and species such as bocaviruses*,* enteroviruses*,* rotaviruses, and sapoviruses (196). Besides, it also include some disease-associated viruses such as herpesviruses, polyomaviruses, anelloviruses, adenoviruses, papillomaviruses, and others (197). However, despite the presence of these pathogenic viruses (pathobionts) most humans remain asymptomatic, so it has been suggested that these viruses have become part of the metagenome of normal individuals remaining dormant within the host (198,199).

1.2.6.2. Bacteriophages

The human GIT contains about 10^{15} bacteriophages (phageome) (200). Phages can be categorized in two mainly groups: ***lytic or virulent phages***, which use the host cell's replication mechanism to produce more phages and then lysate the cell releasing phage virions, and ***lysogenic or temperate***

phages, which incorporate their genetic material into the host cell as prophages an replicate with the cell (201) (**Figure 11**). Sometimes, the second type of phages do not integrate and exist as a circular or linear plasmid (202). It has recently discovered another group of bacteriophages, known as *pseudolysogenic phages*, which neither integrate into the host genome nor lysate the bacterial host cell (201). On the other hand, it is important to note that, recently, a group of DNA phages, called crAssphage, has been identified. CrAssphages are highly abundant in GM and they have been predicted to infect *Bacteroides* species (203), although its relevance is still unknown.
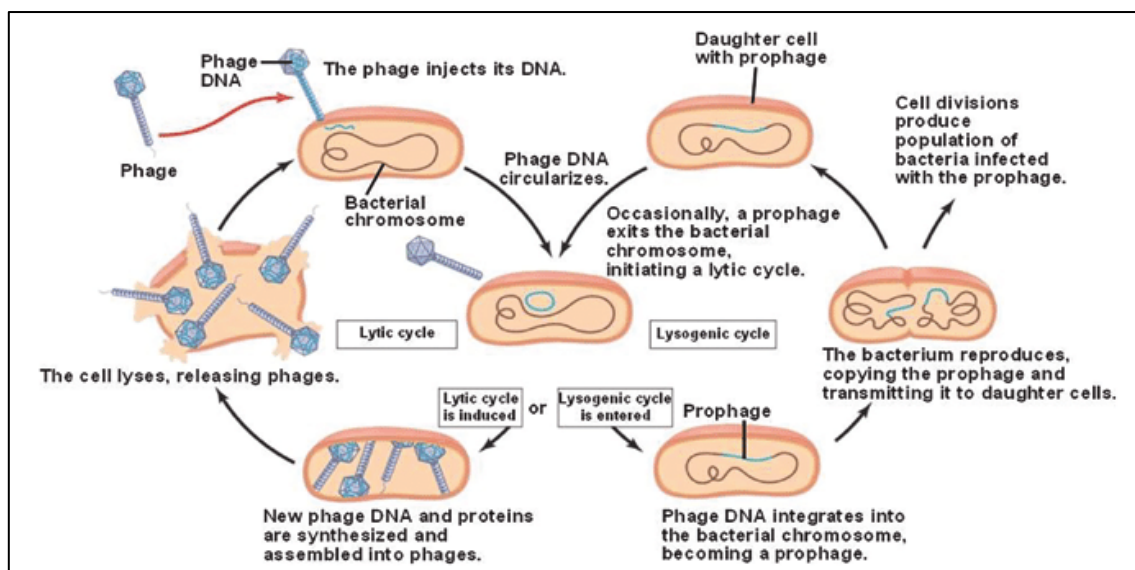
Figure 11. Bacteriophage lytic and lysogenic cycle. From Vander *et al.*, 2018 (204). DNA, deoxyribonucleic acid.

1.2.6.3. Gut virome composition, development, and establishment

While our knowledge about composition and development of gut bacteriome is large, we have a little understanding of gut virome acquisition (197). The lack of viral like particles (VLPs) in the first faecal samples of new-borns seems to indicate that gut virome is acquired postnatally (205). About a week after born, VLPs numbers reach 10^8/g in faeces. These viruses proceed from dietary, maternal, and environmental sources (205). Then, gut virome develops in parallel with the bacterial component suffering different shifts (206). Later, in

adulthood, gut virome reaches a peak more or less stable in time (196,206). This adult gut virome is mainly constituted by bacteriophages from *Myoviridae*, *Podoviridae*, *Siphoviridae*, *Inoviridae*, and *Microviridae* families, double-stranded DNA viruses (*Adenoviridae*, *Herpesviridae*, *Iridoviridae*, *Marseilleviridae*, *Mimiviridae*, *Papillomaviridae*, *Polyomaviridae*, and *Poxviridae* families), single-stranded DNA viruses (*Anelloviridae* and *Circoviridae* families) double-stranded RNA viruses (*Picobimaviridae* and *Reoviridae*) and single-stranded RNA viruses (*Caliciviridae*, *Astroviridae*, *Virgaviridae*, *Picornaviridae*, *Retroviridae*, and *Togaviridae*). Moreover, it can also contain pathogenic eukaryotic viruses such as rotavirus, norovirus, astrovirus, adenovirus, and enterovirus (197). On the other hand, it has been observed that eukaryotic viral richness is low in infancy and expand thereafter, whereas bacteriophage richness in greatest in early life and decreased with age in addition to suffer a marked shift towards an increased relative abundance of *Microviridae* (206). Besides, members of the *Picornaviridae*, *Adenoviridae, Astroviridae, Anelloviridae, Reoviridae,* and *Caliciviridae* families seem to be predominant in the infant but do not persist during early development (206,207).

Gut virome is more stable than gut bacteriome within individuals (208,209), and similarly, can be influenced by diet (210) and antibiotic use (211). Specifically, antibiotics enrich phages which encodes antibiotic resistance genes to the administrated antibiotic and to other related ones (212).

1.2.6.4. Virome links with other components of the gut microbiome

Virome can influence bacterial evolution, diversity, and metabolism acting as a vehicle for horizontal gene transfer (196,200). Besides, it can trigger dysbiosis through four different mechanisms. In the "*Kill the Winner*" model, phages kill dominant commensal bacteria which are usually growing the fastest and reduce their number in the gut (197). This approach relies on opportunistic contacts and there is limited evidence of this occurring within the gut (213). The second mechanism, the "*Biological Weapon*" model, assume that commensal

bacteria use the phages as weapons to kill competing bacteria (197). The "*Community Shuffling*" model propose that environmental stress factors such as antibiotics, oxidative stress, and inflammation trigger the entrance of prophage into bacteria resulting in lytic infection and altering the balance between symbionts and pathobionts (197,214). Finally, the "*Emerging New Bacterial Strain*", is based on the phages' ability to transfer genes to bacteria modifying their phenotype (197).

1.2.7. Oral microbiota

Oral microbiota is important in health and disease (112). Systemic conditions (and their associated treatments) could have an impact on oral health by reducing salivary flow and affecting the ecological balance of the oral microbiota (215). In this regard, oral microbiota has been revealed to be distinct from that found in other areas such as gut or skin (216). Besides, oral microbiota presents a high α-diversity but a low β-diversity, that is to say, the oral microbiota is very diverse, but the communities are quite similar between individuals (217,218). The analysis of oral microbiota through supra and subgingival plaque samples is often time-consuming (219,220). Because of that, saliva-based analysis has gained considerable attention since it is simple, inexpensive, and non-invasive (221–223).

1.2.7.1. Oral microbiota composition, development, and establishment

The oral cavity becomes a major point of entry of microorganisms in the human body (224). The oral microbiota is composed by hundreds of microbial species including bacteria, viruses, archaea, fungi, and protozoa that coexist and interact in oral biofilms to maintain homeostasis (224–227). Thanks to the development of omics techniques, genome database specific to oral microorganisms have been developed, including the Human Oral Microbiome database (HOMD) (228) and the Core Oral Microbiome (CORE) database (229). Besides, the Human Microbiome Consortium has sequenced the genomes of oral

bacteria allowing the reduction of the number of unassigned reads in metagenomic analysis (230).

Oral microbiota can be acquired from the birth canal, mother's skin, air, food, water, and other fluids, but saliva (from the mother or from other individuals in close contact) is the main route (231). Besides, the mode of delivery has been associated with specific oral microbiome patterns in 3- to 6-month-old infants (232).

The diversity of the oral microbiota increases during the first months of life, being the main pioneer oral bacterial species *Streptococcus salivarius*, *Streptococcus mitis*, and *Streptococcus oralis*. These early colonizers are followed by gram-negative anaerobes such as *Prevotella melaninogenica*, *Fusobacterium nucleatum*, and *Veillonella* spp. Then, at the time of teeth eruption, bacterial species such as *Streptococcus sanguinis* begin to colonize the oral cavity (233). Finally, from the first month of life to the adulthood, the oral microbiota becomes more diverse being very influenced by environmental factors such as diet (234).

1.2.7.2. Oral microbiota dysbiosis

The most abundant members of the oral microbiota are commensal microorganisms beneficial for oral health, but pathogens also co-exist in a symbiosis state providing some kind of "colonization resistance" and downregulation of damage helping to maintain the normal development of host tissues and defences (235). However, constant changes in the environment can disturb these symbiotic interactions between microbe-microbe and microbe-host and trigger dysbiosis, which is characterized by the outgrowth of pathogens and the increased risk of disease development (236). In this context, untreated dental caries is the most common disease. In fact, severe periodontitis is the sixth most common disease affecting humans globally (237). Moreover, increasing evidence shows that oral bacteria may spread and be associated with infections in other parts of the body (238) such as the brain in Alzheimer disease (239).

1.2.7.3. Oral and gut microbiota interactions

It has been recently showed that there is an ongoing direct migration of bacteria from the mouth to the gut even in healthy individuals (240). In most individuals, there is no apparent clinical consequences of this migration, and this may be a necessary mechanism to shape the GM. However, some oral bacteria appear to cause gut inflammation (241–243), and multiple clinical studies have associated the presence of "oral" bacteria in the gut with inflammatory diseases (244–246) such as HIV infection (247,248).

1.3. HIV infection and microbiota

1.3.1. Role of bacterial translocation and chronic inflammation in HIV infection

Life expectancy in HIV-infected people has significantly increased thanks to the improvement in clinical management and, specially, by the extended use of ART. Indeed, HIV infection is considered a chronic disease, although life expectative is not as long as that observed in non-infected people or general population (49). This fact has been associated with premature and accelerated aging (inflammaging), among other factors (249). The acceleration of the aging process leads to immunosenescence, which is characterized by a continuous activation of the immune system and a low-grade chronic inflammation (250). Thus, HIV patients are predisposed to co-morbidities and natural aging symptoms more frequently seen in elderly people. Therefore, HIV patients have higher rates of cardiovascular disease (CVD), mainly atherosclerosis, and also non-AIDS (acquired immune deficiency syndrome) cancers, frailty (loss of muscle mass, osteoporosis, and muscle weakness), kidney and/or liver diseases, and neurologic complications such as dementia, compared to uninfected subjects of the same age (251–257).

HIV infection is characterized by a set of structural changes of the gut epithelial barrier, immunological shifts, and modifications in the composition and

functionality of the GM. In normal physiological conditions, the microorganisms are in the intestinal lumen interacting with the intestinal cells in a state of symbiosis but, when HIV infection occurs, depletion of lymphocytes T CD4+ takes place in the GALT. Besides, although lymphocytes T CD4+ represent the most affected cells during HIV infection (258), other cell types are also infected during HIV infection. In fact, an altered functionality of lymphocytes T CD8+ (cluster of differentiation 8), lymphocytes B, and innate immune cells have also been observed (259,260). Concerning lymphocytes B, an hyperactivation and a dysregulation lead to altered antibody production during HIV infection (261). DCs are also altered (262–264) and macrophages show a reduced capability for phagocytosing bacterial products in addition to be targets for HIV infection (265,266). All these facts are accompanied by a rupture of the integrity of the epithelial barrier, as mentioned before, due to the appearance of focal breaches, a decreased expression of epithelial repair tight junction genes, and an increased permeability (265,267–269). This rupture of the epithelial barrier during HIV infection triggers alterations in the intestinal lumen and also in the composition of the microbiota (at least at bacteria level) (270). This dysbiosis favors the passage of microorganisms and their components to the *lamina propria* and, hence, to the circulation, which is known as bacterial translocation (BT) (265,266,268,271–294) and which undergoes subsequent intestinal and systemic inflammation (295) (**Figure 12**). It is interesting to point out that SIV-infected natural host do not develop AIDS despite high levels of virus replication and do not show evidence of BT, which might explain the lack of immune activation and disease progression in these animals (272,296). In addition, external administration of bacterial products in these natural host induces immune activation, increase viral load, and trigger the depletion of lymphocytes T CD4+ (297). Thus, the importance of BT in immune activation and disease progression is corroborated.
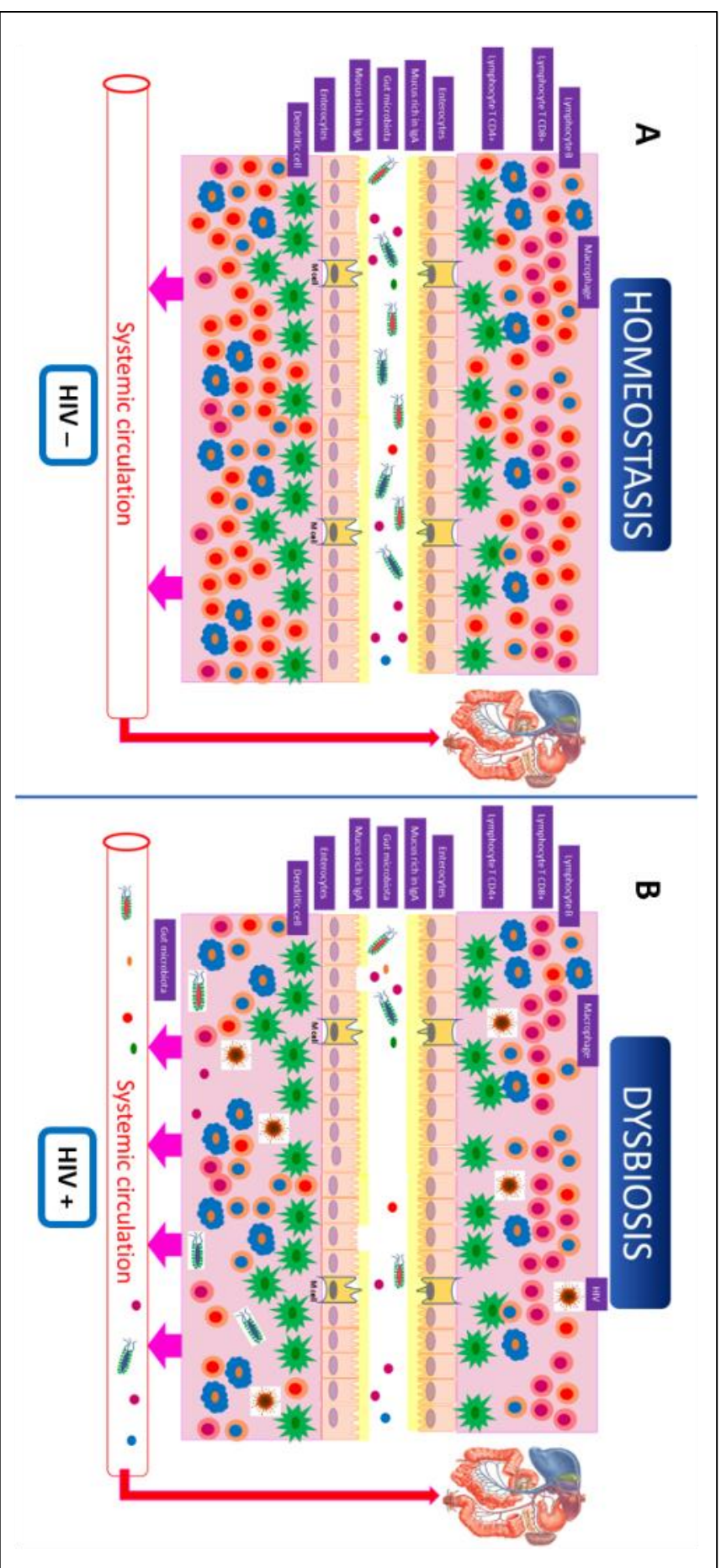
Figure 12. A) Gut homeostasis. **B)** Gut dysbiosis after HIV infection. From Pérez-Matute *et al.*, 2017 (298). CD4 (cluster of differentiation 4), CD8 (cluster of differentiation 8), HIV (human immunodeficiency virus), IgA (immunoglobulin A).

Specifically, BT was firstly described in HIV-infected patients in 2006 by Brenchley *et al.* (272). As mentioned above, bacterial products such as lipopolysaccharide (LPS) induce a significant increase of proinflammatory cytokine production via toll-like receptors (TLRs) contributing to immune activation and inflammation (299). TLRs are transmembrane receptors expressed in numerous cell types that play an important role in the mechanism of innate immunity of the intestinal epithelium, recognizing bacterial, viral, parasites or self-derived ligands, initiating several signalling cascades, and inducing the synthesis and release of factors related to inflammation such as TNF-α, interleukin 1 (IL-1), and interleukin 6 (IL-6) (300). In normal physiological conditions, TLRs play a pivotal role in the regulation of intestinal inflammation and immune tolerance inducing a basal state of activation which ensures mucosal homeostasis (300). However, after exposure to physiological stressors such as remote infection, changes on GM composition or high concentration of LPS, an increased TLR activity occurs, which induces the release of proinflammatory cytokines, triggers apoptosis and inhibits intestinal repair, which damages the epithelial layer (300). These effects may be initiated but also propagated by the TLR-activated leukocytes (300).

In this context, soluble cluster of differentiation 14 (sCD14) and soluble cluster of differentiation 163 (sCD163) are two clusters of differentiation that act as indicators of BT. sCD14 is secreted by activated monocytes (by proteolytic processing) after the join of LPS to toll-like receptor 4/MD-2 (TLR-4/MD-2) complex mediated by lipopolysaccharide binding protein (LBP) and membrane cluster of differentiation 14 (mCD14). sCD14 can join, in turn, to more LPS and transfer it to mCD14 triggering the activation cascade of a greater number of monocytes (301) (**Figure 13**). On the other hand, cluster of differentiation 163 (CD163), expressed in monocytes, has also two forms, membrane cluster of differentiation 163 (mCD163) and sCD163. mCD163 is responsible for the removal of plasma hemoglobin through endocytosis of the very high-affinity complex hemoglobin–haptoglobin, thus, preventing the oxidative stress triggered by free hemoglobin through the release of the free iron, bilirubin, and carbon monoxide. Moreover, sCD163 acts in the immune system but its role has not

been clearly defined, up to now. Its plasma levels are elevated in pathologies such as diabetes, obesity, liver disease, and atherosclerosis, all of them characterized by a low-grade inflammation (302). Regarding HIV-infection, only one study has reported a statistically significant relationship between the levels of sCD14 and sCD163 and new atheromatous plaque formation in HIV patients (303).
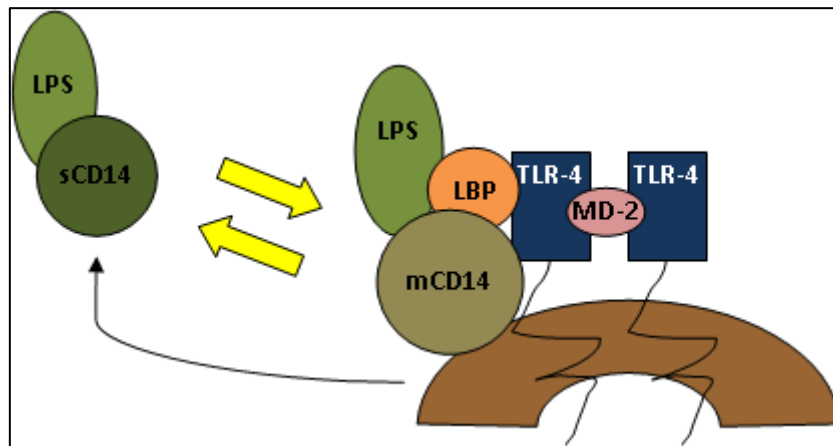
Figure 13. sCD14 pathway. Original contribution made with PowerPoint. LBP (lipolysaccharide binding protein), LPS (lipopolysaccharide), mCD14 (membrane cluster of differentiation 14), sCD14 (soluble cluster of differentiation 14), TLR-4 (toll-like receptor 4).

Finally, as a consequence of this increased BT and innate cell activation, systemic levels of proinflammatory cytokines such as interferon α (IFN-α), IL-1, IL-6, interleukin 18 (IL-18), and TNF-α are observed (263,304). All these processes triggered by HIV infection -even under ART- constitute what is called as "persistent chronic immune activation" (305) and the degree of this immune activation is very important because it represents the strongest correlation with disease progression, morbidity, and mortality (305–310). In addition, this state of chronic inflammation that persists in HIV infection despite ART is also associated with different disorders that limit the quality of life of these patients, such as the cardiovascular events.

In this context, it is of great interest the relation observed between very high levels of trimethylamine N-oxide (TMAO), produced by GM, and the development of future cardiovascular events such as atherosclerosis, as has been recently recognised in non-HIV-infected patients (311–316). In fact,

elevated blood levels of TMAO are associated with worse outcomes in patients with CVD, such as coronary artery disease or heart failure, and with higher mortality (312,316–320). TMAO derives from choline (vitamin B), carnitine and betaine (trimethylglycine) that are present in diet (mainly in milk, red meat, fish, vegetables, and mushrooms) and that are degraded by the action of trimethylamine (TMA) lyases present in GM producing TMA. TMA is subsequently processed by hepatic monooxygenases leading to TMAO (**Figure 14**). In HIV patients, several studies have also demonstrated the relation between TMAO and cardiovascular events (321–324). In one of these studies, high levels of TMAO were significantly associated with an increased risk of plaque incidence in the carotid artery (324). Furthermore, levels of TMAO were associated with higher levels of sCD14 and sCD163 (324). Other study demonstrated an independent association between higher TMAO concentrations and higher cardiovascular risk and between higher TMAO concentrations and multimorbidity (presenting ≥3 comorbidities) in HIV-infected patients (325). In contrast, in the study from Haismman *et al.*, 2017, no differences in TMAO blood levels were observed between naive and ART-treated HIV patients, although high levels of its precursors, carnitine and betaine, were increased in untreated HIV patients compared to treated ones (326). It will be necessary to ensure if the lack of differences observed in that study between naive and ART-treated people could be explained by diet. Thus, if diet were similar among both groups, it could be suggested that GM composition and/or functionality is different among both groups in terms of the ability to metabolize TMAO's precursors. In addition, the lack of differences observed in this study did not discard a significant increased cardiovascular risk in HIV-infected patients. In fact, other biomarkers of CVD should also be analysed since a very recent study has failed to find a strong association between TMAO, gut dysbiosis, and inflammation in HIV infection (327).
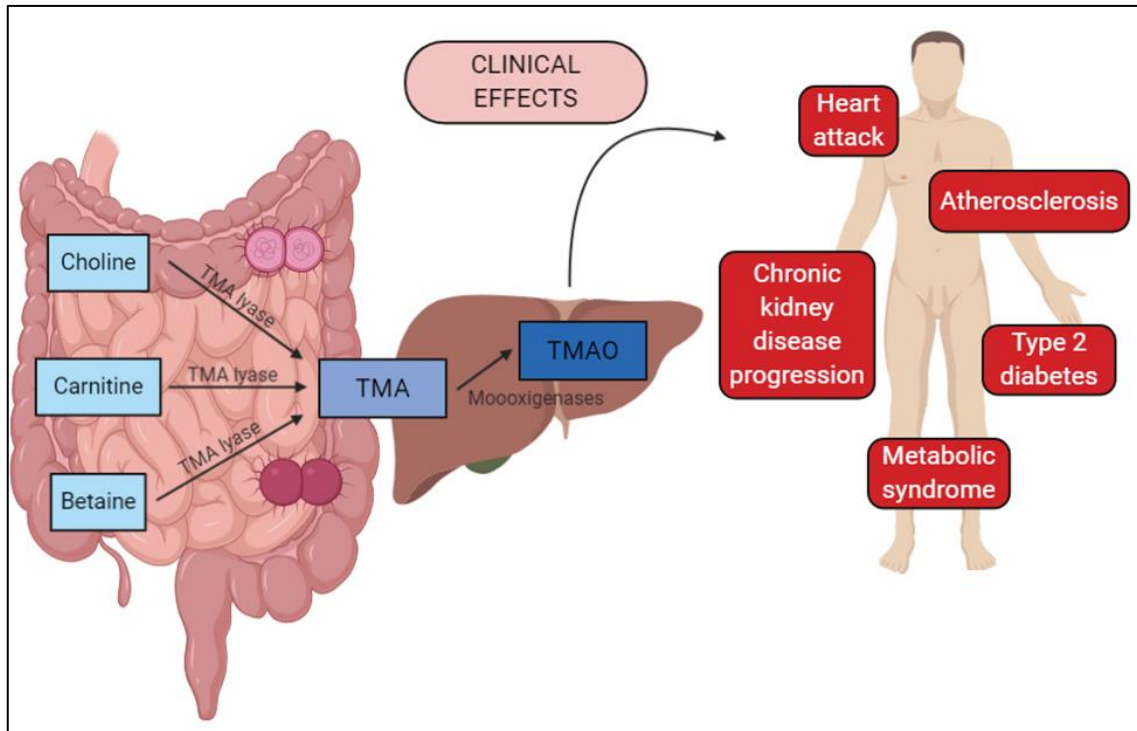
Figure 14. Processing pathway of choline, carnitine, and betaine from diet to produce TMAO and clinical effects of TMAO. Original contribution made with BioRender. TMA (trimethylamine), TMAO (trimethylamine N-oxide).

1.3.2. Gut bacteriome composition in HIV infection

GM dysbiosis (focused on bacteriome) has been associated with the deleterious events that take place in gut during HIV infection and that are associated with a low-grade of chronic inflammation and immunosenescence (described before). Specifically, HIV infection has been associated with a reduced bacterial diversity in gut (328–330), although other studies did not find differences in bacterial diversity between naive patients, ART-treated patients, and controls (248,331–333). Thus, more studies are required in this field. On the other hand, several studies have reported a characteristic profile in naive patients compared to a general population with a depletion in Clostridia class an *Bacteroides spp*, an overgrowth of Enterobacteriaceae, and an increase in the genus *Prevotella* (334). In this regard, a lower abundance of several *Bacteroides* species has been observed to impair the functions of natural killer (NK) cells, which limit BT and chronic immune activation (335). Besides, a study reported a greater abundance of Proteobacteria phylum (which promote inflammation) and

a lower abundance of Bacteroidia class (which limit inflammation) in naive patients, which has been linked to an increased T cell activation, a lower secretion of interleukin 17 (IL-17) and interleukin 22 (IL-22), and a higher presence of inflammatory markers (248). Among the Firmicutes phyla, whose abundance seems to be decreased in naive patients (331), *Faecalibacterium prausnitzii* has arisen as a very interested candidate because it is an obligate anaerobe belonging to Lachnospiraceae family, which has anti-inflammatory properties and whose depletion has been reported during HIV infection (328,329,331). Moreover, the reduction in the amount of other protective bacteria such as bifidobacteria and lactobacilli has been reported in naive patients compared to general population (336). Recent studies have also highlighted the influence of sexual orientation and mode of transmission in the composition of GM in HIV-infected patients (337–339). It is worth pointing out that this GM dysbiosis triggered by HIV infection cannot be fully reversed by ART. In fact, very few studies have analyzed the effects of different ART therapies on BT and GM composition. In this context, a previous study from our group carried out with a small number of patients under INSTIs (RAL) showed levels of inflammation and BT similar to uninfected controls and a significant improvement in GM richness (270). Another issue to consider when investigating what is happening at gut level in HIV infection is the metabolic pathways by which GM could influence HIV immunopathogenesis. In this context, it has been revealed that the microbiota associated with HIV-infected individuals is enriched in genes involved in several pathogenic processes such as LPS biosynthesis and, on the contrary, associated with depletion of genes involved in amino acid metabolism and energy processes (248), some of the process in which GM has an important role as has been described before.

1.3.3. Virome composition in HIV infection

There are very few studies focused on the effects of HIV infection and ARTs on gut virome. These studies have been carried out in different matrix such as plasma, semen, cervix, saliva, and faeces, which complicates to extract

general conclusions. Next, we summarize the most relevant results of these different studies.

1.3.3.1. Plasma virome of HIV-infected patients

In 2012, Li *et al.* compared the plasma virome (only DNA viruses) of naive patients (4 males and six males with 36 ± 7 years) with that of a control population (non-infected) (6 males and 5 females with 24 ± 3 years) through whole genome amplification (WGA) using Illumina Solexa sequencing (340). They observed that the HIV/AIDS plasma virome was dominated by bacteriophages (85.51% of total plasma virome) and human endogenous retroviruses (HERVs) K (14.34% of total plasma virome). HERVs are remnant of gene line retroviral integration (341) and are generally considered functionally defective but it has been observed higher levels in autoimmune disorders, malignancies, and HIV infection (342,343). HERV K represents the more recently integrated and active group and it has been extensively associated to HIV infection (343–346). Besides, the bluetongue virus, which infects ruminants (347,348), was also found contributing to 1.15% of the plasma total virome. Among phages, the most abundant one was *Bacteriophage* (40.97% of total plasma virome), followed by *Enterobacteria phage* (25.75% of total plasma virome) and *Pseudomonas phage* (17.79% of total plasma virome). In contrast, in the control population the dominant group of viruses was *Torque teno virus* (TTV) (87.20% of total plasma virome), followed by *Torque teno midi virus* (TTMDV) (10.12%), *SEN virus* (2.03% of total plasma virome) and *small anellovirus* (0.65% of total plasma virome).

A few years later, in 2013, Li *et al*. analysed the DNA and RNA virome in the plasma of HIV-infected patients with low (<200 cells/µl) versus high (>700 cells/µl) lymphocytes T CD4+ (35 patients between both groups) through MiSeq platform (349). The plasma virome of HIV subjects contained viral sequences from HIV, GB virus C (GBV-C), hepatitis B virus (HBV), hepatitis C virus (HCV), anellovirus, and HERVs. Coinfection with GBV-C is common among HIV-infected people and has been linked with slower disease progression, lower mortality rate, and longer survival (350,351). On the other hand, anelloviruses, which have not

been associated with human disease (352), seemed to be higher in the low-CD4+ group than in the high-CD4+ group, suggesting an imbalance in the control of anellovirus replication.

In 2016, Li *et al.* analysed the plasma virome of ART-treated HIV-infected patients (19 patients; age range 37-57 (mean 47.8 $\pm$ 5.1 years) with a male/female ratio of 17/2) using MiSeq platform (353). The anellovirus sequences were identified in all 19 individuals and sequences of HVB, HCV, and GBV-C were also detected. The anelloviruses reads showed no significant association with either lymphocytes T CD4+ or CD8+ or the percentage of activated lymphocytes T CD4+ or CD8+ (HLA-DR+ CD38+ CD3+), so they seem not to have an important role in T-cell activation. Among anellovirus sequences, the *Alphatorquevirus* group 3 (18 strains detected in 9 individuals) was the most prevalent one, followed by *Betatorquevirus* (8 strains detected in 5 individuals) and *Alphatorquevirus* group 1 (6 strains detected in 6 individuals).

Finally, in 2021, *Liu et al*. analysed the plasma virome of naive and ART-treated HIV-infected men who have sex with men (MSM) (22 HIV- MSM, 30 HIV+ naive MSM with CD4>200, 20 HIV+ naive MSM with CD4<200 and 29 HIV+ ART-treated MSM; age range 23-43) compared to HIV- MSM (22 individuals) and non-MSM as controls (20 individuals) using NovaSeq platform (354). Most clean reads were unclassified (~57%) and viral reads accounted for ~10% of cleaned reads. The plasma virome of these participants were dominated by eukaryotic viruses (98.0% of total viral reads), followed by bacteriophages (1.7% of total viral reads) and unclassified viruses (0.3% of total viral reads). Eleven eukaryotic viral families were detected, including DNA viruses *Anelloviridae*, *Hepadnaviridae*, *Genomoviridae*, *Papillomaviridae*, *Adenoviridae*, *Circoviridae,* and *Herpesviridae*, and RNA viruses *Flaviviridae* and *Picornaviridae*. Besides HIV-1 (identified in 65 out of 71 HIV + samples), the most frequently detected viruses from these individuals included anellovirus, pegivirus, HBV, HCV, and HERVs. Other viruses included papillomavirus, influenza virus, α-herpesvirus, adenovirus, and gemykibivirus. Compared to non-MSM individuals, MSM did not show changes in overall plasma viral reads. However, HIV infection significantly

increased the abundance of plasma viral reads. Besides, although the viral abundance of individuals receiving ART was higher than that of HIV- MSM, ART successfully controlled the shedding of different viruses. Moreover, HIV infection led to a decrease in phage abundance and increase in eukaryotic virus abundance and ART usage could restore the virome profile towards that of HIV-individuals. Finally, compared to non-MSM, MSM had a lower abundance of allenovirus, and HIV infection increased its abundance, while ART could decrease it. On the other hand, compared to non-MSM, MSM had a higher abundance of pegivirus, and HIV infection decreased its abundance.

1.3.3.2. Semen virome of HIV-infected patients

In 2020, Li *et al.* investigated the semen virome of 13 samples from naive HIV-infected samples and 36 from ART-treated HIV-infected MSM using Illumina MiSeq (2x250 base pairs (bp)) (355). Members of four families of eukaryotic viruses were detected: anelloviruses, cytomegalovirus (CMV), papillomavirus, and HIV. Samples with plasma CD4 counts less than 350 cells/µl had higher detection rate for anellovirus, CMV, and human papillomavirus (HPV) than those with CD4 counts higher than 350 cells/µl, although it was not statistically significant (35.8% *vs.* 20%, p=0.27). Samples with detectable plasma HIV viremia and naive patients (not on ART) also had higher detection rate of these viruses (43.7% *vs.* 15.4%, p=0.04; and 42.8% *vs.* 17.8%, p=0.08; respectively).

1.3.3.3. Cervix virome of HIV/HPV coinfected women

In 2019, Siqueira *et al*. studied the cervix DNA virome of 19 HIV/HPV coinfected women (with a mean age of 28 years) at three time points: second trimester of pregnancy (timepoint A) and at six (timepoint B) and 12 months (timepoint C) after delivery (356). The sequencing was carried out through Illumina HiSeq 2500. The four viral families more representative were *Papillomaviridae* (86% of the reads), *Anelloviridae* (12% of the reads), *Genomoviridae* (2% of the reads), and *Herpesviridae* (0.06% of the reads). The normalized number of anellovirus reads per total reads showed a statistically

significant negative correlation with lymphocytes T CD4+ counts (r=-0.499, p=0.03) in addition to the normalized number of anellovirus reads per virus reads (r=-0.490, p=0.033) and the percentage of anellovirus reads (r=-0.525, p=0.021). Besides, 41 different HPV types were identified belonging to the *Alphapapillomavarius* genus.

1.3.3.4. Salivary virome of HIV-infected patients

Only one study has been carried out focused on salivary virome and it has been developed in HIV-infected MSM. Thus, in 2021, Guo *et al*., analysed the salivary DNA virome of HIV-infected MSM without treatment (naive) using a Illumina platform (357). The participants were split into 5 groups: non-infected (control group) (n=5), HIV RNA positive but HIV antibody negative (stage 0) (n=5), CD4>500 cells/μl (stage 1) (n=5), CD4 between 499 and 200 cells/μl (stage 2) (n=5) and CD4<200 cells/μl (stage 3) (n=5). In summary, 43 genuses were detected in all groups, and each group had its unique virus genus, except from stage 3 group (*Luz24likevirus* and *Felixounalikevirus* for stage 0 group, *Epsilonretrovirus*, *Phifllikevirus*, *Spbetakilevirus,* and *Rhadinovirus* for stage 1 group, *Simplexvirus* for stage 2 group, and *Chilikevirus* for control group). Besides, stage 1 group was more similar to control group, whereas stage 2 group was more similar to stage 3 group. The analysis of differential abundance revealed that the unique *Lymphocryptovirus* was significantly enriched in the stage 3 group (LDA value=5.32441, p=0.00859), *Retroviridae* (LDA value=4.58279, p=0.01227), *Hpunakilevirus* (LDA value=4.35265, p=0.01666), *Roseolovirus* (LDA value=4.310001, p=0.01036), and *Mimivirus* (LDA value=5.05485, p=0.01391) were more abundant in the stage 0 group and, finally, *Pbunalikevirus* (LDA value=4.37982, p=0.03503) and *Schizot4likevirus* (LDA value=4.09366, p=0.04403) showed lower abundances in HIV-infected groups compared to control group.

1.3.3.5. Faecal virome of HIV-infected patients

In 2016, Monaco *et al.* studied the enteric DNA virome of HIV-infected naive patients (n=23), HIV-infected ART-treated patients (n=21) and HIV-negative subjects (n=21) using an Illumina MiSeq platform (358). In general, sequences were most frequently assigned to bacteriophages of *Caudovirales* order or *Microviridae* family, to several eukaryotic viruses such as *Adenoviridae* and *Anelloviridae*, and to "unclassified" viruses. However, there were no statistically significant differences between the control group and HIV-infected patients for *Adenoviridae*, *Anelloviridae*, *Circoviridae*, and *Papillomaviridae* sequences. Regarding *Adenoviridae*, more sequences were observed in HIV-infected patients with CD4<200 cells/µl compared to the controls or HIV-infected patients with CD4>200 cells/µl (p=0.0026), but there were no significant differences based on therapy (p=0.0754). Moreover, *Anelloviridae* sequences significantly differed by both CD4 counts (p=0.0239) and treatment status (p=0.0282). Specifically, samples from HIV-infected patients with CD4<200 cells/µl were more likely to contain *Anelloviridae* sequences compared to HIV-infected patients with CD4>200 cells/µl (p=0.0238), but there were no significant differences between HIV-infected patients with CD4<200 cells/µl and control group (p=0.0990). Besides, *Circoviridae* was the most frequently detected eukaryotic virus (present in 75% of all samples), but there were no statistically significant differences in the number or prevalence of *Circoviridae* sequences by CD4 counts (p=0.4530 and p=0.8746, respectively) or treatment status (p=0.3984). Finally, *Papillomaviridae* sequences were found in 23% of the samples, but were not differentially represented based on CD4 counts (p=0.1115 and p=0.1253, respectively) or treatment status (p=0.5552). On the other hand, there were no significant differences in *Richness* or *Shannon index* of bacteriophage families or genuses by HIV-infection, CD4 counts, or treatment status. Furthermore, there were no significant correlations between bacteriophage and bacterial richness and diversity.

Thus, as can be observed in **Table 2.** , only one study has investigated the impact of HIV infection and ARTs on gut virome, and it has only focused on DNA

viruses. Because of that and seeing that HIV infection has a potent effect on the intestine, more studies are needed in this regard.

Table 2. Studies focused on the effects of HIV infection and ARTs on gut virome.

Author	Sample	Control (number)	HIV+ naive (number)	HIV+ ART (number)	Does HIV alter gut virome?	Is ART able to restore gut virome?
Monaco *et al.,* (2016)	Stool	21	23	21	Yes	Partially
Li *et al.,* (2011)	Plasma	11	10	-	Yes	-
Li *et al.,* (2013)	Plasma	-	35	-	-	-
Li *et al.,* (2016)	Plasma	-	-	19	-	-
Liu *et al.,* (2021)	Plasma	42	50	29	Yes	Partially
Guo *et al.,* (2021)	Saliva	5	20	-	Yes	No
Li *et al.,* (2020)	Semen	-	13	36	-	Partially
Siqueira *et al.,* (2019)	Cervix	-	19	-		

ART (antiretroviral treatment), HIV (human immunodeficiency virus).

1.3.4. Oral bacteriome composition in HIV infection

Along with gut alterations and subsequent systemic disturbances, HIV infection has also been associated with a variety of oral manifestations. Interestingly, oral microbiota seems to play a key role on such alterations (37,298,359). Opportunistic oral infections are common among HIV-infected people and have been linked to deteriorated immune function and weight loss (360–362). Some of these oral manifestations linked to oral microbiota are oral candidiasis, HIV salivary gland disease, HPV-associated oral lesions,

xerostomia, and ulcerations (363). Besides, ART itself can increase oral microbial translocation due to the inhibition of epithelial cell repair (364) and proliferation (365).

Li *et al*., 2014 reported that in comparison to HIV-negative individuals, HIV-infected patients had higher levels of total cultivable microbes in saliva, including streptococci, *Streptococcus mutants*, lactobacilli, and *Candida* (359). Again, Li *et al*., 2021 showed that α-diversity of oral microbiota of naive patients was significantly decreased compared to control group whereas ART was not able to revert this effect. Comparing naive patients to the control group, it was observed an increased abundance of *unidentified Prevotellaceae* and a decreased abundance of several groups of bacteria such as *Lactobacillus*, *Rothia*, *Lautropia*, and *Bacteroides*. Besides, ART treatment triggered an increase in *Bradhyrhizobium* (366). On the other hand, Presti *et al.*, 2018 reported that the most abundantly detected bacterial phyla in the saliva of naive patients were Bacteroidetes, Firmicutes, and Proteobacteria, with lower relative abundance of Fusobacteria, Spirochaetes, Actinobacteria, and Tenericutes. Following 24 weeks of ART, the dominant phyla remained similar and there was no significant difference either in α or in β-diversity (367). Moreover, Imahashi *et al.*, 2021 did not observe differences either in α or in β-diversity between controls, naive patients, and ART-treated patients. Besides, they described that the three major genera in the salivary microbes (*Prevotella*, *Streptococcus*, and *Veillonella* (359,367,368)) were not differentially abundant between the three groups (369).

2.HYPHOTESIS

- HIV infection has become a chronic infection thanks to the use of ARTs. However, life expectancy of HIV-infected patients, although increased, it is not the same as that of the general population. This fact is probably due to a chronic inflammation state that persists in HIV-infected patients despite ART. An altered GM favours BT and such chronic inflammatory state.

- Several studies have demonstrated that HIV infection has a significant impact on gut and oral microbiota, specifically on bacteriome. However, no concluding studies have been developed concerning HIV infection effects on virome.

- INSTIs-based treatments are the preferred choice for the treatment of naive patients. A previous work from our group (270) reported that HIV-infected patients treated with these drugs (RAL) exhibited a gut bacteriome profile more similar to that of a control non-infected population, which suggests a healthier gut.

Thus, the hypothesis of this Doctoral Thesis is that **novel INSTIs-based treatments are able to restore the effects of HIV infection on GM (both bacteriome and virome), oral bacteriome, and markers of BT, inflammation, cardiovascular risk, and gut permeability.**

3.OBJECTIVES

The main objective of this Doctoral Thesis was to deeply characterize GM composition (both bacteriome and virome) and oral bacteriome of HIV-infected patients in comparison with non-HIV-infected subjects, and to analyse the impact of INSTIs-based treatments.

More specifically, the objectives were as follows:

1. To investigate the actions of INSTIs-based therapies on the state of chronic inflammation and increased BT induced by HIV infection compared to non-infected subjects.
2. To assess the impact of HIV infection and INSTIs-based treatments on gut bacteriome compared to a non-HIV-infected population.
3. To deeply analyse the impact of HIV infection and INSTI-based treatment on gut virome composition compared to a non-HIV-infected population.
4. To study the potential associations between gut virome and gut bacteriome composition in the studied populations.
5. To evaluate the impact of HIV infection and INSTIs-based treatments on salivary bacteriome compared to a non-HIV-infected population.

4. MATERIAL AND METHODS

4.1. Patient recruitment

HIV-infected patients (naive and under ART) were recruited from the Infectious Diseases Department at Hospital Universitario San Pedro (HUSP) (Logroño, Spain) from March 2019 to February 2021. The group of HIV-infected ART-treated patients included HIV-infected patients in first line of treatment to avoid confounding effects due to previous treatments. Six of the naive patients correspond to six of the ART-treated patients recruited both before treatment and after one year of treatment. Treatment was based on INSTIs (DTG or BIC) with a backbone based on one or two NRTIs for at least one year and with viral load <20 copies/ml in the last six months (**Table 3**). All HIV-infected patients were immune responders. The presence of AIDS, mode of transmission, and coinfection with HBV and/or HCV were also registered. In case of coinfection, degree of liver fibrosis was evaluated by FibroScan® (Echosens, Paris, France) method. This method consists of the passage of a 50-megahertz wave through the liver from a small transducer placed in an intercostal space near the right love of the liver. This device measures the velocity of the wave (in meters per second) and determines the degree of liver damage. The more quickly the wave passes through the liver, the more liver damage shows the patient. The results of the measurements were converted to kilopascal (KPa) (370) and patients were classified according to the METAVIR scoring system (F0, no fibrosis; F1, portal fibrosis without septa; F2, portal fibrosis and few septa; F3, numerous septa without cirrhosis; F4, cirrhosis) (371). CD4+ T-cell, CD8+ T-cell counts, and viral load were measured using flow cytometry (NAVIOS EX, Beckman Coulter) and COBAS 6800 Analyzer (Roche Molecular Systems Inc., Branchburg, New Jersey, USA), respectively, as a clinical procedure in the HUSP. Healthy patients (non-HIV-infected patients) were also recruited as control group (n=26). Patients recruited during COVID pandemic did not report any symptoms related to COVID before the date of sample collection and were not vaccinated in the previous month of the enrolment. For both HIV-infected patients and controls, following

exclusion criteria were applied: <18 years, patients who do not sign the informed consent, pregnant women, individuals with inflammatory disease in the last 2 months, patients treated with antibiotics*, anti-inflammatory drugs, immunosuppressive drugs, statins or probiotics in the last 2 months, individuals with renal insufficiency, patients with neoplasms, individuals with history of intestinal surgery (except from appendectomy or cholecystectomy), IBD, celiac disease, chronic pancreatitis, or any other syndrome related to intestinal malabsorption (270). Patients treated with statins were excluded because it was demonstrated that this therapy can cause gut dysbiosis (372,373). Finally, weight, height, waist circumference, systolic and diastolic pressure, alcohol consumption, and smoking habits were also registered from all participants.

*Antibiotic therapy influences virome, not by affecting VLPs directly but by affecting the prokaryote host (374).

Table 3. INSTIs-based treatments used in HIV-infected patients.

INSTI	Backbone	Number of patients
Dolutegravir	Abacavir and lamivudine	10/15 (66.67%)
	Lamivudine	2/15 (13.33%)
Bictegravir	Emtricitabine and tenofovir alafenamide	3/15 (20.00%)

HIV (human immunodeficiency virus infection), INSTI (integrase strand transfer inhibitor).

This study was performed following the Helsinki Declaration and was approved by the Committee for Ethics in Drug Research in La Rioja (CEImLAR) (28 February 2019, reference number 349). All participants provided their written informed consent.

4.2. Biochemical parameters, immunological analyses, and mass spectrometry approaches

4.2.1. Plasma and serum preparation

Blood samples from HIV-infected patients were collected at HUSP while blood samples from control population were collected at Center for Biomedical Research of La Rioja (CIBIR) thanks to the help of the Head nurse from the Health Centre 7 Infantes de Lara. In all cases, individuals had 12 hours of fasting and two different commercial tubes were used in order to obtain plasma and serum from blood.

Plasma samples were collected in Vacutainer tubes treated with ethylenediamine tetraacetic acid (EDTA) (BD Vacutainer® spray coated K2EDTA Tubes). After collection, tubes were centrifuged 10 minutes at 3000g and 4°C to remove cells from plasma. Immediately, plasma was aliquoted in several Eppendorf tubes with micropipettes to avoid subsequent freeze-thaw cycles and was stored at -80°C for further analysis.

Serum samples were collected in Vacutainer tubes (BD Vacutainer® Plus Plastic Serum Tubes) which contain a gel to help the separation of the clot. After collection, tubes were leaved 30 minutes at room temperature to allow the blood to clot and then, the clot was removed by centrifugation 10 minutes at 3000 g and 4°C. Immediately, serum was aliquoted in several Eppendorf tubes with micropipettes to avoid subsequent freeze-thaw cycles and was stored at -80°C for further analysis.

4.2.2. Biochemical parameters

Serum levels of glucose, triglycerides, total cholesterol, low density lipoprotein (LDL), high density lipoprotein (HDL), glutamic oxalacetic transaminase or aspartate aminotransferase (GOT/AST), and pyruvic glutamic

transaminase or alanine aminotransferase (GPT/ALT) were measured at HUSP using an AutoAnalyzer (Cobas C702, Roche, Madrid, Spain).

4.2.3. Immunological assays: enzyme-linked immunosorbent assay and Luminex Screening Assay

To analyse markers of BT, inflammation, cardiovascular risk, and gut permeability from serum and faeces samples collected from HIV-infected patients and a healthy population, enzyme-linked immunosorbent assays (ELISAs) and Luminex Screening Assays were used. All these analyses were performed with commercially available kits and according to the manufacturer's instructions.

4.2.3.1. Enzyme-linked immunosorbent assay principle

ELISA is an immunological assay commonly used to measure antibodies, antigens, proteins, peptides, and glycoproteins in biological samples. In this Doctoral Thesis the quantitative sandwich enzyme immunoassays from Merck Millipore (Darmstadt, Germany) and from BÜHLMANN (Amherst, USA) have been used. In this type of ELISA, a specific antibody for the antigen of interest (capture antibody) is pre-coated onto a microplate. Then, standards and samples are pipetted into the wells and any antigen of interest present is bound by the capture antibody. After washing away any unbound substance, an enzyme-linked antibody specific for the antigen of interest (biotin-labelled detection antibody) is added to the wells. The next step is to remove any unbound detection antibody and, finally, a substrate solution is added to the wells. This substrate solution contains streptavidin-labelled horseradish peroxidase (HRP) (which binds to the biotin-labelled antibody) and its specific substrate. Colour is developed in proportion to the amount of antigen bound in the initial step. Colour development is stopped and its intensity is measured in a plate reader spectrophotometer at the wavelength indicated by the manufacturer (**Figure 15**) (375).
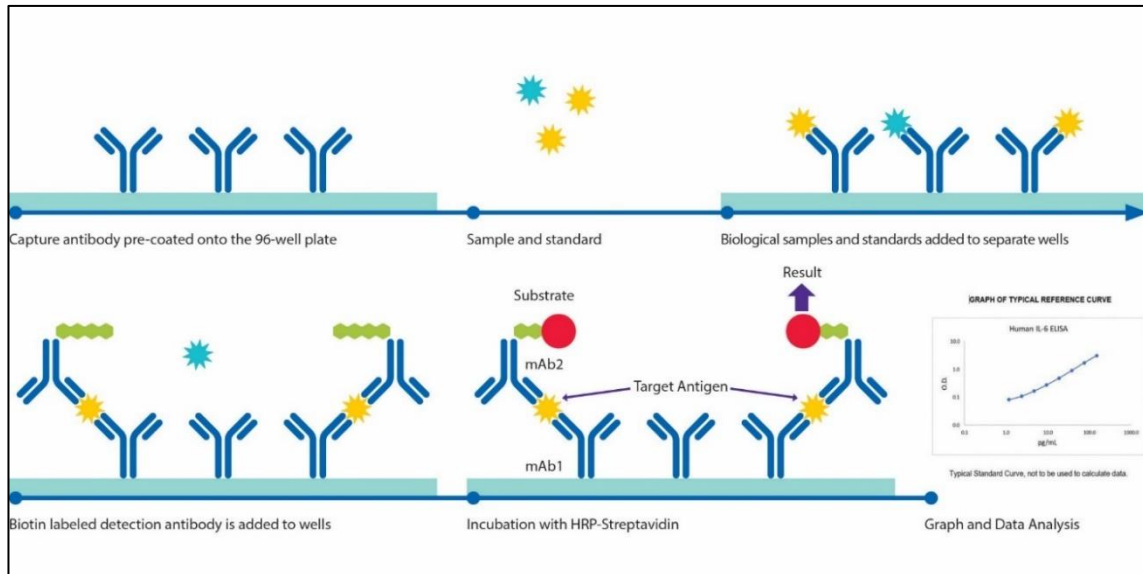
Figure 15. Illustration of how sandwich ELISA works. From Sigma-Aldrich webpage (376). ELISA (enzyme-linked immunosorbent assay), HRP (horseradish peroxidase).

Analytes measured using enzyme-linked immunosorbent assay

ELISA was performed to determine the serum levels of insulin and two markers of intestinal integrity: intestinal fatty acid binding protein (iFABP) and calprotectin in HIV-infected patients and controls. Results were measured using a POLARstar Omega plate reader spectrophotometer (BMG LABTECH). The detailed information of the assay is summarized in **Table 4**.

Table 4. Parameters measured using sandwich ELISA.

Physiological relevance	Analyte	Sample	Wavelength
Glucose metabolism	Insulin	Serum without diluting	450 nm
Gut permeability	iFABP	Serum diluted 1/250	450 nm
Gut permeability	Calprotectin	Faeces diluted 1:7500	450 nm

ELISA (enzyme-linked immunosorbent assay), iFABP (intestinal fatty acid binding protein).

The values of glucose (measured by AutoAnalyzer Cobas C702 (Roche, Madrid, Spain) and insulin levels were used to calculate the "homeostasis model assessment insulin resistance index" (HOMA-IR) as follows, according to the report by Matthews *et al.,* 1985 (377).

$$HOMA - IR\ index = \frac{fasting\ glucosa\ \left(\frac{mg}{dl}\right) \times fasting\ insulin\ \left(\frac{mU}{L}\right)}{405}$$

4.2.3.2. Luminex Screening Assay principle

A Luminex assay is a type of immunoassay that precisely measures multiple analytes in one sample. The Luminex® xMAP® technology is a bead-based immunoassay that allows the detection of up to 100 analytes simultaneously. Color-coded microspheres (beads) are internally dyed with different proportions of red and infrared fluorophores that correspond to a distinct spectral signature, or bead region. The quantification of multiple cytokines and other biomarkers in a sample provides critical information about biological processes and diseases (378).

Antibodies specific to a desired analyte are coupled to a unique bead region and are incubated with sample. After washing away unbound materials, samples are incubated with a mixture of biotinylated detection antibodies and a streptavidin-phycoerythrin (PE) reporter. Using a Luminex instrument, beads are excited by one laser (red) to determine the bead region and corresponding assigned analyte. Another laser (green) determines the magnitude of the PE-derived signal, which is proportional to the amount of analyte bound. Multiple readings are taken at each bead region, ensuring robust detection (378) (**Figure 16**).
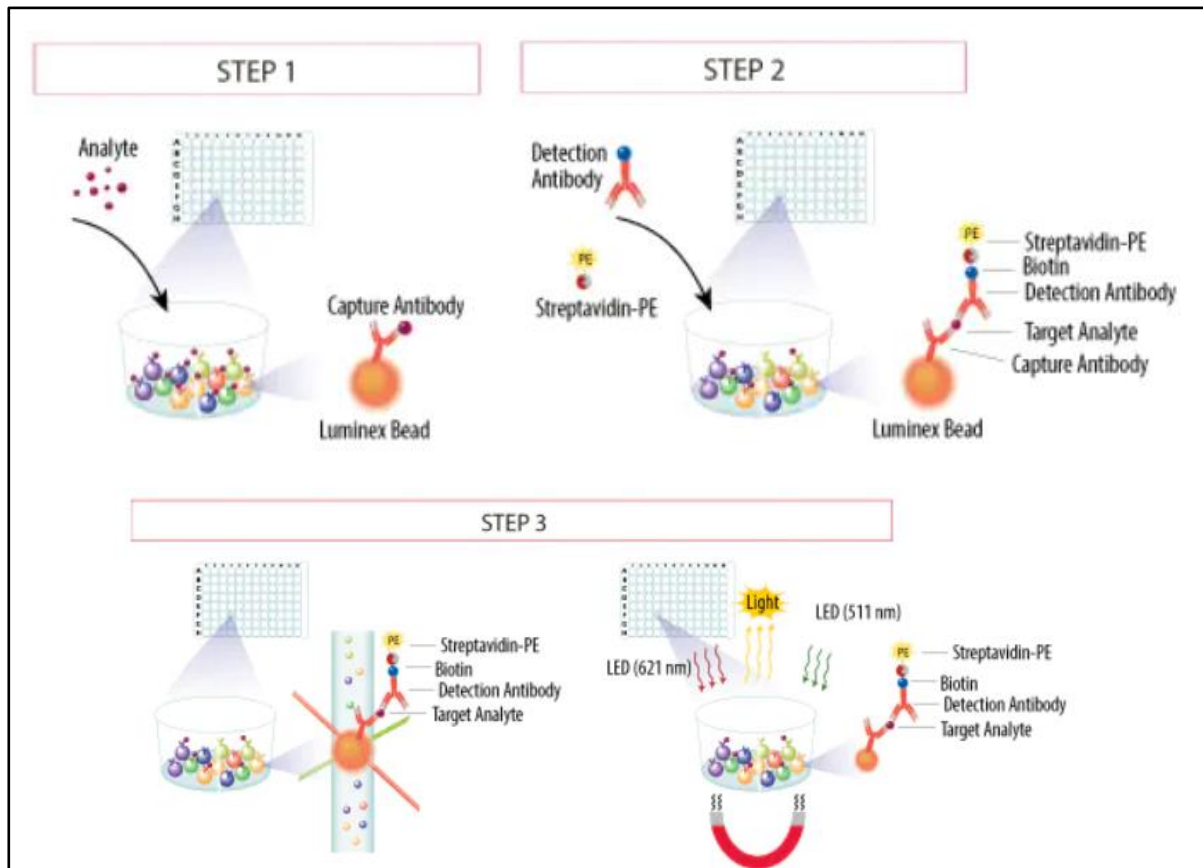
Figure 16. Illustration of how Luminex assay works. From R&D webpage (378). PE (phycoerythrin).

Analytes measured using Luminex Screening Assay

Luminex was performed to determine the levels of several markers of BT (sCD14 and LBP), inflammation markers (IL-6, interleukin 1β (IL-1β), TNF-α, and monocyte chemoattractant protein 1 (MCP1)) and cardiovascular risk markers (intracellular adhesion molecule 1 (ICAM-1), vascular cell adhesion molecule 1 (VCAM-1), and plasminogen activator protein 1 (PAI-1)) in serum of HIV-infected patients and control population. Results were measured using a Luminex® FLEXMAP 3D® (R&D Systems) located in HUSP. The detailed information of the assays is summarised in **Table 5**.

Table 5. Parameters measured using Luminex assay.

	Analyte	Sample	Wavelength
Markers of BT	sCD14	Serum diluted 1/2	Red laser: 635 nm Green laser: 532 nm
	LBP	Serum diluted 1/2	
Inflammation markers	IL-6	Serum diluted 1/200	
	IL-1β	Serum diluted 1/200	
	TNF-α	Serum diluted 1/200	
	MCP-1	Serum diluted 1/200	
Cardiovascular risk markers	ICAM-1	Serum diluted 1/200	
	VCAM-1	Serum diluted 1/200	
	PAI-1	Serum diluted 1/2	

BT (bacterial translocation), ICAM (intracellular adhesion molecule 1), IL-1β (interleukin 1β), IL-6 (interleukin 6), LBP (lipopolysaccharide binding protein), MCP-1 (monocyte chemoattractant protein 1), PAI-1 (plasminogen activator protein), sCD14 (soluble cluster of differentiation 14), TNF-α (tumour necrosis factor α), VCAM-1 (vascular cell adhesion molecule).

4.2.4. Mass spectrometry techniques

4.2.4.1. Analysis of trimethylamine N-oxide

TMAO was measured from serum samples of both HIV-infected patients and control population in the Institute of Grapevine and Wine Sciences (ICVV) (Logrono, Spain).

Firstly, 150 µl of serum were mixed with 500 µl of methanol containing internal standard (TMAO D6 0.1 ppm) in a 1.5 ml Eppendorf tube. Secondly, the mixture was vortexed for 30 seconds and centrifuged 20 min at 9000 rpm. Then, the supernatant was transferred to another 1.5 ml Eppendorf and 500 µl of MiliQ water was added. Finally, the sample was vortexed for 10 seconds and filtered with a 0.22 µm polyvinylidene fluoride (PVDF) filter over a 12x32 mm glass screw neck vial.

TMAO in samples was quantified by Ultra Performance Liquid Chromatography (UPLC, Nexera Shimadzu) coupled to a triple quadrupole (QQQ) mass spectrometer detector (SCIEX 3200QTRAP), equipped with electrospray interface (ESI). Chromatographic separation was performed on an

Acquity UPLC BEH HILIC (1.7 µm, 2.1x100 mm) column (Waters). Chromatographic conditions were as follows: eluent A 10 mM ammonium acetate in water; eluent B 10 mM ammonium acetate in water/acetonitrile (ACN) (1/10); flow 0,3 ml/min; column temperature 30 °C; injection volume 2.5 L; eluent gradient 0 min 100%B, 10 min 10% B, 11 min 10% B. Concentration of TMAO was determined from calibration curve using peak area ratio of the analyte to its deuterated internal standard (TMAO D6).

4.2.4.2. Analysis of short-chain fatty acids

Short-chain fatty acids (SCFAs) such as acetic, propanoic, isobutanoic, butanoic, isopentanoic, pentanoic, and hexanoic acid were measured from serum samples of both HIV-infected patients and control population in the ICVV.

400 µl of serum were placed in a 12x32 mm glass crimp top vial containing 120-140 mg of KCl. Then, it was added 65 µl of HCl and 400 µl of *terc*-butylethylether (tBuEtO) containing internal standards (valproic acid 0.41 ppm and heptanoic acid 0.82 mm). Vials were immediately capped with an aluminium cap with polytetrafluoroethylene (PTFE)/silicon septum and sealed. Samples were vigorously shaken at room temperature for 30 minutes and centrifuged 5 min at 4696 g. Upper organic phase was analysed by gas chromatography coupled to MS (GC-MS) using a 7890C Series gas chromatography coupled to a 7000C Series Triple Quad GC/MS triple quadrupole mass spectrometer (Agilent Technologies Inc., Wilmington, DE, USA) with a multi-purpose sampler (MPS) automatized liquid sample injection system (Gerstel GmbH & Co. KG, Múlheim an der Ruhr, Germany). Chromatography separation was performed in a capillary column TG-WaxMS (30 m x 0.25 mm intern diameter, 0.25 µl film) (Thermo Scientific™). A volume of 3 µl of sample was automatically injected into a split/splitless inlet (in splitless mode) kept at 250 °C. Helium was used as carrier gas at a flow rate of 1 ml/min in constant flow mode. The oven program was set as follows: an initial temperature of 40 °C for 5 min, increased to 150 °C at a rate of 3 °C/min, then increased to 240 °C at a rate of 15 °C/min and held at 240 °C for 10 min. Total analysis time was 57.7 min. Detection was performed with the

mass spectrometer operating in SIM mode (dwell time 75 ms) by electronic impact ionisation with 70 eV ionization energy.

GERSTEL Maestro software (Gerstel GmbH & Co. KG) and MassHunter Workstation Software: GCMS Acquisition, version B.07.02 (Agilent Technologies Inc.) were used for data acquisition. Firstly, peak identification was made by comparison of retention times and ion spectra from fatty acids real standards and spectra form the NIST mass spectral library. Analyte quantification was performed by external calibration comparing the area of each analyte in samples with calibration curves. Calibration curves for each analyte were made from the chromatographical analysis data of standard solutions at different concentrations. MassHunter Workstation Software: GCMS Qualitative Analysis, version B.07.00 (Agilent Technologies Inc.) was used for data analysis and sample quantification.

4.3. Fecal samples

4.3.1. Collection of samples

All patients and healthy volunteers received a sterile tube and the following instructions for the collecting of fecal samples:

- Urinate before defecating.
- Clean the perineal area with a sponge with soap.
- Rinse the perineal area with plenty of water.
- Dry the perineal area with a clean and unused towel.
- Defecate in a urinal or, otherwise, in a clean and dry place.
- Open the tube without touching the edges.
- Collect a small amount of stool (about the size of a walnut) that has not touched the sides of the urinal with a spoon which is situated on the inside of the tube.
- Close the tube.
- Store the tube in a fridge at 4-5 °C until its transportation to the CIBIR (within 24 hours).

4.3.2. Bacteriome

4.3.2.1. DNA extraction

Fresh stool samples were received at CIBIR, aliquoted in tubes (150-250 mg) and stored at -80 °C for further analysis. Then, stool samples were unfrozen, and faecal DNA was extracted using the Real Microbiome Fecal DNA Kit (Durviz, Valencia, Spain) following manufacturer's instructions. Then, purity, concentration, and quality were determined by a Nanodrop spectrophotometer 1000 (Thermo Scientific, USA), a Qubit 3.0 fluorometer (Thermo Fisher Scientific, MA, USA), and a Fragment Analyzer (Agilent, USA).

The Real Microbiome Fecal DNA Kit (Durviz, Valencia, Spain) has been developed for a quick and efficient purification of microbial DNA from different faecal sources for microbiota studies. The procedure includes an efficient lysis of microorganisms by a combination of heat and chemical-mechanic disruption with specific beads. Then, inhibitors are discarded by precipitation with a buffer and, finally, the sample is purified by its passage through a column, washing, and elution.

4.3.2.2. 16S rRNA gene sequencing and bioinformatic analysis

Samples were amplified for the 16S rRNA gene hypervariable regions V3-V4. Sequencing was performed using an Illumina sequencer (MiSeq, 2x300 bp, paired end) at the Genomics & Bioinformatics Core Facility at CIBIR. Computational analysis was performed with the help of the Genomics & Bioinformatics Core Facility at CIBIR.

The first step was to check the quality of reads by the quality control tool FastQC program. Then, the Qiime2 pipeline (379) was used along the bioinformatic analysis. Firstly, the raw sequences already demultiplexed (mapping the barcodes to the samples they belong) by the Illumina sequencer were denoised. In this step, performed by the DADA2 software, it takes places

the trimming of sequencing adapters and primer regions, the filtering of noisy reads, the dereplicate of our sequences to reduce repetition, the joint of paired reads, the identification of amplicon sequence variants (ASVs) at 99% of sequencing similarity, and the elimination of chimeras. Secondly, we used the SILVA database (380) trained with the V3-V4 amplification primers using during the wet-lab process to do the taxonomic assignation at 70% of confidence (**Figure 17**).

The α and β-diversity were analysed as follows: α-diversity is a measure of sample-level species richness, whereas β-diversity describes inter-subject similarity of microbial composition and facilitates the identification of broad differences between samples. The measure of α-diversity was analysed using *Observed Features*, *Chao1 index*, *Fisher's alpha*, *Pielou's index*, *Shannon index*, and *Simpson index*. *Observed features*, *Chao1 index*, and *Fisher's alpha* are based in richness, *Pielou's index* is based in evenness and *Shannon index* and *Simpson index* are based in diversity (richness + evenness). The measure of β-diversity was analysed using Bray Curtis and visualized using Principal Coordinate Analysis (PCoA) by R software (version 4.0.5) and R Studio (version 1.4.1105). Finally, the analysis of the differential composition of microbiomes was carried out with the ANCOM methodology (381) at phylum, order, and genus taxonomic levels. This methodology accounts for the underlying structure in the data and its widely used for comparing the composition of microbiomes in two or more populations, with no assumptions of population distribution.
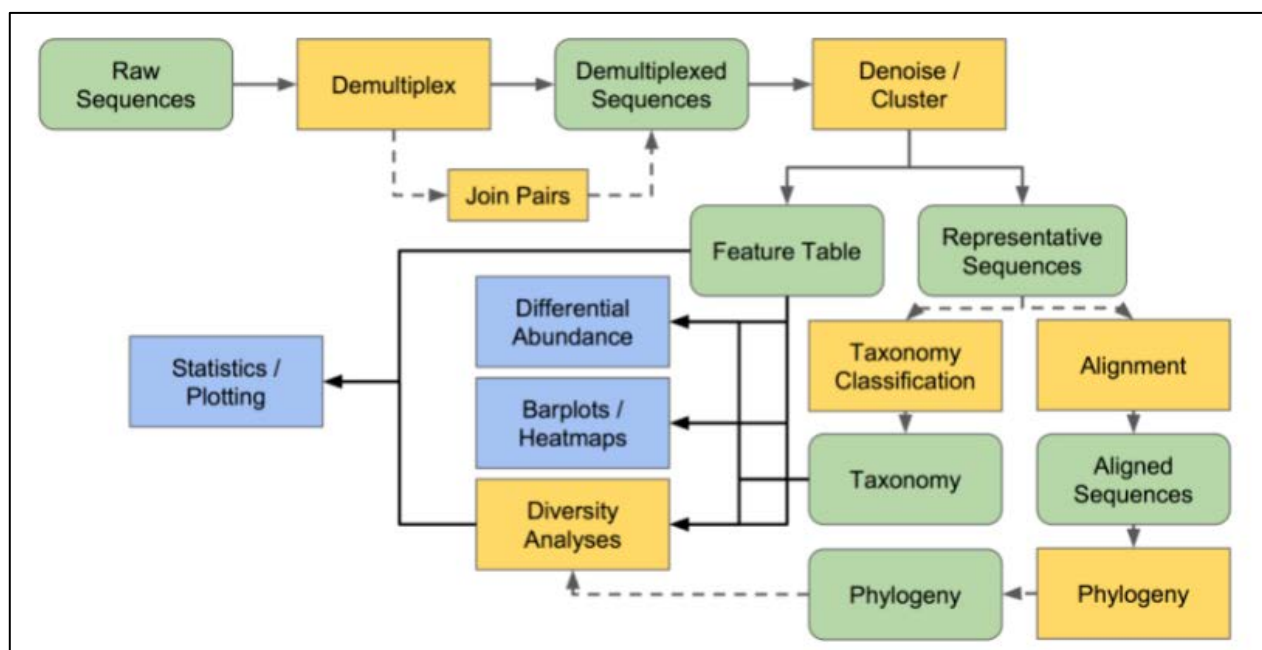
Figure 17. Workflow for examining amplicon sequence data. From Qiime2 webpage (379).

4.3.3. Virome

4.3.3.1. DNA and RNA extraction

Fresh stool samples were received at CIBIR, collected, aliquoted in tubes with O-ring caps (45-55 mg) and stored at -80 ºC for further analysis. Later, stool samples were thawed and fecal viral DNA and RNA were extracted using the NetoVIR protocol (382). To carry out this procedure, I moved to the Laboratory of Viral Metagenomics of the Rega Institute (KU Leuven, Belgium), where this protocol was previously developed. The aliquots were suspended in sterile dPBS (10%) and homogenized using the MINILYS homogenizer (Bertin Technologies) for 1 min at 3000 rpm. Homogenates were centrifuged for 3 min at 17000 g and filtered using a 0.8 µm polyethersulfone (PES) filter (Sartorius). Filtrates were treated with micrococcal nuclease (New England Biolabs) and benzonase (Novagen) at 37 °C for 2h. Viral nucleic acids were extracted using the QIAMP® Viral RNA mini kit (Qiagen, Venlo, Netherlands) without addition of carrier RNA to the lysis buffer. Subsequently, random amplification was performed using a modified version of the WTA2 kit (Sigma-Aldrich) with the following parameters: 94 °C for 2 min, 17 cycles of 94 °C for 30 sec, and 70 °C for 5 min. The WTA2 products were purified using the MSB Spin PCRapace kit (Stratec Molecular).

Quantification of purified product was performed using Qubit™ dsDNA HS Assay Kit with the use of a Qubit 2.0 fluorometer (Thermo Fisher Scientific, MA, USA). Sequencing libraries were prepared using the Nextera XT DNA Library kit (Illumina). Sizes of the libraries were checked with the Bioanalyzer 2100 using the High Sensitivity DNA kit (Agilent Technologies, USA) (**Figure 18**).
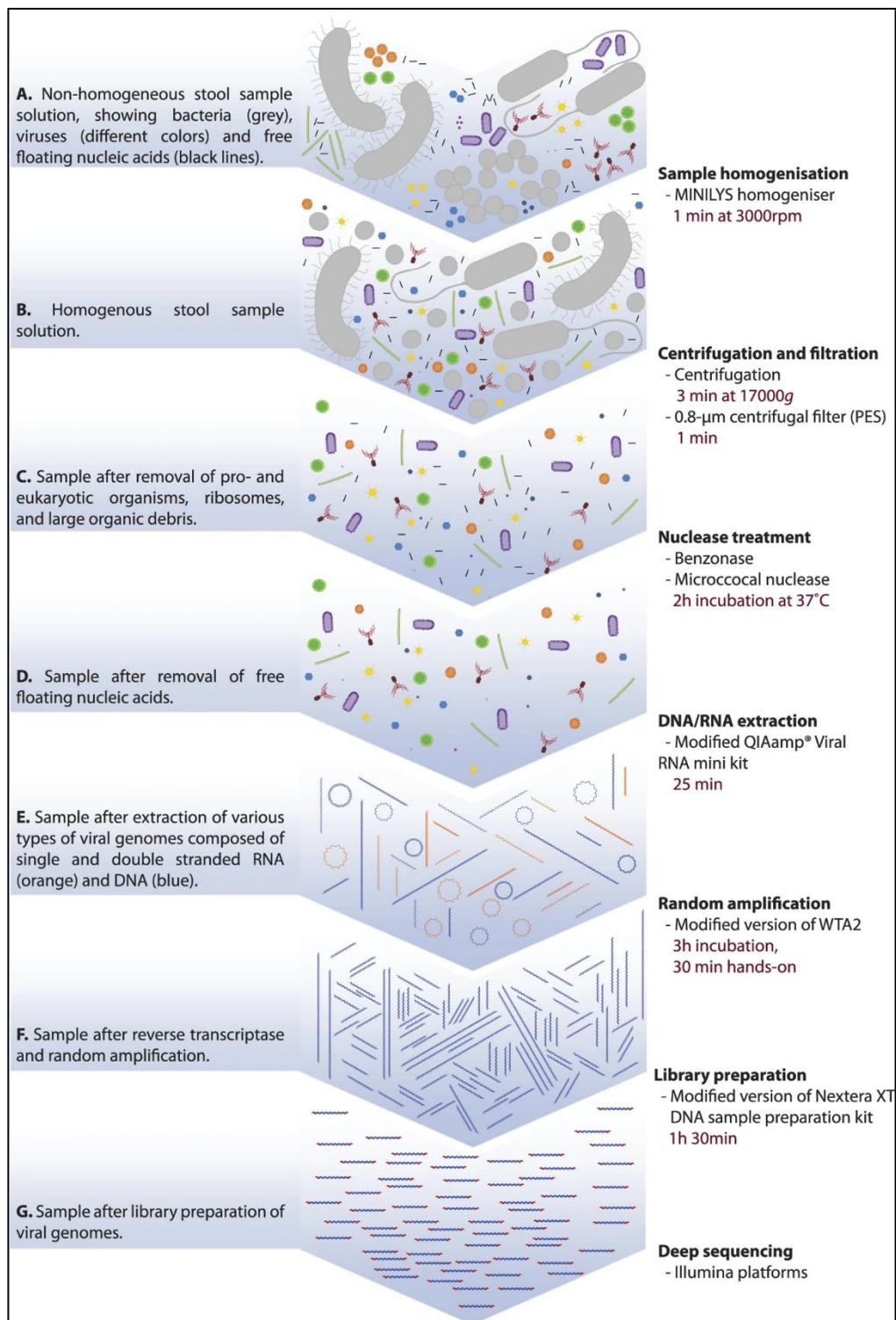
Figure 18. Workflow of NetoVIR protocol. From Conceição-Neto *et al.*, 2015 (383).

4.3.3.2. Sequencing and bioinformatic analysis

Sequencing was performed using NextSeq 500 high-throughput Illumina platform (2x150 bp paired-end, Nucleomics Core facility, KU Leuven, Belgium). Computational analysis was performed following ViPER protocol (384). Ambiguous bases, low-quality reads, primers, and adapter sequences were removed with Trimmomatic (v0.39) (385). Sequencing mapping to the "contaminome" (coming from the sequencing of the four negative control (PBS) included during the extraction procedure) were removed using Bowtie2 (v2.4.2) in "very-sensitive" mode (386).

Quality-controlled reads were *de novo* assembled into a set of contigs with MetaSPAdes (v3.15.3) using 21, 33, 55 and 77 k-mer length (387). A set of non-redundant scaffolds was obtained by clustering the contigs with a length greater than 500 bp at 95% average nucleotide identity and 85% coverage using CheckV's clustering scripts (388). Instead of calculating abundances by mapping the quality-filtered reads to the complete set of non-redundant scaffolds, reads were only mapped against the representatives of the cluster containing a scaffold from that sample to avoid false-positive detection of closely related sequences. Abundances per sample were obtained by mapping the quality-controlled reads back to the set of representative scaffolds using bwa-mem2 (v2.2.1) (389). Representative scaffolds with a horizontal coverage of 70% or higher were kept for further analyses.

Eukaryotic viruses

Eukaryotic viruses were identified and classified by homology-based approaches. The representative scaffolds set was compared against the National Center for Biotechnology Information (NCBI) nucleotide database using BLASTN (v2.11.0, e-value ≤ 1e-10) (390), and against a non-redundant protein sequence database using DIAMOND (v.2.0.13, sensitive mode) (391) (nonredundant [nr] and nucleotide [nt] databases downloaded from NCBI) and CAT (v5.2.3) (392).

Classification was based on the principle of lowest common ancestor as determined by the ktClassifyBLAST module in KronaTools (v2.8) (393).

Prokaryotic viruses

Prokaryotic viruses (bacteriophages) were identified using Virsorter2 (v2.2.3) with score $\geq$ 0.5 (394). The completeness of these contigs was determined with CheckV (v0.8.1) (388). Bacteriophages were selected for further analysis based on a combination of Virsorter2 identification and $\geq$ 50% completeness. Classification was performed as described in the previous section. Additionally, taxonomic classification was expanded using marker gene approaches as determined by Cenote-Taker2 (v2.1.3) (395). The lifestyle of bacteriophages was determined based on the appearance of lysogeny-specific genes. These genes were predicted using the functional annotation module of Cenote-Taker2 (395) and can be found in **Table 6**. The host of bacteriophages was determined using Random Forest Assignments of Hosts (RaFAH, v0.3). Bacterial hosts were predicted on phylum level with score $\geq$ 0.14 (396).

Table 6. Predicted lysogenic-specific genes and their functions used for the prediction of the lifestyle of bacteriophages.

Lysogenic-specific genes	Function
Integrase or INTEGRASE	Integrase
Phage_integrase_family_protein	Integrase
SITE_SPECIFIC_RECOMBINASE_XERD	Integrase
Excisionase_from_transposon_Tn916	Excisionase
DNA_binding_domain,_excisionase_family	Excisionase
Repressor_protein_CI	Repressor
P22_AR_repressor_domain_protein	Repressor
REPRESSOR_PROTEIN	Repressor
Cro/C1-type_HTH_DNA-binding_domain	Repressor
Phage_regulatory_protein_Rha_(Phage_pRha)	Repressor
Uncharacterized_ATPase,_putative_transposase	Transposase
MU TRANSPOSASE	Transposase
PROPHAGE_LAMBDALM01_ANTIGEN	Prophage domain
Mu-like_prophage_DNA_circulation_protein	Prophage domain
Mu-like_prophage_I_protein	Prophage domain
ParB protein	Lysogenic recombination
CHROMOSOME_PARTITIONING_PROTEIN_PARB	Lysogenic recombination

CrAss-like bacteriophages

A custom database of 998 CrAss-like bacteriophages was created by combining the CrAss-like genomes of 3 large datasets. We found 55 genomes in Refseq, 249 genomes in Guerin *et al*., 2028 (203), and 694 genomes in Yutin *et al.*, 2018 (397). Bacteriophages selected in previous section were compared against this custom nucleotide database using BLASTN (v2.11.0, e-value ≤ 1e-5, %coverage ≥ 10000 bp) to identify CrAss-like viruses (390) .

Statistical analysis

The α and β-diversity were analysed using phyloseq (398). The measure of α-diversity was analysed using *Observed Features*, *Fisher's alpha*, *Shannon index*, *Simpson index*, and *Pielou's index* with the plot_anova_diversity function of the microbiomeSeq package. Besides, correlations between α-diversity from

bacteriome and phages was analysed using rcorr and corrplot packages from R. The measure of β-diversity was analysed using Bray Curtis (ordinate function from phyloseq package) and visualized using PCoA (plot_ordination function from phyloseq package) and statistically significant differences were evaluated with PERMANOVA (adonis2 and pairwise.adonis functions from the vegan package). Finally, the analysis of the differential composition of microbiomes was carried out with DESeq2 at phylum and class taxonomic levels regarding phages and at phylum, family, and genus taxonomic levels regarding eukaryotic viruses. When required, statistical significance was evaluated with the adequate non-parametric test. All these analyses were performed using R (v3.6.3) and R Studio (v1.2.1335).

4.4. Saliva samples

4.4.1. Collection of samples

All patients and healthy volunteers received a sterile 50 ml Falcon and the following instructions for the collecting of saliva samples:

- Stay at least 1 hour without eating.
- Rinse the mouth.
- Wait 10 minutes.
- Wash hands and put on gloves.
- Collect the sample (approximately 2 ml) spitting inside de Falcon.
- Store the tube in fridge at 4-5 °C until its transportation to the CIBIR (within 24 hours).

4.4.2. DNA extraction

Fresh saliva samples were received at CIBIR, aliquoted in tubes (approximately 500 µl) and stored at -80 °C for further analysis. Then, saliva samples were unfrozen, and saliva DNA was extracted using a modified version of the DNeasy® Blood and Tissue kit (Qiagen, Venlo, Netherlands). Then, purity,

concentration, and quality were determined by a Nanodrop spectrophotometer 1000 (Thermo Fisher Scientific, MA, USA), a Qubit 3.0 fluorometer (Thermo Fisher Scientific, MA, USA), and a Fragment Analyzer (Agilent, USA).

This protocol has been adapted by customers from the DNeasy animal and cell protocol for the purification of DNA from fresh or frozen animal saliva. The procedure includes a homogenisation and an efficient lysis of microorganisms by a combination of heat and chemical disruption. Then, the sample is purified by its passage through a column, washing, and elution.

4.4.3. 16S rRNA gene sequencing and bioinformatic analysis

The same procedure used for sequencing the bacteriome of faeces samples already aforementioned has been carried out for the 16S rRNA gene sequencing of salivary samples (section 4.3.2.2).

4.5. Statistical analysis

Results are presented as mean ± standard error of the mean (SEM) for quantitative variables and as percentage for qualitative variables. Boxplots indicates the median, the first and third quartile, and the minimum and maximum values. Categorical variables were analysed using the Chi-square or Fisher's exact test. Normal distribution of quantitative variables was checked using the Shapiro-Wilk test. Comparison between two groups was performed using unpaired t test or U-Mann Whitney depending on the normality of the data. Besides, in the case of longitudinal studies, the comparison between two groups was performed by paired t test or Wilcoxon regarding the normality of the data. Comparison between three or more groups was analysed using ANOVA followed by Tukey post-hoc regardless the normality of the data, considering that parametric tests are robust enough to be applied to non-parametric samples. Relationships between variables were analysed by Pearson or Spearman depending on the normality of the data. P values < 0.05 and false discovery rates

(FDRs) < 0.05 were considered as statistically significant. Statistical analysis was performed using GraphPad Prism 8 (GraphPad Prism®, La Jolla, California, USA), R software (version 4.0.5), and R Studio (version 1.4.1105).

Figure 19 summarizes all the steps carried out in the present Doctoral Thesis.
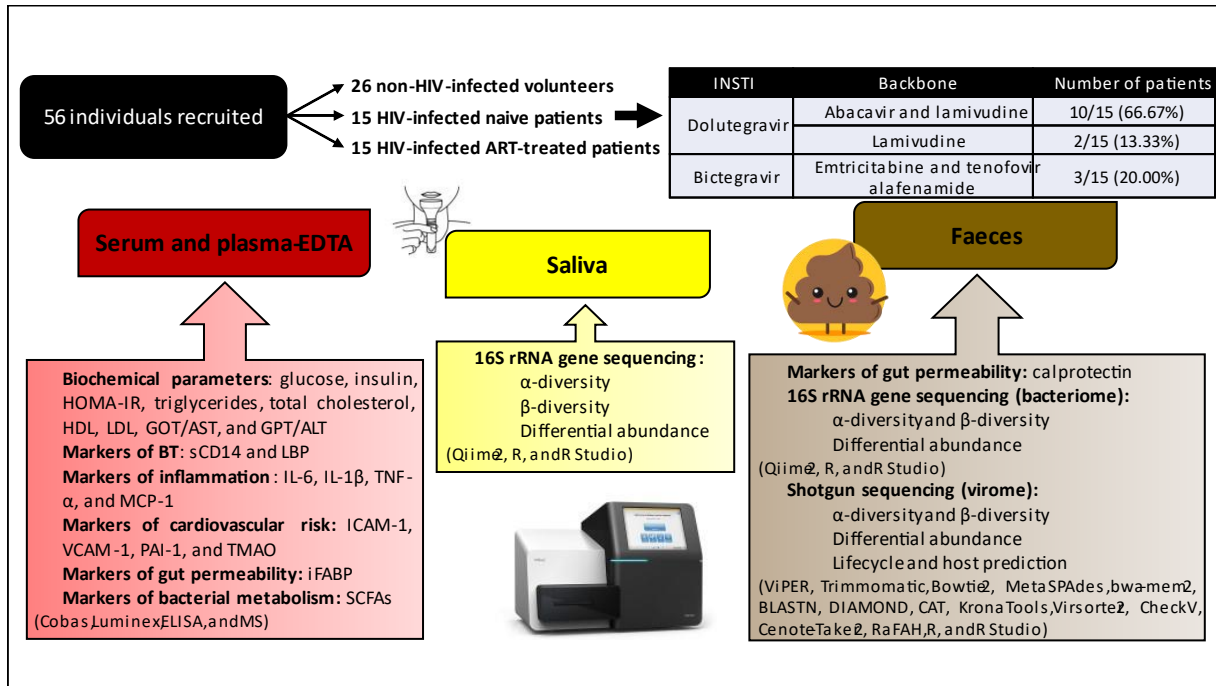
Figure 19. Workflow of the present Doctoral Thesis. Original contribution made with PowerPoint. ART (antiretroviral treatment), EDTA (ethylenediamine tetraacetic acid), ELISA (enzyme-linked immunosorbent assay), GOT/AST (glutamic oxalacetic transaminase or aspartate transaminase), GPT/ALT (pyruvic glutamic transaminase or alanine aminotransferase), HDL (high density lipoprotein), HIV (human immunodeficiency virus), HOMA-IR (homeostasis model assessment insulin resistance index), ICAM-1 (intracellular adhesion molecule 1), iFABP (intestinal fatty acid binding protein), IL-1β (interleukin 1β), IL-6 (interleukin 6), INSTIs (integrase strand transfer inhibitors), LBP (lipopolysaccharide binding protein), LDL (low density lipoprotein), MCP-1 (macrophage chemoattractant protein 1), PAI-1 (plasminogen activator protein 1), RaFAH (Random Forest Assignments of Host), rRNA (ribosomal ribonucleic acid), sCD14 (soluble cluster of differentiation 14), SCFAs (short chain fatty acids), TMAO (trimethylamine N-oxide), TNF-α (tumor necrosis factor α), VCAM-1 (vascular cell adhesion molecule 1).

5.RESULTS

5.1.   Patient characteristics

Table 7 shows the main characteristics of the recruited population. Viral load of naive patients was 622,252.9 ± 341,039.3 copies/ml, whereas INSTIs-treated patients showed indetectable viral load (<20 copies/ml), as expected. INSTIs-treated patients showed nadir CD4 counts of 526.53 ± 56.30 cells/µl. The average time under treatment was 33.27 ± 5.04 months. Statistically significant differences were observed between the naive group and INSTIs-treated patients in CD4 levels (p<0.01) and CD4/CD8 ratio, both higher in the INSTIs-treated group. Statistically significant differences were also observed between the control and the naive group in terms of gender (p<0.01), age (p<0.05), systolic blood pressure (p<0.05), diastolic blood pressure (p<0.05), and smoking habits (p<0.05). In fact, males were less represented in the control group (34.62%) in contrast to HIV-infected patients (80.00% and 86.67% in naive and INSTIs-treated patients, respectively). Mean age of the control group was higher than that observed in the naive group. However, no differences were observed among the controls and INSTIs-treated patients or among the naive and INSTIs-treated patients. Both systolic and diastolic blood pressure were higher in the naive group compared to the control group although no differences were observed when the controls were compared to INSTIs-treated patients and among both HIV-infected groups. Of note, none of the naive HIV-infected patients suffered from hypertension (based on clinical records). Thus, these differences could be explained as "white coat hypertension" generated in those patients that have just received the news of being HIV-positive. Smoking habits were also higher in the naive group and in INSTIs-treated group compared to the control group (11.54% *vs.* 46.67% and 66.67%, respectively). No differences were observed either in the mode of transmission, or in AIDS events (only one naive patient suffered from it), or in the coinfection with virus C or B (only two INSTIs-treated patients presented coinfection with virus C and a low grade of fibrosis of F0/F1).

Table 7. Characteristics of healthy uninfected controls and HIV-infected patients (naive and under INSTIs-based treatment).

	Control	Naive	INSTIs-treated	p value
Number of patients	26	15	15	-
Gender (men)	9/26 (34.62%)	13/15 (86.67%) **	12/15 (80.00%) **	0.002
Age (years)	43.58±2.31	33.87±2.85 *	43.67±3.39	0.033
BMI (kg/m²)	24.30±0.69	23.23±1.05	23.51±0.85	0.616
Waist circumference (cm)	85.35±2.55	83.83±2.86	85.13±2.15	0.916
Systolic blood pressure (mmHg)	120.58±2.76	135.67±5.67 *	129.73±6.02	0.050
Diastolic blood pressure (mmHg)	72.19±1.94	81.87±3.31 *	77.80±3.24	0.035
Alcohol active	3/26 (11.54%)	0/15 (0.00%)	1/15 (6.67%)	0.578
Smoking active	3/26 (11.54%)	7/15 (46.67%) *	10/15 (66.67%) ***	0.001
CD4 (cells/µl)	-	464.07±76.46	850.53±101.68	0.006
Nadir CD4 (cells/ µl)	-	464.07±76.46	526.53 ± 56.30	0.517
CD4/CD8 ratio	-	0.53±0.13	0.84±0.10	0.027
Mode of transmission	-	HS: 6/15 (40.00%)	HS: 7/15 (46.67%)	0.716
	-	MSM: 9/15 (60.00%)	MSM: 7/15 (46.67%)	
	-	Parenteral: 0/15 (0.00%)	Parenteral: 1/15 (6.66%)	
AIDS	-	1/15 (6.67%)	0/15 (0.00%)	1
Coinfection with virus C	-	0/15 (0.00%)	2/15 (13.33%)	0.483
Coinfection with virus B	-	0/15 (0.00%)	0/15 (0.00%)	1

Qualitative variables are represented as absolute number (percentage), while quantitative variables are represented as mean ± standard error mean. P value refers to the comparison between two (naive *vs.* INSTIs) or three (control *vs.* naive *vs.* INSTIs) groups, as appropriate. Asterisks indicate statistically significant differences with respect to control group (*p<0.05, **p<0.01, and ***p<0.001). AIDS (acquired immunodeficiency syndrome), BMI (body mass index), HIV (human immunodeficiency virus), HS (heterosexual), INSTIs (integrase strand transfer inhibitors-based treatment), MSM (men who have sex with men).

On the other hand, **Table 8** shows the biochemical characterization of the population recruited for this study. Glucose levels and the insulin resistance index, the HOMA-IR, were significantly higher in the naive group compared to the control (p<0.05). However, differences were not observed between the controls and INSTIs-treated group, suggesting that INSTIs-based treatment ameliorates this metabolic disturbance induced by HIV. Besides, triglyceride levels were higher in HIV-infected patients, being more potent in those naive participants. Although no statistically significant differences were observed in cholesterol

levels, a significant reduction on HDL was only observed in naive patients (p<0.001 *vs.* control) but disappeared in INSTIs-treated HIV-infected patients.

Table 8. Biochemical parameter of healthy, uninfected controls, and HIV-infected patients.

	Control	Naive	INSTIs-treated	p value
Glucose (mg/dl)	87.64±1.77	94.73±2.42 *	93.00±2.20	0.039
Insulin (µU/ml)	9.25±1.54	13.16±1.78	9.90±0.57	0.190
HOMA-IR	2.03±0.33	3.40±0.52 *	2.19±0.16	0.030
Triglycerides (mg/dl)	73.28±5.21	124.47±14.95 **	117.87±17.73 *	0.004
Cholesterol (mg/d)	184.40±5.66	160.27±8.70	179.87±8.76	0.065
HDL (mg/dl)	62.42±3.83	39.53±2.77 ***	51.47±3.76	0.001
LDL (mg/dl)	110.26±4.26	95.93±7.57	99.00±6.47	0.167
GOT/AST (U/L)	20.88±1.62	21.29±1.74	18.86±1.25	0.607
GPT/ALT (U/L)	18.68±1.60	23.00±2.29	18.43±1.72	0.211

Variables are represented as mean ± standard error mean. P value refers to the comparison between three groups (control *vs.* naive *vs.* ART). Asterisks indicated statistically significant differences with respect to control group (*p<0.05, **p<0.01, and ***p<0.001). GOT/AST (glutamic oxalacetic transaminase or aspartate aminotransferase), GPT/ALT (pyruvic glutamic transaminase or alanine aminotransferase), HDL (high density lipoprotein), HOMA-IR (homeostatic model assessment-insulin resistance), INSTIs (integrase strand transfer inhibitors-based treatments), LDL (low density lipoprotein).

5.2. Bacterial translocation, inflammation, cardiovascular risk, and gut permeability markers

Figure 20 shows the results obtained from the analysis of BT, inflammation, and cardiovascular risk markers in the studied population. HIV infection was accompanied by a significant increase in BT (p<0.05 and p<0.001 for LBP and sCD14 respectively) (**Figure 20A**), although this increase was completely abolished after one year of INSTI-based treatment (**Figure 20B**) reaching statistical significance among the naive and INSTIs-treated patients (p<0.01 and p<0.001 for LBP and sCD14 respectively). No differences were observed either in IL-6 or in TNF-α, well-known markers of inflammation (**Figure 20C**). However, although no significant differences were observed on TNF-α levels when all HIV-infected patients were analysed together, when they were split into two groups depending on ART regimen (naive *vs.* INSTIs), a significant

increase was observed in naive patients ($p<0.05$) that was completely reversed in those patients under INSTIs-based regimen (**Figure 20D**). Regarding the analysis of cardiovascular risk markers, no significant differences were observed with any of the parameters analysed when the control group was compared with all HIV-infected patients analysed together (**Figure 20E**). However, when HIV-infected patients were separated into a naive group and a INSTIs-treated group, the naive group presented higher levels of VCAM-1 and PAI-1 reaching statistical significance ($p<0.001$ in both cases) while no differences were observed on ICAM-1 and TMAO. The increases observed in VCAM-1 and PAI-1 were clearly reversed in INSTIs-treated group ($p<0.001$ regarding VCAM-1 and $p<0.01$ regarding PAI-1, INSTIs *vs.* naive) and, consequently, no differences were observed when the INSTIs-treated patients were compared to uninfected volunteers (**Figure 20F**).
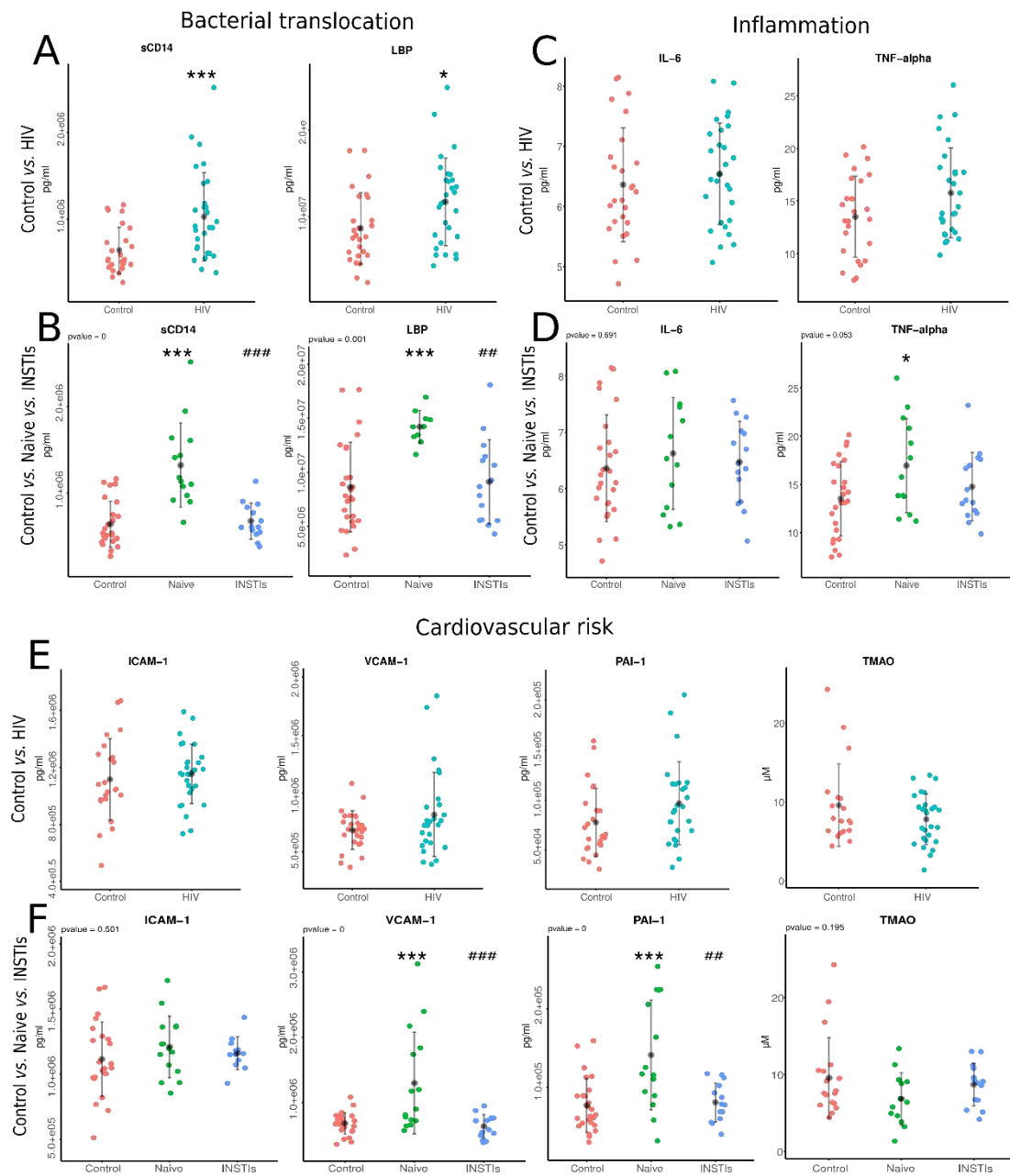
Figure 20. Levels of BT (**A** and **B**), inflammation (**C** and **D**), and cardiovascular risk markers (**E** and **F**) in the studied population. *p<0.05 *vs.* control, ***p<0.001 *vs.* control, ##p<0.01 *vs.* INSTIs, and ###p<0.001 *vs.* INSTIs. HIV (human immunodeficiency virus), ICAM-1 (intracellular adhesion molecule 1), IL-6 (interleukin6), INSTIs (integrase strand transfer inhibitors-based treatment), LBP (lipopolysaccharide binding protein), PAI-1 (plasminogen activator protein 1), sCD14 (soluble cluster of differentiation 14), TMAO (trimethylamine N-oxide), TNF-alfa (tumor necrosis factor α), VCAM-1 (vascular cell adhesion molecule 1).

In line with these results, we carried out a small pilot study in which six naive patients were recruited and samples were also collected after one year under treatment. Thus, we carried out a longitudinal approach and, although the sample size was quite small (n=6), the results revealed that systemic levels of VCAM-1 and PAI-1 were significantly reduced after the treatment (p<0.05 in both cases *vs.* naive), corroborating the potent effect of INSTIs-based treatments on these cardiovascular markers (**Figure 21**).
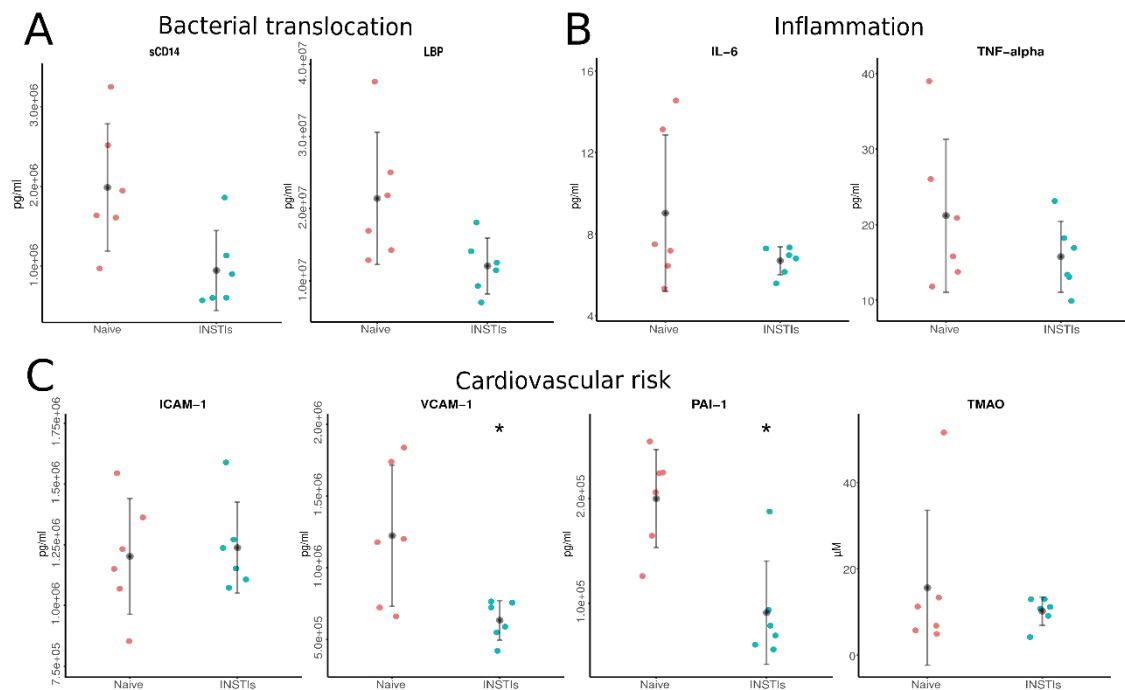
Figure 21. Levels of BT (**A**), inflammation (**B**), and cardiovascular risk markers (**C**) comparing INSTIs-treated patients before and after one year of treatment. *p<0.05 *vs*. control. ICAM-1 (intracellular adhesion molecule 1), IL-6 (interleukin6), INSTIs (integrase strand transfer inhibitors-based treatment), LBP (lipopolysaccharide binding protein), PAI-1 (plasminogen activator protein 1), sCD14 (soluble cluster of differentiation 14), TMAO (trimethylamine N-oxide), TNF-alfa (tumor necrosis factor alfa), VCAM-1 (vascular cell adhesion molecule 1).

We also investigated the effects of DTG and BIC separately. **Figure 22** indicates that DTG exerted a more powerful reducing effect on BT than BIC, but these results could also be due to the significant higher number of patients included in this group. Thus, it is difficult to extract general conclusions in this concern.
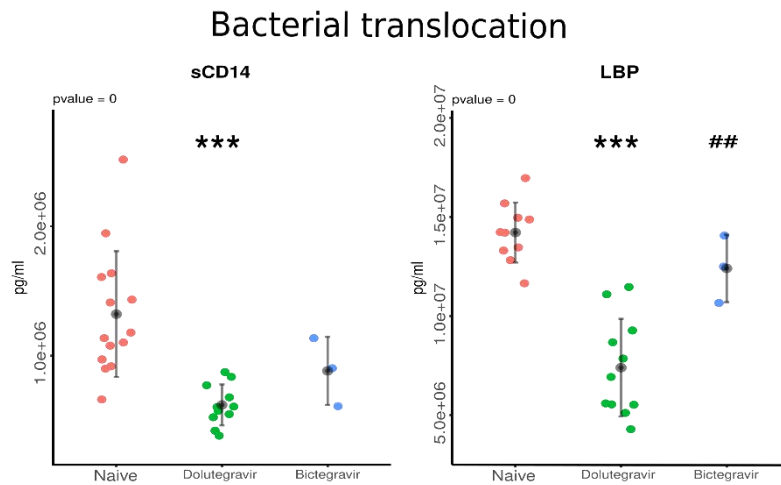
Figure 22. Levels of BT comparing naive patients to patients taking DTG and BIC. ***p<0.001 *vs.* naive and ##p<0.01 *vs.* DTG. BIC (bictegravir), DTG (dolutegravir), LBP (lipopolysaccharide binding protein), sCD14 (soluble cluster of differentiation 14).

Finally, **Figure 23** shows that HIV infection was accompanied by a statistically significant increase in faecal calprotectin levels, a marker of gut permeability (p<0.01 *vs.* control). Furthermore, a statistically significant increase in faecal calprotectin levels was only observed in naive patients (p<0.05 *vs.* control), that was not present in INSTIs-treated patients (p=0.291). However, considering iFABP, another marker of gut permeability, differences were not observed.
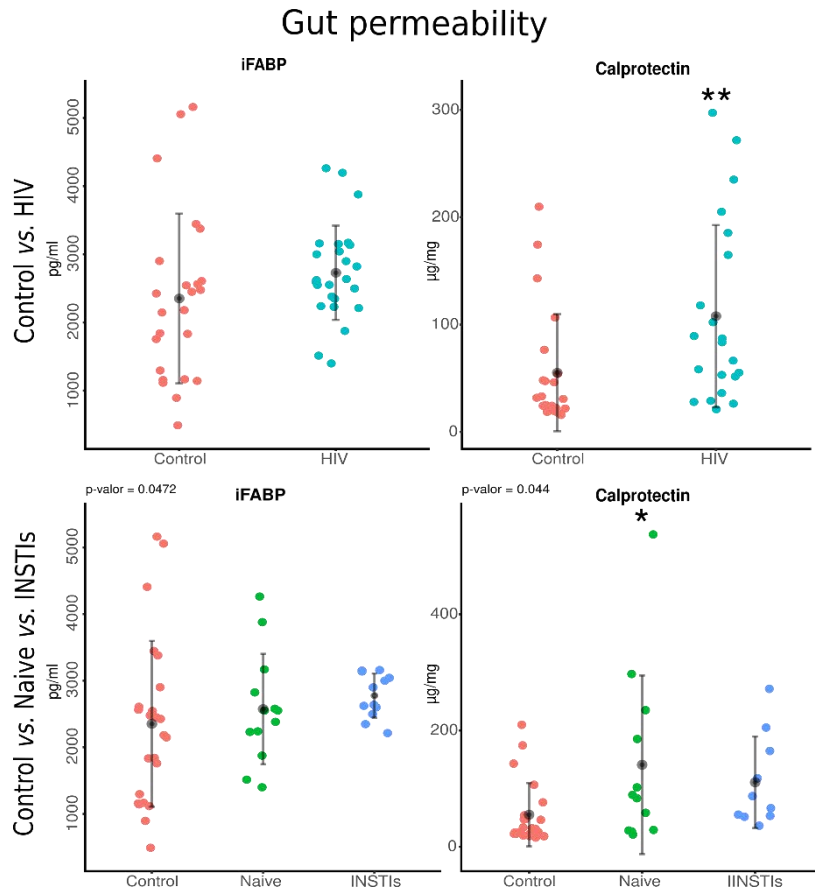
Figure 23. Levels of iFABP and calprotectin in the studied population. *p<0.05 *vs.* control and **p<0.01 *vs.* control. HIV (human immunodeficiency virus), iFABP (intestinal fatty acid binding protein), INSTIs (integrase strand transfer inhibitors-based treatment).

5.3. Gut derived short chain fatty acids

A statistically significant reduction in serum concentration of acetic acid, butanoic acid, pentanoic acid, and hexanoic acid was observed in HIV-infected population compared to controls (p<0.05-p<0.001) (**Figure 24A**). This reduction was independent of ART as can be observed in **Figure 24B**, except for acetic acid, where ART seems to reverse such the decrease induced by HIV infection as no significant differences were observed when compared with the controls.
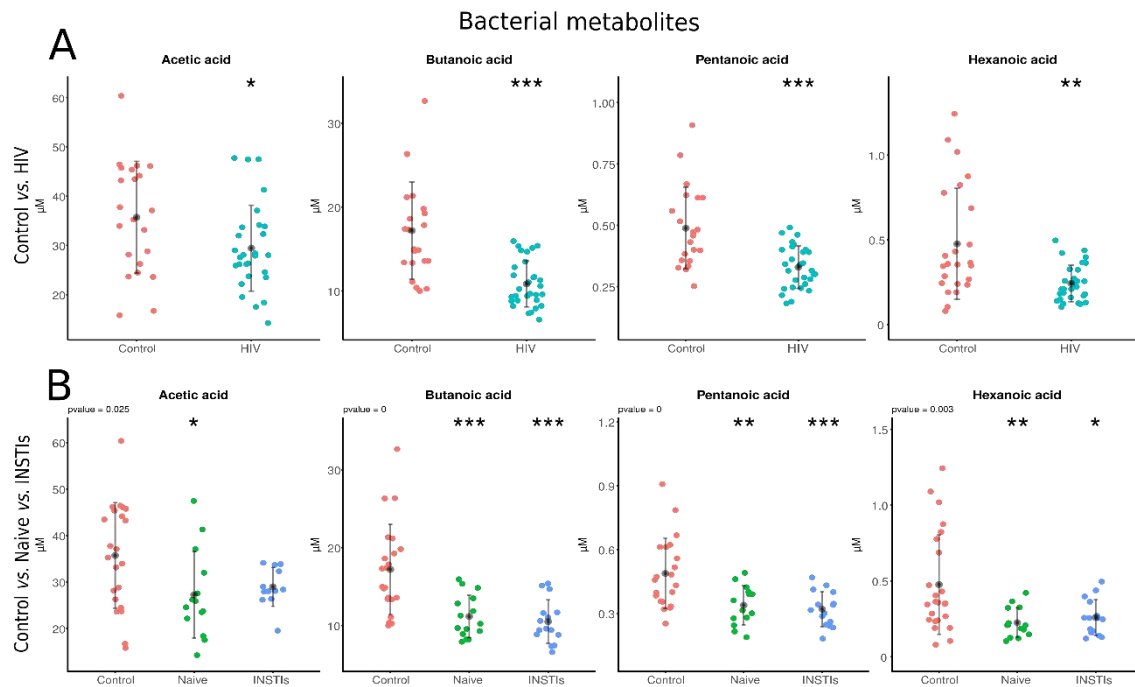
Figure 24. Levels of bacterial metabolites in the studied population. *p<0.05 *vs.* control, **p<0.01 *vs.* control, and ***p<0.001 *vs.* control. HIV (human immunodeficiency virus), INSTIs (integrase strand transfer inhibitors-based treatments).

5.4. Gut bacterioma diversity and composition

5.4.1. Alpha diversity of gut bacteriome

A significant decrease in *Observed features* and *Chao1* index was observed in naive group compared to controls (p<0.05 in both cases). Such decrease was not present in INSTIs-treated group when compared to controls, suggesting some kind of reversion due to the treatment (**Figure 25**). No statistically significant differences were observed either in *Fisher's alpha*, or in *Pielou's evenness*, or in *Shannon index*, or in *Simpson index*.
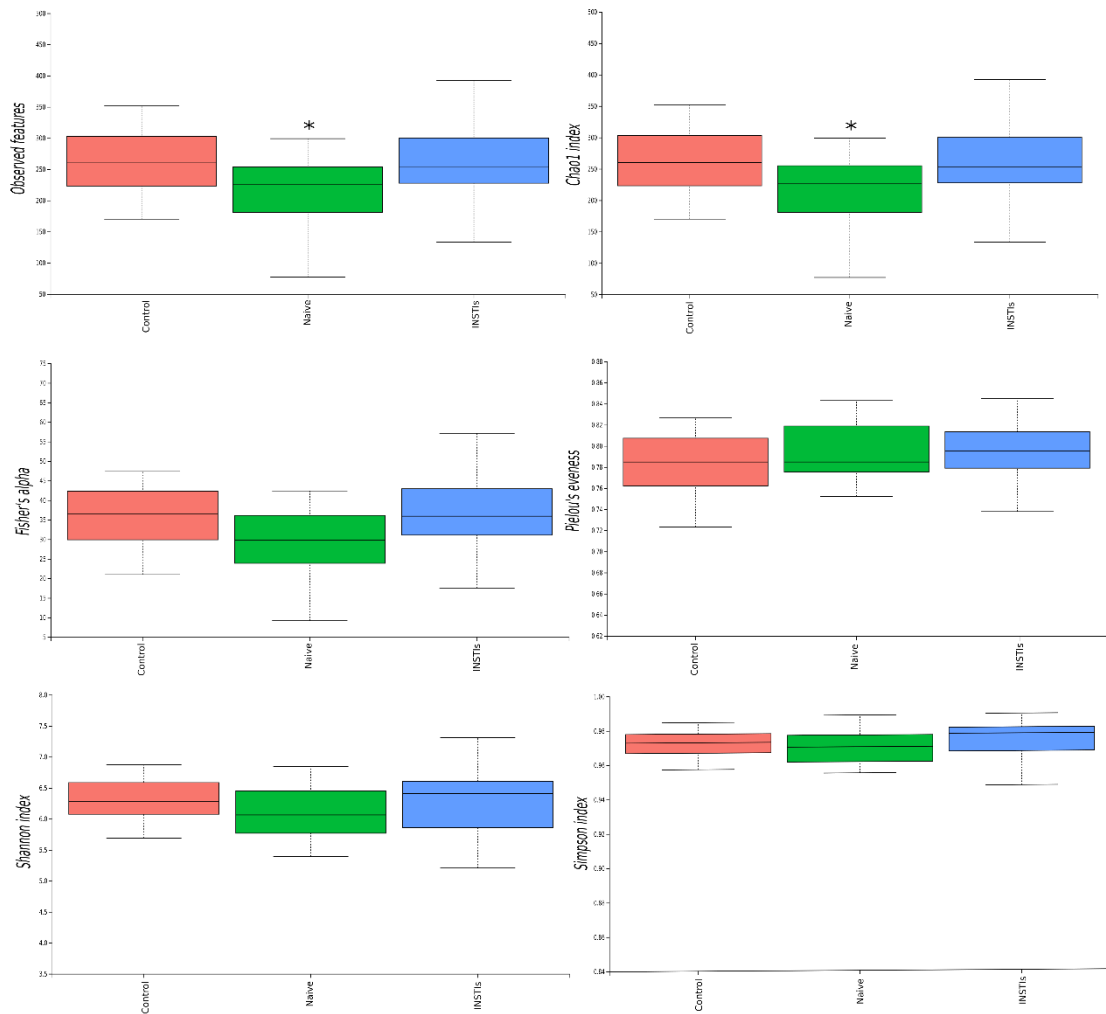
Figure 25. Different indexes of α-diversity from bacteria in faecal samples of the studied population. *p<0.05 *vs.* control. INSTIs (integrase strand transfer inhibitors-based treatments).

5.4.2. Beta diversity of gut bacteriome

Figure 26 shows the PCoA from the studied population. Control group is clearly different from naive group (p<0.01) and INSTIs-treated group (p<0.01). However, statically significant differences were not observed between the naive group and INSTIs-treated patients in terms of β-diversity as can be observed in **Figure 26**.
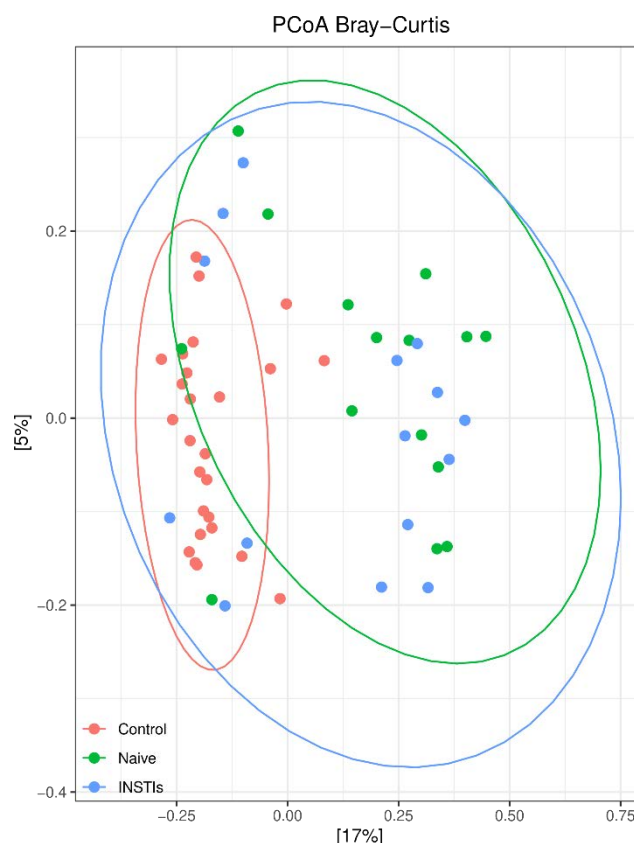
Figure 26. PCoAs from bacteria in faecal samples of the studied population (accounting for 22% of the total variation [Component 1 = 17% and Component 2 = 5%]). Results are plotted according to the first two principal components. Each circle represents a sample: red circles represent the uninfected volunteers, green circles represent the naive group and blue circles represent the INSTIs-treated group. The clustering of samples is represented by their respective 95% confidence interval ellipse. p<0.05 naive *vs.* control and p<0.05 INSTIs *vs.* control. INSTIs (integrase strand transfer inhibitors-based treatments).

5.4.3. Differential abundance of gut bacteriome

Concerning GM composition, a total of 16 phyla and 42 orders were detected. The two most abundant phyla in gut were Bacteroidetes (20.27%-64.21%) and Firmicutes (13.57%-77.01%). In the order level, Bacteroidales (20.27%-64.21%) and Clostridiales (11.41%-64.47%) were the most abundant.

When comparing controls to naive patients, increases in phylum level were not revealed. An increase in the order Aeromonadales (phylum Proteobacteria) and in the genus *Succinivibrio* (order Aeromonadales, phylum Proteobacteria) and *Prevotella 2* (order Bacteroidales, phylum Bacteroidetes) were observed in the naive group compared to controls (**Table 9**). In contrast, HIV infection was

accompanied by a decrease in the phylum Verrucomicrobia and in the genera *Erysipelotrichaceae UCG-003* (order Erysipelotrichales, phylum Firmicutes) and *Catenibacterium* (order Erysipelotrichales, phylum Firmicutes) in the naive group compared to controls (**Table 9**). When controls were compared against INSTIs-treated HIV-infected patients, an increase in the phyla Spirochaetes and Cyanobacteria, in the order Aeromonadales (phylum Proteobacteria) and in the genera *Succinivibrio* (order Aeromonadales, phylum Proteobacteria) and *Catenibacterium* (order Erysipelotrichales, phylum Firmicutes) were observed in the treated group (**Table 9**). A decrease in the phyla Bacteroidetes and Actinobacteria in INSTIs-treated group compared to the control group was also detected, although no specific orders or genera were decreased in this group of patients compared to healthy volunteers (**Table 9**). Finally, when comparing naive group and INTSIs-treated group an increase in the phylum Cyanobacteria and in the order Gastranaerophilales (phylum Cyanobacteria) were observed in the INSTIS-treated group along with a decrease in the phyla Bacteroidetes and Fusobacteria.

Table 9. Bacterial taxonomical orders that present a differential abundance in the faeces of the studied population.

Control *vs.*					
Naive			**INSTIs**		
Category	**Taxonomic group**	**W**	**Category**	**Taxonomic group**	**W**
			Phylum	Spirochaetes	9
			Phylum	Cyanobacteria	6
Order	Aeromonadales	41	Order	Aeromonadales	42
Genus	*Succinivibrio*	285	Genus	*Succinivibrio*	307
Genus	*Prevotella 2*	285	Genus	*Catenibacterium*	286
Phylum	Verrucomicrobia	9	Phylum	*Bacteroidetes*	4
			Phylum	*Actinobacteria*	4
Genus	*Erysipelotrichaceae UCG-003*	303			
Genus	*Catenibacterium*	292			

INSTIs (integrase strand transfer inhibitors-based treatments).

5.5.   Gut virome analysis

5.5.1.   Reads and contigs distribution

After the sequencing and the quality control, 48.8% of the reads (99,038,911 reads) mapped to viruses (**Figure 27A**) and, of them, 98.8% belonged to phages and 1.2% to eukaryotic virus (**Figure 27C**). Among the rest of the reads, 40% mapped to bacteria, 9.8% to other microorganisms, and only 1.4% were unannotated (**Figure 27A**). On the other hand, only 0.4% of the contigs (coming from the assembling of the reads after quality control) mapped to viruses (**Figure 27B**) and, of them, 88.6% belonged to phages and 11.4% to eukaryotic viruses (**Figure 27D**). Among the rest of the contigs, 93.7% belonged to bacteria, 4.9% to other, and 1% to unannotated (**Figure 27B**).
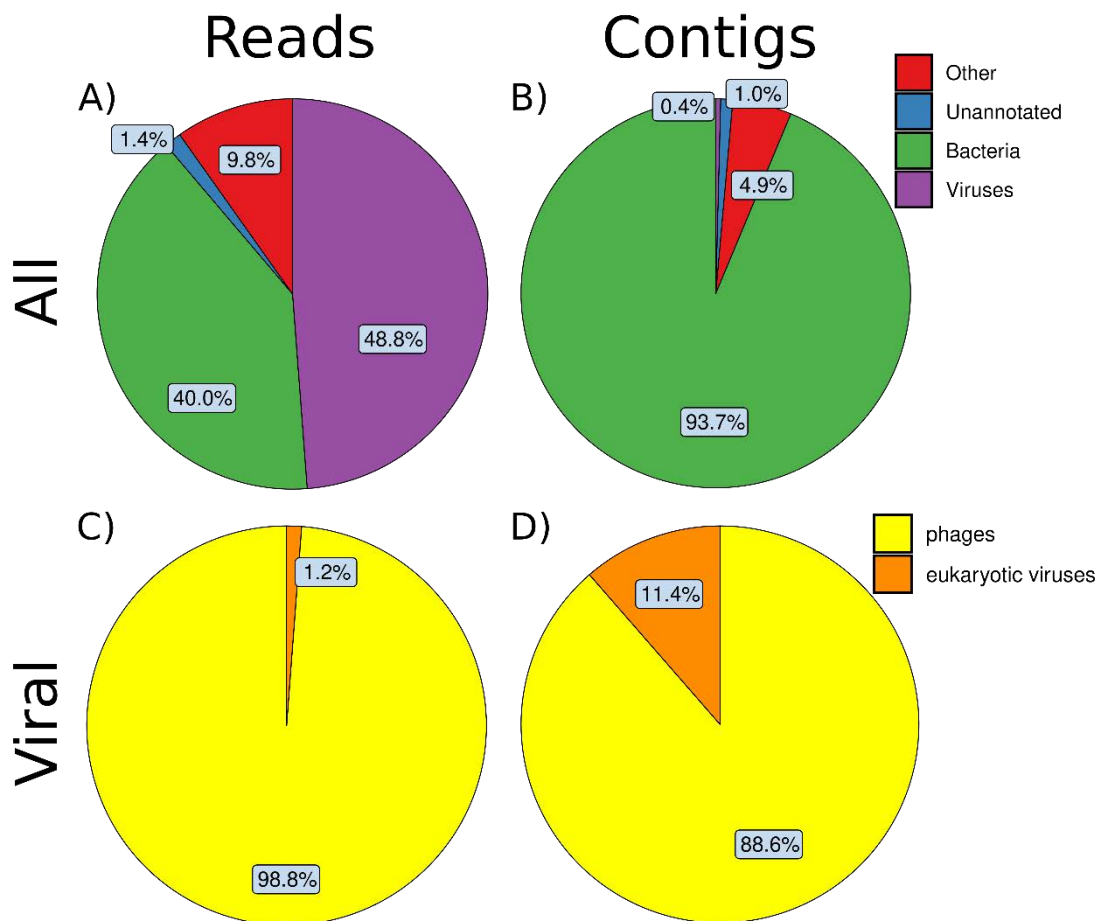
Figure 27. Percentage of the reads (**A** and **C**) and the contigs (**B** and **D**) that correspond to different superkingdoms (**A** and **B**) and viral categories (**C** and **D**).

5.5.2. Eukaryotic virus diversity and composition

5.5.2.1. Alpha and beta diversity of eukaryotic viruses

The analysis of α-diversity of eukaryotic viruses did not show statistically significant differences in the indexes analysed (*Observed features*, *Simpson index*, *Shannon index*, and *Pielou's evenness*) (**Figure 28**). However, a slightly decreased tendency was observed in *Observed features*, *Simpson index*, and *Shannon index* in the naive group compared to the controls, which seems to be reverted after INSTIs-based treatment. In the same line as α-diversity, the analysis of β-diversity did not reveal a different clustering between the three groups (**Figure 29**).
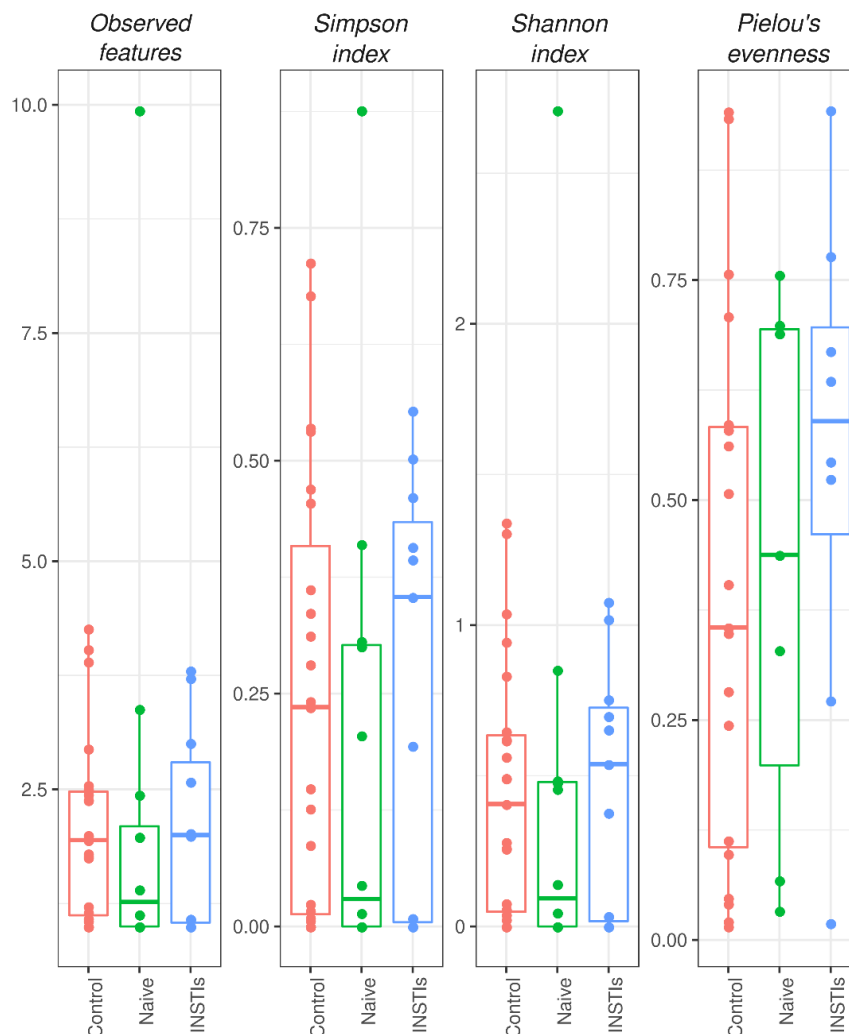
Figure 28. Different indexes of α-diversity from eukaryotic viruses in faecal samples of the studied population. INSTIs (integrase strand transfer inhibitors-based treatment).
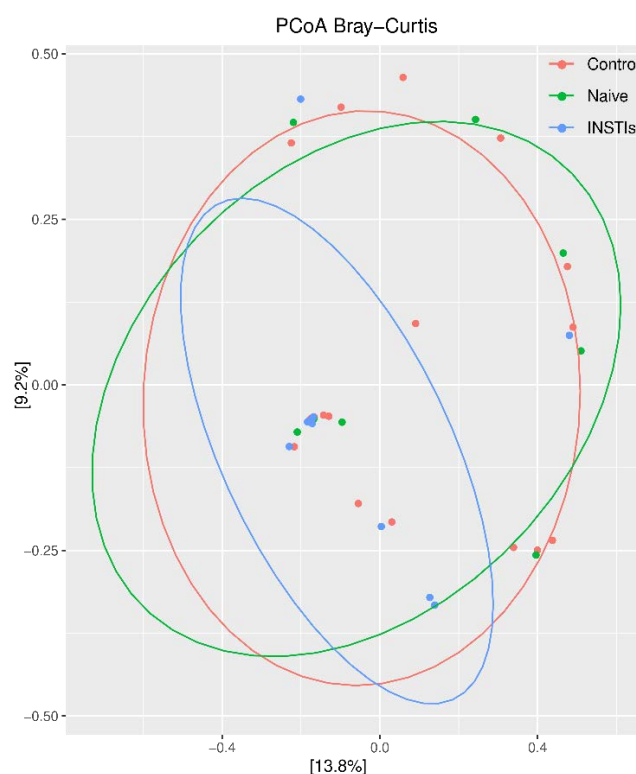
**Figure 29**. PCoAs from eukaryotic viruses in faecal samples of the studied population (accounting for 23% of the total variation [Component 1 = 13.8% and Component 2 = 9.2%]). Results are plotted according to the first two principal components. Each circle represents a sample: red circles represent the uninfected volunteers, green circles represent the naive group and blue circles represent the INSTIs-treated group. The clustering of sample is represented by their respective 95% confidence interval ellipse. INSTIs (integrase strand transfer inhibitors-based treatment).

5.5.2.2. Distribution of eukaryotic viruses

Eukaryotic viruses were classified into three groups: animal infecting viruses (4 families), plant and fungi infecting viruses (9 families), and small circular viruses (7 families). **Figure 30** shows the presence of these viruses and their relative abundance comparing their presence in controls subjects and naive and INSTIs-treated groups to provide a first view of their distribution. Our data revealed that plant and fungal viruses are the most prevalent, with members of the *Virgaviridae* family being the most abundant, followed by small circular viruses. Although plant viruses are likely passengers, they were the only group found in more than 50% of all samples. On the other hand, animal infecting viruses were rare. Due to the low percentage of reads belonging to eukaryotic

viruses compared to those belonging to phages and the wide deviation between samples, DESeq analysis did not reveal differentially abundant eukaryotic viruses among the three groups.
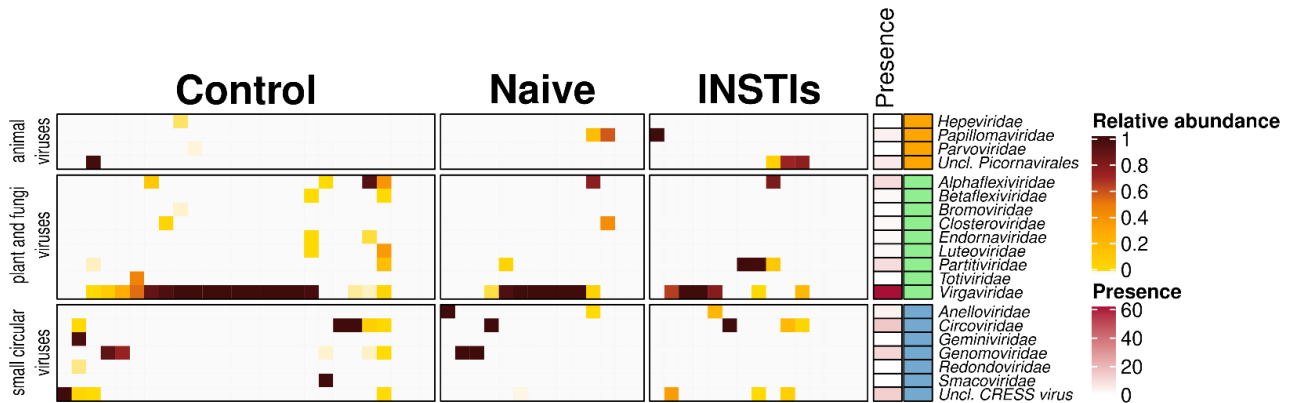
Figure 30. Heatmap of the distribution of eukaryotic viruses between control, naive, and INSTIs groups. The relative abundance and the presence of the different families between three groups is shown (animal infecting viruses, plant and fungi infecting viruses, and small circular viruses). INSTIs (integrase strand transfer inhibitors-based treatment).

5.5.3. Phage diversity and composition

5.5.3.1. Alpha diversity of phages

A significant decrease in *Observed features* and *Fisher's alpha* indexes was observed in HIV-naive patients compared to controls (p<0.01 and p<0.05 respectively). Such decrease was not present in INSTIs-treated group when compared to controls (**Figure 31**). No differences were observed either in *Simpson index, or Shannon index*, or in *Pielou's evenness*.
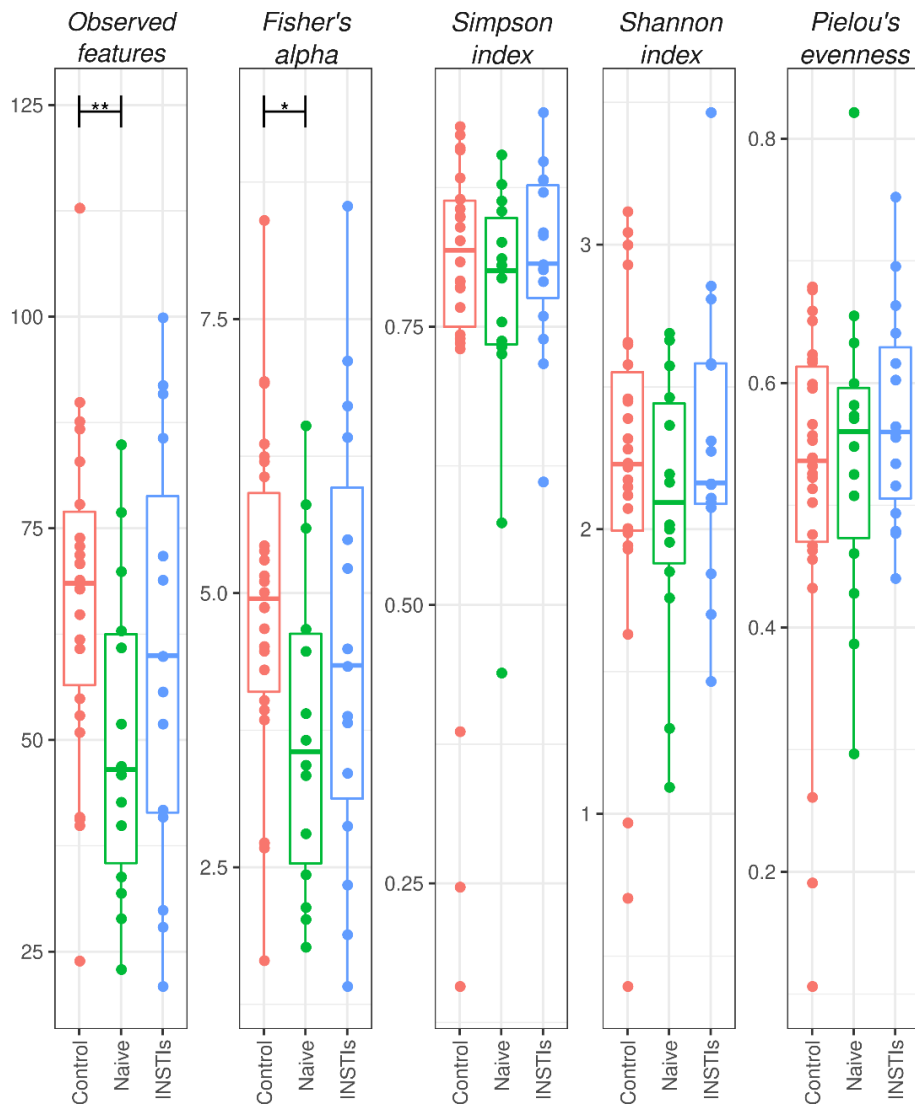
Figure 31. Different indexes of α-diversity from phages in faecal samples of the studied population. *p<0.05 *vs*. control, **p<0.01 *vs*. control. INSTIs (integrase strand transfer inhibitors-based treatment).

5.5.3.2. Beta diversity of phages

Figure 32 shows the PCoA obtained from the studied population. The control group is clearly different from the naive group (p<0.01) and the INSTIs-treated group (p<0.01). However, statistically significant differences were not observed between the naive group and the INSTIs-treated patients in terms of β-diversity, although it is worth mentioning that samples coming from INSTIs-treated patients grouped more closely together compared to those of naive patients, as can be observed in **Figure 32**.
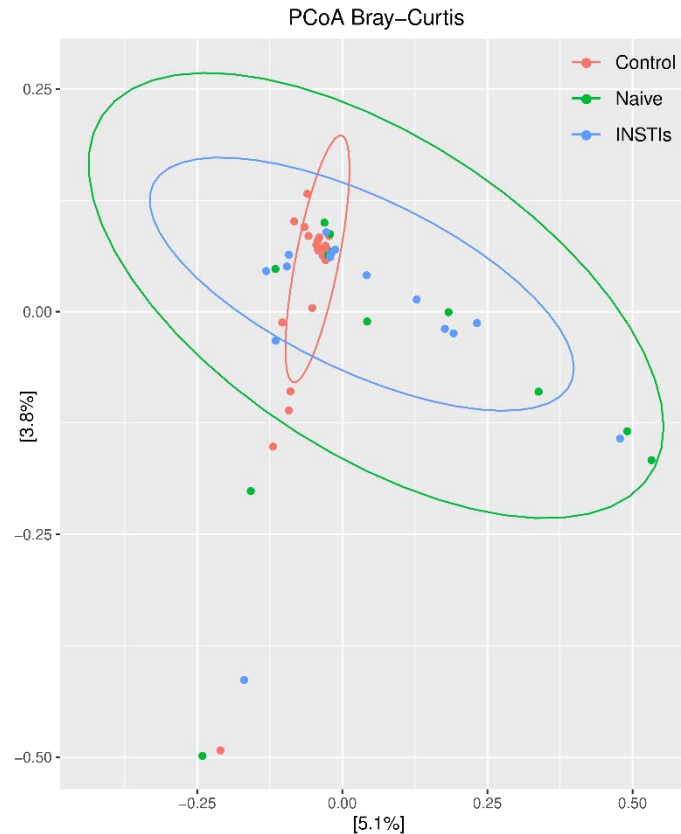
Figure 32. PCoAs from phages in faecal samples of the studied population (accounting for 8.9% of the total variation [Component 1 = 5.1% and Component 2 = 3.8%]). Results are plotted according to the first two principal components. Each circle represents a sample: red circles represent the uninfected volunteers, green circles represent the naive group and blue circles represent the INSTIs-treated group. The clustering of samples is represented by their respective 95% confidence interval ellipse. p<0.01 naive *vs.* control and p<0.01 INSTIs *vs.* control. INSTIs (integrase strand transfer inhibitors-based treatment).

5.5.3.3. Differential abundance of phages

DESeq analysis revealed an increase in members of the *Caudoviricetes* class in naive patients compared to the non-infected group and a decrease in *Malgrandaviricetes* class in INSTIs-treated patients compared to the control group. However, differences between naive and INSTIs-treated patients were not detected (**Table 10**).

Table 10. Phage taxonomical orders which present a differential abundance in the faeces of the studied population.

	Control *vs.*					
	Naive			**INSTIs**		
	Category	**Taxonomic group**	**padj**	**Category**	**Taxonomic group**	**padj**
⬆	Phylum	Uroviricota	0,011			
	Class	*Caudoviricetes*	0,011			
⬇				Phylum	Phixviricota	<0,001
				Class	*Malgrandaviricetes*	<0,001

INSTIs (integrase strand transfer inhibitors-based treatments).

5.5.3.4. Lifecycle prediction of phages

Comparison between controls and HIV-infected groups revealed a statistically significant increase in the relative abundance of lysogenic phages in HIV-infected patients ($p < 0.05$ *vs.* control) (**Figure 33A**), that was not reversed after INSTIs-based treatment (**Figure 33B**). These differences couldn't be solely explained by changes in the relative abundance of *Caudoviricetes* class (**Figure 33C** and **Figure 33D**).
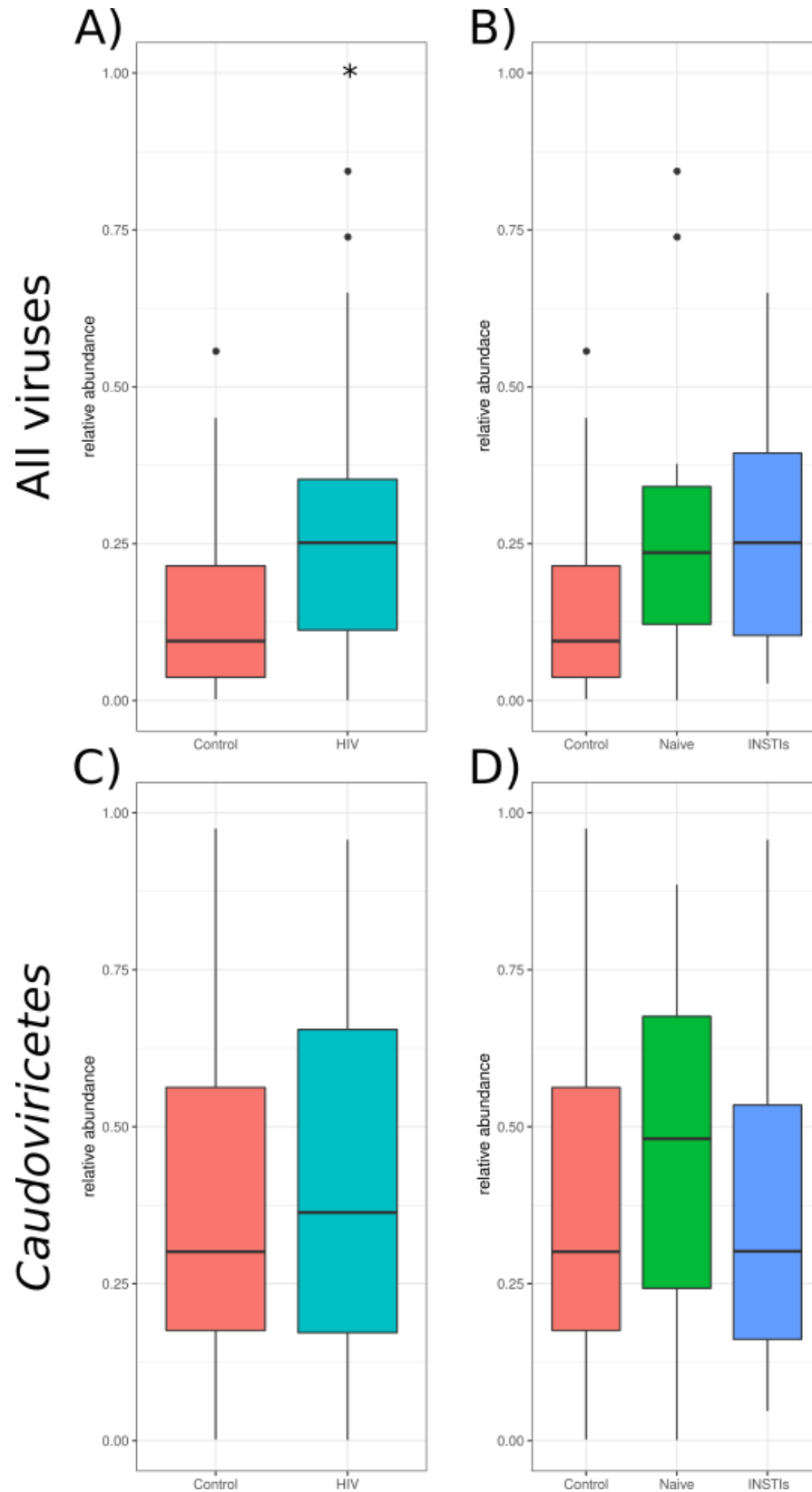
Figure 33. Relative abundance of the lysogenic phages comparing control group *vs.* HIV-infected patients and control group *vs.* naive patients *vs.* INSTIs-treated patients taking into account all viral classes (**A** and **B**) and only *Caudoviricetes* class (**C** and **D**). *p<0.05 *vs.* control. HIV (human immunodeficiency virus), INSTIs (integrase strand transfer inhibitors-based treatment).

5.5.3.5. Host prediction of phages

Figure 34A shows the host prediction of the four classes of phages detected (*Caudoviricetes*, *Duplopiviricetes*, *Faserviricetes*, and *Malgrandaviricetes*) and of those viruses which were unable to be classified (Unannotated). *Caudoviricetes* were predicted to mainly infect members of the phyla Firmicutes followed by Bacteroidetes phylum. *Malgrandaviricetes* were predicted to mainly infect members of the Proteobacteria phylum followed by Firmicutes and Chloroflexi phyla. The main host of *Duplopiviricetes* and *Faserviricetes* couldn't be detected and, therefore, was identified as "unknown".

Finally, the comparison between the relative abundance of the phages infecting each bacterial phylum revealed that INSTIs-based treatments were not able to restore the decrease observed in the relative abundance of Proteobacteria-infecting phages (p<0.05 HIV *vs.* control) (**Figure 34B** and **Figure 34C**).
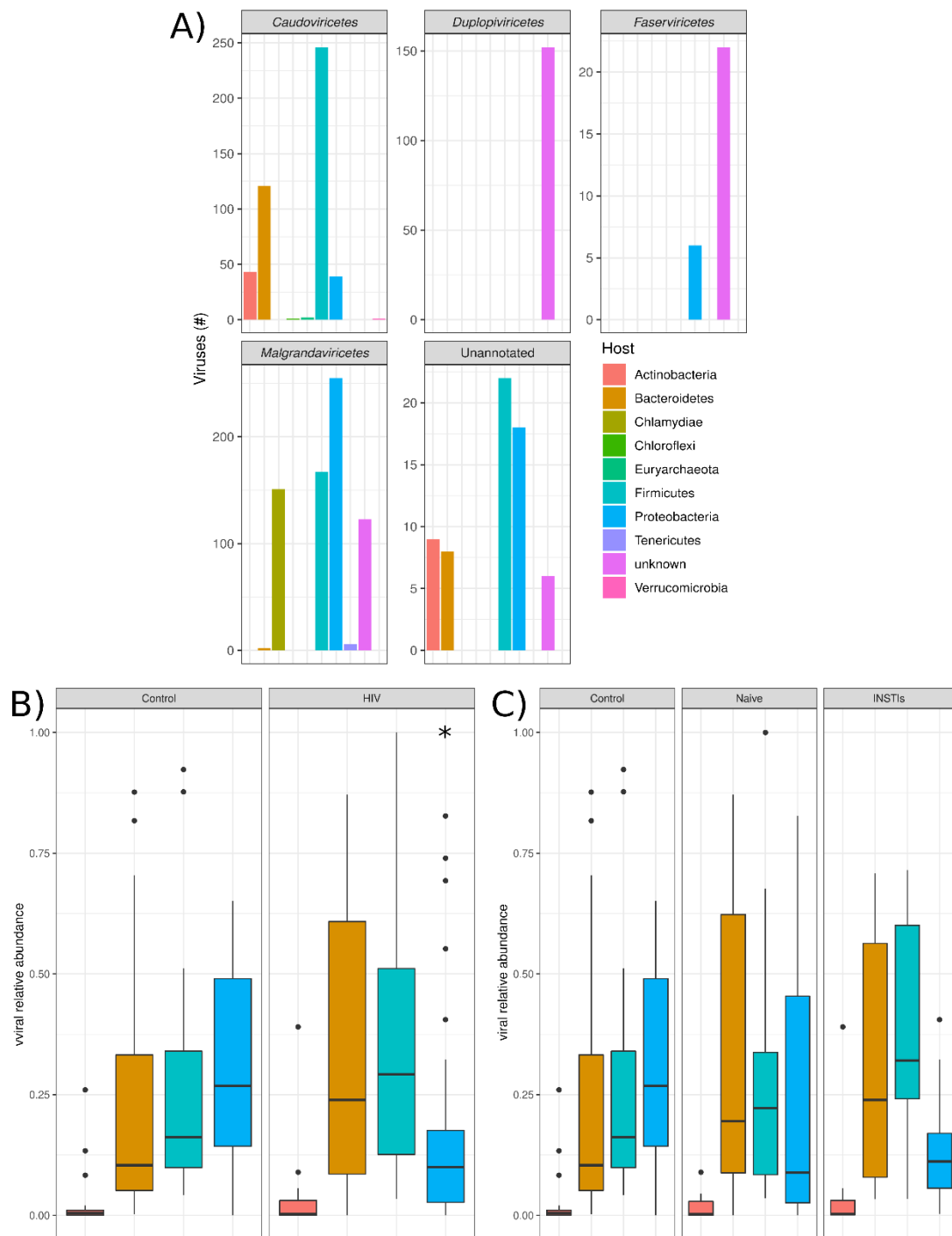
Figure 34. Host prediction of the phages belonging to different classes. **A)** Prediction of which bacteria are infected by phage grouped based on class-level taxonomy. **B)** Differences between control and HIV-infected patients in the relative abundance of the phages infecting bacterial phyla. **C)** Differences between control, naive, and INSTIs in the relative abundance of the phages infecting bacterial phyla. *p<0.05 *vs.* control. INSTIs (integrase strand transfer inhibitors-based treatment).

5.5.3.6. Correlation between α-diversity of gut bacteriome and α-diversity of gut phages

Finally, we wanted to detect possible correlations between indexes of α-diversity from bacterioma and from phages (**Figure 35**). As expected, all bacteriome α-diversity indexes correlated between them as well as all phages α-diversity indexes did. In addition, all bacteriome richness indexes (*Observed features*, *Chao 1 index*, and *Fisher's alpha*) and *Shannon index* correlated with the following phages indexes: *Observed features*, *Chao1 index*, and *Simpson index*, but not with *Fisher's alpha* or *Shannon index*.
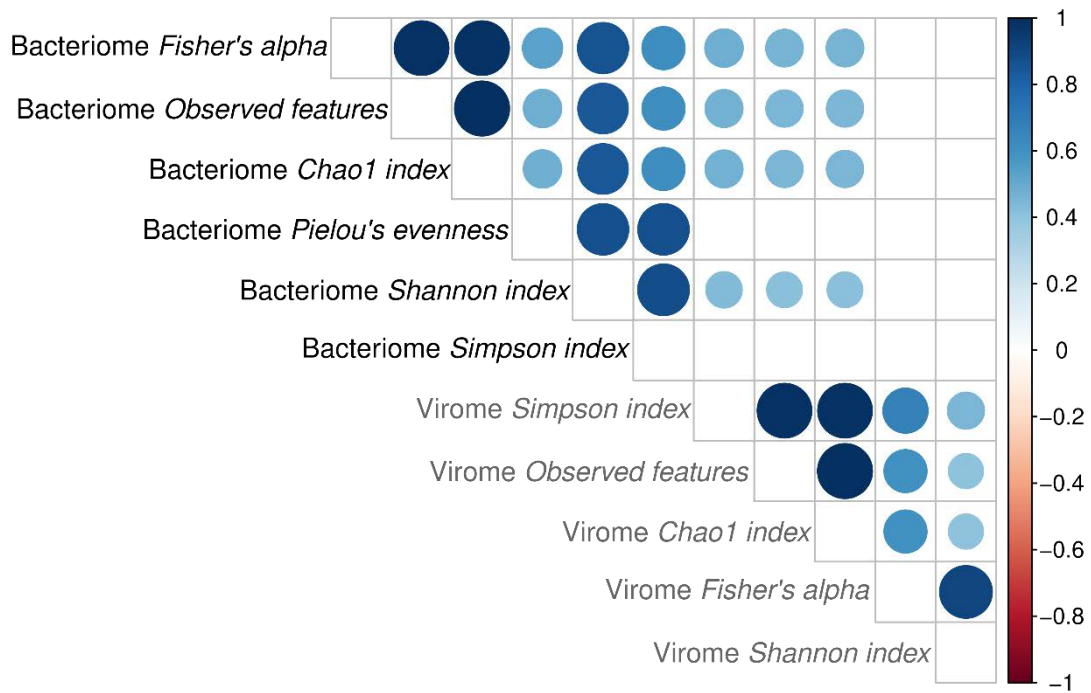
Figure 35. Correlation plot between α-diversity indexes from bacteria and phages. Only significant correlations (p<0.01) are shown.

5.6. Oral bacterioma diversity and composition

5.6.1. Alpha and beta diversity of oral bacteriome

The analysis of the α-diversity of oral bacteriome did not show statistically significant differences in the indexes analysed among the three groups of subjects (*Observed features*, *Chao1 index*, *Fisher's alpha*, *Pielou's evenness, Simpson index*, and *Shannon index*) (**Figure 36**). Similarly, the analysis of β-diversity did not reveal a different clustering between the three groups (**Figure 37**).
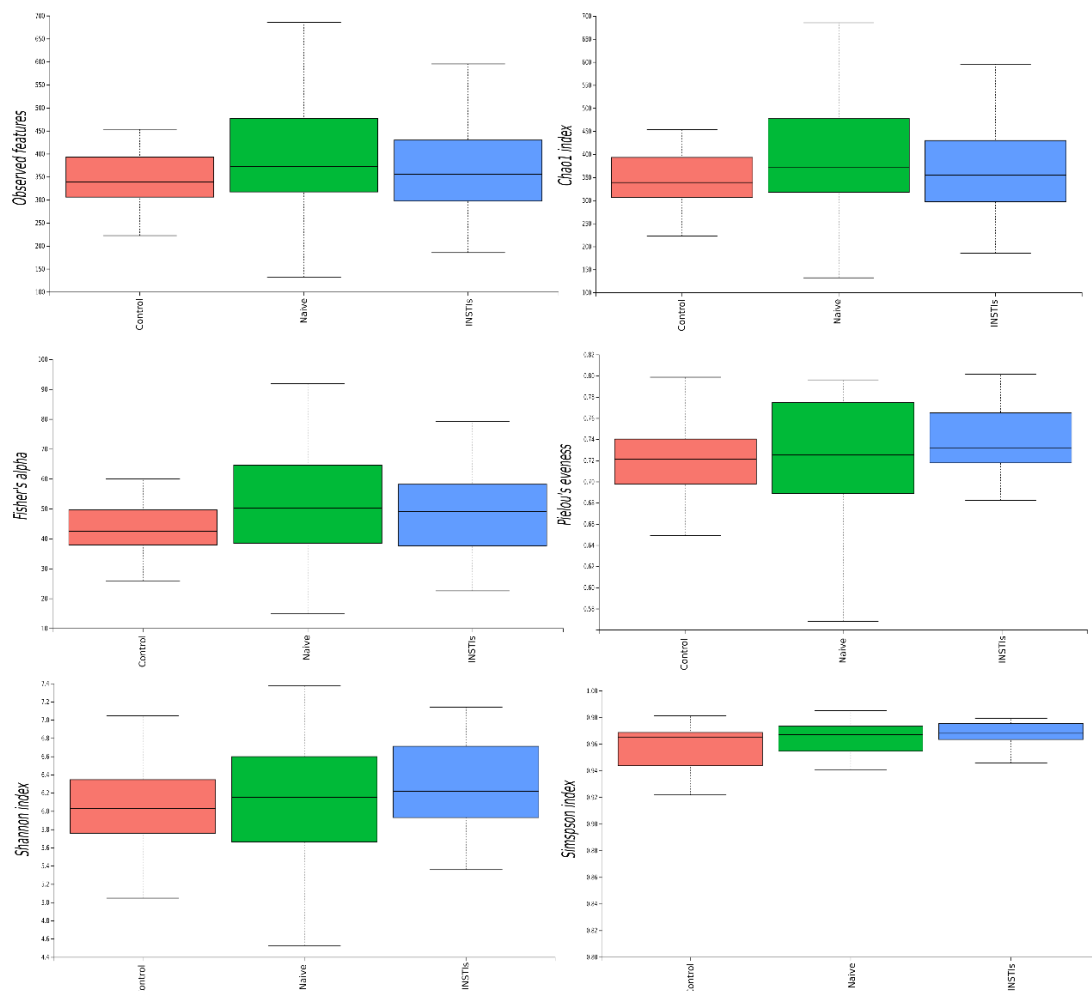
Figure 36. Different indexes of α-diversity from bacteria in salivary samples of the studied population. INSTIs (integrase strand transfer inhibitors-based treatments).
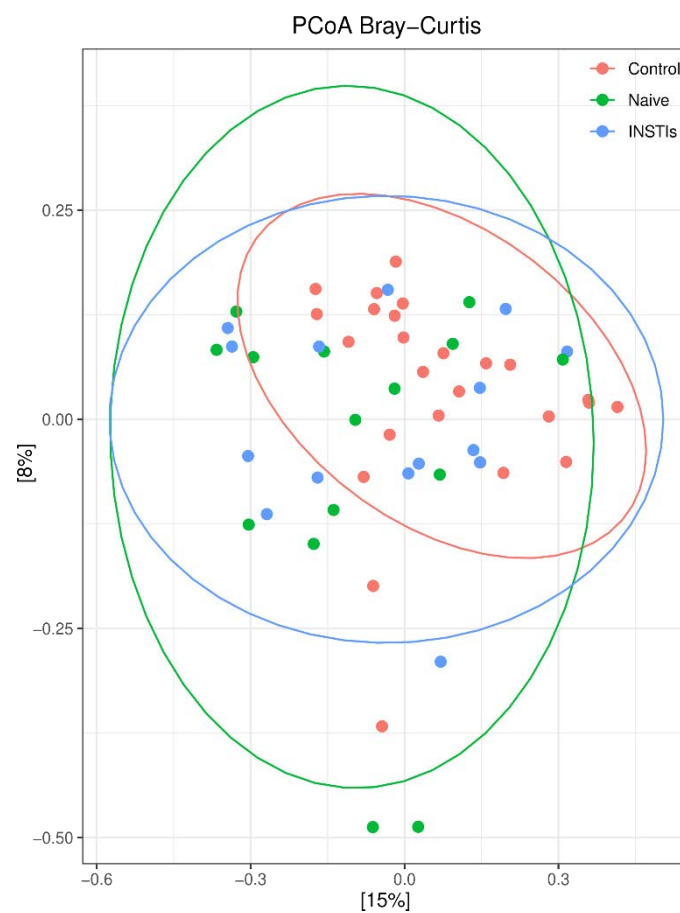
Figure 37. PCoAs from bacteria in salivary samples from the studied population (accounting for 23% of the total variation [Component 1 = 15% and Component 2 = 8%]). Results are plotted according to the first two principal components. Each circle represents a sample: red circles represent the uninfected volunteers, green circles represent the naive group and blue circles represent the INSTIs-treated group. The clustering of samples is represented by their respective 95% confidence interval ellipse. INSTIs (integrase strand transfer inhibitors-based treatments).

5.6.2. Differential abundance of oral bacteriome

Concerning oral microbiota composition, a total of 20 phyla and 68 orders were detected. The three most abundant phyla in saliva were Bacteroidetes (12.61%-64.16%), Firmicutes (7.37%-66.14%), and Proteobacteria (0.12%-54.40%). In the order level, Bacteroidales (10.05%-63.13%), Lactobacillales (2.65%-56.11%), and Betaproteobacteriales (0.04%-42.54%) were the most abundant.

When comparing controls to naive patients, an increase in the phylum Proteobacteria, in the order Acholeplasmatales (phylum Firmicutes), and in the genera *Ezakiella* (order Tissierellia, phylum Firmicutes) and *Acholeplasma* (order

Acholeplasmatales, phylum Firmicutes) were observed in the naive group compared to controls (**Table 11**). On the other hand, when controls were compared against INSTIs-treated HIV-infected patients, an increase in the phylum Tenericutes, in the order Acholeplasmatales (phylum Firmicutes), and in the genera *Acholeplasma* (order Acholeplasmatales, phylum Firmicutes) and *uncultured Eubacteriaceae bacterium* (order Eubacteriales, phylum Firmicutes) were detected (**Table 11**). No differences were observed between naive group and INSTIs-treated group.

Table 11. Bacterial taxonomical orders that present a differential abundance in the saliva of the studied population.

Control *vs.*					
Naive			**INSTIs**		
Category	**Taxonomic group**	**W**	**Category**	**Taxonomic group**	**W**
Phylum	Proteobacteria	13	Phylum	Tenericutes	19
Order	Acholeplasmatales	66	Order	Acholeplasmatales	57
Genus	*Ezakiella*	130	Genus	*Acholeplasma*	178
Genus	*Acholeplasma*	124	Genus	*uncultured Eubacteriaceae bacterium*	162

INSTIs (integrase strand transfer inhibitors-based treatment).

6. DISCUSSION

Integrase inhibitors are recommended by international guidelines (78,399,400) as a key component of ART in the treatment of naive HIV-infected patients. In particular, their efficacy, tolerability, and low drug-drug interaction profile have made them the preferred choice as part of the first-line regimen in treatment-naive individuals (401). Here we report that current antiretroviral regimens based on INSTIs are able to reverse the impact of HIV infection on BT and systemic inflammation reaching similar levels than those observed in an uninfected/control population. These results suggest potent beneficial actions of this class of antiretrovirals on gut and in potential age-related complications such as cardiovascular events. In addition, our study confirms that the results previously observed with RAL (270) can be extrapolated to other INSTIs used for treatment of HIV-infected patients. On the other hand, we have demonstrated the effects of HIV infection and INSTIs-based treatment on gut bacteriome, bacteriophages, and eukaryotic virus abundances as also on salivary bacteriome. To our knowledge, this is the first time that DNA and RNA viruses have been identified in gut of HIV-infected people along with the characterization of gut bacteriome in the same individuals. Thus, this study implies a "snapshot" needed to identify if INSTIs-based treatments are able to restore gut dysbiosis not only at bacterial (270) but also at viral level.

As deeply described in the introduction section of this Doctoral Thesis, the BT triggered by HIV infection is associated with subsequent intestinal and systemic inflammation (295) and with the predisposition of HIV-infected patients to co-morbidities such as CVD (251). Several studies have reported elevated serum levels of sCD14 and have demonstrated that this marker independently predict mortality and thrombotic risk (288,402). Our study clearly showed that ART-based on INSTIs reduced the levels of sCD14 and LBP reaching similar serum levels than those observed in control population. These results could have a positive impact on the inflammaging state present in these patients (253) and improve their quality of life. Moreover, we have revealed that this effect is mainly

present in those patients taking DTG, while BIC seems to be less efficient reducing BT in HIV-infected patients. However, the number of patients included when we split INSTIs-treated group into two is very small and more studies with larger cohorts will be needed to confirm such findings. Anyway, our study clearly revealed the positive effects of both treatments, analysed together, on BT. An increase in the inflammatory cytokine TNF-α in the naive group, which was not present in the INSTIs-treated group, was also observed in our study. This fact suggests a mild recuperation of the inflammatory state in HIV-infected people under INSTIs-based therapy. These results are similar to those obtained in an observational study analysing the effects of different INSTIs (RAL, EVG or DTG) on markers of inflammation and BT (403). Besides, in this study they revealed that EVG is the INSTIs which seem to have a worsen impact on inflammation and BT (341). Thus, this could potentially reduce future HIV-related complications associated with inflammation. In fact, we have observed that INSTIs-based treatments are able to reduce cardiovascular risk markers VCAM-1 and PAI-1 which could suggest a reduced risk of CVD, as stated in a previous study (404). Furthermore, our "small and quite limited" longitudinal study demonstrated the ability of these drugs to counteract the HIV-induced inflammatory state, although the limited number of patients included in this analysis make difficult to extrapolate such results to the whole HIV-infected population. Regarding faecal calprotectin, several studies have shown that its concentrations are highly correlated with histopathological and endoscopic findings in IBD (405) and, in fact, it is used as a measurement of gut permeability and inflammation in IBD (405). In our study, we revealed an increase of faecal calprotectin due to HIV-infection that was completely reversed after INSTIs-based treatment. These results are in contrast with those from Eckard *et al.,* 2021 (406) and Ancona *et al.,* 2021 (407), who did not detect a recovery of faecal calprotectin levels after ART. These differences could be due to the different treatment used, what could suggest a strong protective role of INSTIs-based treatments in terms of gut permeability. Furthermore, calprotectin is a very good marker of the "intestine state" (405) and our results suggest a recovery at this level after INSTIs-based

treatment, which seems to be associated with the effects observed at systemic level with markers of BT, inflammation, and cardiovascular risk.

Our results have also showed that HIV infection reduces bacterial richness/diversity, as previously demonstrated (408), whereas ART based on INSTIs was able to counteract this process. These results mimic those previously observed by our group with RAL (270) and, therefore, point towards a similar trend in all INSTI-based regimens, confirming a class effect irrespective of the drug used. However, long-term suppressive INSTI-based ART was not able to completely restore the compositional changes induced by HIV-infection on gut and only partial improvements were observed. Thus, HIV infection was associated with an increase in Aeromonadales order (phylum Proteobacteria) mainly triggered through the increase in genus *Succinivibrio* (Aeromonadales order constitutes 0.23%-26.78% of the bacterial reads and *Succinivibrio* genus until 26.78%). This increase was not reversed by the INSTIs and should be studied in depth in the future given the fact that previous studies suggested that *Succinivibrio* could be associated with defects in gastrointestinal functions such as diarrhoea and abdominal pain (409–412). However, none of the patients included in our study reported such problems. Our results also showed an increase of *Prevotella 2* (phylum Bacteroidetes) associated with HIV-infection, which was not present in INSTIs-treated patients, suggesting a partial recovery after treatment. This increase observed in *Prevotella* could be associated with the elevated inflammation observed in naive patients since increased *Prevotella* abundance is associated with augmented Th17-mediated mucosal inflammation, which is in line with the marked capacity of *Prevotella* in driving Th17 immune responses *in vitro*. Furthermore, *Prevotella* stimulate epithelial cells to produce interleukin 8 (IL-8), IL-6, and C-C motif chemokine ligand 20 (CCL20), which can promote mucosal Th17 immune responses and neutrophil recruitment (413). Thus, these results could suggest that HIV increases inflammation (confirmed by the increase in serum TNF-α levels and also at gut level based on calprotectin data) and INSTI-based treatments are able to improve this pro-inflammatory effect at gut and systemic level through the modulation of this bacterial genus. However, more studies are needed in this regard. On the other hand,

Verrucomicrobia phylum and *Erysipelotrichaceae UCG-003* genus (phylum Firmicutes) were decreased in the naive group. In this context, *Akkermansia muciniphila* belonging to phylum Verrucomicrobia has been reported to be a sentinel for gut permeability having benefits in HIV-infected people (414), so probiotics based on *Akkermansia muciniphila* could have a positive effect on HIV-infected patients in terms of gut health. Moreover, an increase in Spirochaetes and Cyanobacteria phyla and a decrease in Bacteroidetes and Actinobacteria phyla were observed in INSTIs-treated patients when compared to uninfected individuals. These effects were not observed in naive patients, at least at phylum level, suggesting a direct effect of INSTIs. There are few studies analysing the relation of these phyla and HIV infection, but recent studies have shown that spirulina and other compounds extracted from Cyanobacteria can alleviate oxidative stress and inflammation in aspirin-induced gastric ulcer in mice (415) and could even exert anti-HIV activities (416). Thus, the increase observed after INSTIs-based treatment could be of great interest from a clinical point of view although more studies are needed. Besides, Bacteroidetes phylum has been reported to include some significant clinical pathogens (417) and has also been found to decrease in INSTI-treated patients in other studies (270,334), which corroborates our results. Regarding Actinobacteria, this phylum includes some genera with beneficial properties to human health such as *Collinsela*, related to butyrate production (418), and *Bifidobacterium*, which has numerous positive health benefits (419). Thus, the slight decrease observed in INSTIs-treated patients compared to controls should be further address in depth.

On the other hand, our study showed a decrease in the concentration of acetic acid, butanoic acid, pentanoic acid (valproic acid), and hexanoic acid (caproic acid) in HIV-infected subjects, including both naive and INSTIs-treated patients. These SCFAs are generated by the fermentation of dietary fibers by GM and evidence indicates that are key players in regulating beneficial effects on GM and health (420). Specifically, a study revealed that acetic acid suppresses colonic inflammation in germ-free (GF) mice (421) and butanoic acid has also been demonstrated to exert important actions related to cellular homeostasis such as anti-inflammatory, antioxidant, and anti-carcinogenic functions (422). On

the other hand, hexanoic acid has revealed anti-inflammatory effects and a role in maintaining the integrity of the gastrointestinal epithelial barrier through regulation of mucus production and tight junction expression (423), and was previously shown to protect against dysbiosis and expansion of pathogenic bacteria in animal (424). The fact that levels of these SCFAs are not restored after INSTIs-based treatments is interesting and should be studied to evaluate if a longer treatment is able to restore them and the implications for health.

Our study revealed that in stools collected from controls and HIV-infected patients, most of the viral reads and contigs belonged to phages, while eukaryotic viruses were less abundant. These findings are in line with previous studies that highlight that bacteriophages are the vast majority of the viral component in the human gut (425). The lack of differences in α and β-diversity of eukaryotic viruses could be due to the low number or reads obtained belonging to these viruses. However, a slightly non-significant tendency of a decreased richness and diversity in naive patients compared to the controls were observed, along with a partial recovery after INSTIs-based treatments although it did not reach statistical significance Our results also revealed that plant and fungal infecting viruses (mainly members of the *Virgaviridae*) were the most abundant eukaryotic viruses, followed by small circular viruses and animal infecting viruses, suggesting that most of the eukaryotic viruses are diet derived. These results differ from those obtained by Monaco *et al.*, 2016 (358), who reported that *Adenoviridae*, *Anelloviridae*, *Circoviridae,* and *Papillomaviridae* viruses, all of them animal infecting viruses, were the most abundant eukaryotic viruses in the enteric virome of HIV-infected subjects. However, they only analysed DNA viruses, so their viral community is quite different from ours, in which we have included both DNA and RNA viruses. Besides, the HIV cohort analysed in Monaco´s study was different from ours in terms of lifestyle, diet, age, ART, and treatment duration (33.27 ± 5.04 months *vs.* 6.7 years), all of them factors that could have a significant impact on GM profile.

Regarding bacteriophages, a significant decrease in *Observed features* and *Fisher's alpha* indexes was observed in naive patients compared to

uninfected controls. However, INSTIs-based treatment was able to reverse such decrease, since no significant differences were observed among treated patients and the control group. These results are contrary to those obtained by Monaco *et al.*, 2016 (358)*,* who reported no significant differences in *Richness* or *Shannon index* of bacteriophage families or genera by HIV infection or treatment status. The differences among both studies could be due to several factors associated with the population recruited and described before and by the fact that only DNA viruses were analysed in the study of Monaco *et al*., 2016 (358), whereas we have included both DNA and RNA viruses. In fact, phages can be DNA and RNA viruses, therefore, our study is more similar to reality because it assesses the viral community as a whole. However, another very important factor (often overlooked) could be the difference in the bioinformatics approaches carried out. In fact, we have used several recently developed state-of-the-art phage analyses tools (described in Methods section). This might also explain the identification of a different clustering pattern of HIV-infected patients that has not been shown before. A direct correlation between most of the α-diversity indexes from gut bacteriome and those from phages has been observed in our study. These correlations might be explained by the fact that the activation of immune system triggered by HIV infection could have as "targets" both gut bacteria and viruses. However, our results differ from those obtained by Monaco *et al.,* 2016 (358), but the differences could be due to fact that they only analysed DNA viruses and we have included both DNA and RNA viruses, so the communities studied are very different as we studied viral community as a whole.

Our study has also showed a statistically significant increase in *Caudoviricetes* class in naive patients compared to the control group. *Caudoviricetes* are double strand DNA phages that have been revealed to be increased in IBD (426). Therefore, the increase observed in *Caudoviricetes* class might be associated to, or be responsible for, the increased inflammatory state and gut permeability (measured through fecal calprotectin levels) observed in HIV-infected patients that is abolished after INSTI-based treatment (427). Thus, the role of this viral class deserves more attention in the context of HIV infection, inflammation, and gut permeability. On the other hand, we observed a statistically

significant decrease in members of the *Malgrandaviricetes* class (containing circoviruses) in INSTIs-treated patients, although, -up to date- their physiological meaning is unknown. Thus, more studies are needed in order to determine the role of this phage class in the gut in the context of HIV infection and INSTIs-based treatment. Interestingly, we observed an increase in lysogenic phages related to HIV-infection that was not reversed by INSTIs-based treatments. Our hypothesis is that inflammation triggered by HIV-infection creates a stressful state in the enteric environment that, by one side reduces bacteriome α-diversity (427); and, on the other side, induces a selection in phages towards lysogenic profiles since lytic virions have more difficulties to find a new bacterial host to infect. In addition, these effects were not reversed by INSTIs-based treatments, so more studies are required to analyse the possible clinical implications of such findings. We have also revealed for the first time a significant decrease in Proteobacteria-infecting phages in HIV-infected patients, which was not restored by INSTIs-based regimens. These results are very interesting because they correlate with the increase observed in some Proteobacteria taxonomical orders (specifically Aeromonadales order and *Succinivibrio genus)* observed in naive patients (427). These associations among bacteriome and virome are noteworthy since are based on the same individuals (and same samples) and suggest a close interrelationship among bacteriome and virome. In fact, the increase observed in some Proteobacteria taxonomical orders in naive patients could be associated with the decrease revealed in several Proteobacteria-infecting phages. Thus, a phage therapy focused on decreasing *Succinivibrio* presence (from Proteobacteria order) could be an interesting "weapon" to improve the quality of life of these HIV-infected patients since previous studies suggests that *Succinivibrio* could be associated with defects in gastrointestinal functions, such as diarrhoea and abdominal pain (409–412).

Regarding salivary bacterial composition, our study was unable to detect differences in α nor β-diversity among the three groups analysed. Similarly to our results, Presti *et al.,* 2018 (367) were unable to detect differences in α nor β-diversity between the naive group and ART-treated group (treated with EFV/FTC/tenofovir(TDF)). Similarly, Imahashi *et al.,* 2021 (369) did not show

either differences in species richness between HIV negative people and ART-treated HIV-infected subjects. In contrast, Li *et al.,* 2021 (428) revealed a statistically significant decrease in *Chao1 index* and *Shannon index* between the naive group and the control group and also a different clustering between both groups. The differences could be explained by the fact that the populations among both studies were different. In fact, in the study of Li *et al.,* 2021 (428), only HIV-infected MSM patients from Beijing were included, whereas in our study the percentage of MSM were 60.00% in the naive group and only 46.67% in the ART-treated group. In addition, only 15 HIV-infected patients in our study were not Caucasians. Thus, it will be needed to clarify the potential influence of the origin of subjects (in terms of dietary habits) and/or the sexual orientation and mode of transmission of HIV-infection in the composition of oral microbiota in the context of HIV infection. In addition, the hypervariable regions of the 16S rRNA gene analysed were also different between both studies (V4-V5 *vs.* V3-V4 in our study). In fact, and taking into consideration the well-known impact of HIV on GALT, it seems reasonable to detect more differences in gut bacteriome rather than on saliva. However, some taxa were increased in the naive group and in the INSTIs-treated group compared to controls. The three most abundant phyla were Bacteroidetes, Firmicutes, and Proteobacteria, which correlates with the results from Li *et al.*, 2021 (428) and Presti *et al.,* 2018 (367). The clinical impact of these increases should be deeply evaluated.

Finally, it is important to note that this study has some limitations. Some of the patients were recruited during COVID-19 pandemic. However, none of them reported symptoms related to COVID-19 before sample collection and they were not vaccinated in the previous month. In fact, reads belonging to *Coronaviridae* family were not detected in any of the samples collected, so the effects observed could be attributed only to HIV infection and/or ART status. Besides, the number of patients in each group is small (what increases the probability of type-II error), but it was big enough to detect differences between groups, similarly as what has been observed in other studies (349,353). Moreover, some differences between the controls and the HIV-infected groups were detected, such as gender, age, and smoking habits, all of them factors that could have an impact on GM.

However, the two HIV-infected groups were well-balanced in terms of these factors, so the differences observed between them will be independent from these factors and could be attributed to INSTIs-based treatments. In addition, when the control group was compared with all HIV-infected patients (both naive and INSTIs-treated together) no statistically significantly differences were observed in age. Moreover, we performed a study comparing the control/uninfected group *vs.* naive group controlled by age (splitting into two groups, "young" and "aged", according to the median age of the population (38 years)) and only differences were observed on β-diversity, suggesting that age could be a factor that could have a specific impact on gut virome composition although not very strong. However, since the "aged" group only included 3 naive patients from a total of 19, (therefore, the aged group was constituted by almost all treated subjects), the potential role of HIV infection more than age *per se* could be the responsible for such actions. However, more studies with larger cohorts are needed to elucidate the impact of age on gut bacteriome and virome in HIV-infected people. Patients fulfilled a survey focused on dietary habits/patterns to detect those habits that could have an impact on microbiota, such as veganism or excessive consumptions of prebiotics and/or probiotics. None of the patients reported such habits. Finally, the lack of studies carried out in the field of human gut virome makes difficult to compare our results with others. However, we believe that this is more a strength than a limitation, as we contribute to give light to a very exciting and novel field that enrich the knowledge of bacteriome in HIV infection.

To sum up, our study demonstrates that INSTIs, as part of the first-line regimen in treatment-naive individuals, resist and partially restore the actions of HIV infection on BT, subsequent systemic immune, and gut permeability. Thus, INSTIs-based regimens could minimize the disease progression and development of future age-related complications such as CVD. Our study also demonstrates that HIV infection has a direct impact on gut bacteriome and virome (bacteriophages and eukaryotic virus abundances), whereas INSTIs-based treatments were able to mildly reverse these effects, especially on α-diversity indexes, probably because of the strong effects induced by the virus *per se*. In

contrast, HIV-infection and/or INSTIs-based treatments exerted mild effects on salivary bacterial composition.

In general, our results could serve as a first step for future development of coadjuvant therapies (based not only on probiotics/prebiotics but also on phage therapies and/or fecal transplantation) to reduce gut dysbiosis in HIV-infected patients and, therefore, to improve the inflammatory state associated with the infection and the long-term consequences of such state. This will undoubtedly improve the health and quality of life of HIV-infected patients.

7.CONCLUSIONS

1- INSTIs-based treatments were able to reverse the impact of HIV infection on markers of bacterial translocation (sCD14 and LBP), systemic inflammation (TNF-α), cardiovascular risk (VCAM-1 and PAI-1), and gut permeability (calprotectin).

2- INSTIs-based treatments were also able to reverse the impact of HIV-infection on several indexes of α-diversity from gut bacteriome (*Observed features* and *Chao1 index*). However, their effects on gut bacteriome composition were not so marked.

3- Our study confirms that the results previously obtained with raltegravir on gut bacteriome can be partially extrapolated to novel INSTIs-based treatments.

4- Neither HIV-infection nor INSTIs-based treatment had statistically significant effects on the composition of eukaryotic viruses.

5- HIV infection had a significant impact on phages' α-diversity (*Observed Features* and *Fisher's alpha*), β-diversity, differential abundance (some phage taxonomical orders differentially represented), lifecycle (increase of lysogenic phages) and host prediction.

6- INSTIs-based treatment was able to reverse the effects of HIV infection on phages' α-diversity and on the abundance of some phage taxonomical orders.

7- Neither HIV infection nor INSTIs-based treatment exerted a statistically significant impact on α or β-diversity from oral bacteriome. However, some statistically significant differences were observed in the abundance of some bacterial taxonomical orders.

To sum up, our work describes for the first time the impact of HIV infection and, especially, the actions of INSTIs-based treatments, on gut bacteriome and

virome and on oral bacteriome. These results and the conclusions arisen corroborates the good profile described for INSTIs in the treatment of naive HIV-infected patients and could suggest a protective role on the disease progression and in the appearance of future age-related complications such as cardiovascular events. In addition, our research represents a "starting point" to understand the interactions between gut bacteriome and virome. The fully knowledge of such interactions could allow the development of coadjuvant therapies based on microbiota modulation (prebiotics, probiotics, phage therapy, faecal transplantation…) to improve the prognosis and quality of life of these patients.

8.CONCLUSIONES

1- El tratamiento basado en INIs fue capaz de revertir el impacto de la infección por el VIH sobre marcadores de translocación bacteriana (sCD14 y LBP), inflamación sistémica (TNF-α), riesgo cardiovascular (VCAM-1 y PAI-1) y permeabilidad intestinal (calprotectina).

2- El tratamiento basado en INIs fue capaz de revertir el impacto de la infección por el VIH sobre la α-diversidad (*Observed features* y *Chao1 index*) del bacterioma intestinal. Sin embargo, sus efectos sobre la composición del bacterioma intestinal no fueron tan acusados.

3- Nuestro estudio confirma que los resultados obtenidos previamente con raltegravir sobre el bacterioma intestinal pueden ser parcialmente extrapolados a los actuales INIs.

4- Ni la infección por VIH ni los tratamientos basados en INIs tuvieron efectos estadísticamente significativos sobre la composición de los virus eucarióticas.

5- En cuanto a los fagos, la infección por el VIH tuvo un impacto sobre la α-diversidad (*Observed features* y *Fisher's alpha*), la β-diversidad, la abundancia diferencial (algunos órdenes taxonómicos de fagos diferencialmente representados), el ciclo de vida (incrementos de fagos lisogénicos) y la predicción del anfitrión.

6- Los tratamientos basados en INIs fueron capaces de revertir los efectos sobre la α-diversidad y sobre la abundancia de algunos órdenes taxonómicos de fagos.

7- Ni la infección por el VIH ni el tratamiento basado en INIs tuvo un impacto estadísticamente significativo sobre la α o la β-diversidad del bacterioma oral. Sin embargo, se observaron algunas diferencias estadísticamente

significativas en la abundancia diferencial (algunos órdenes taxonómicos bacterianos diferencialmente representados).

En conclusión, nuestro trabajo describe por primera vez el impacto de la infección por el VIH y, especialmente, las acciones de los tratamientos basados en INIs, sobre el bacterioma y el viroma intestinal y sobre el bacterioma oral. Estos resultados y las conclusiones obtenidas corroboran el buen perfil descrito para los INIs en el tratamiento de pacientes VIH naïve y podrían sugerir un efecto protector en la progresión de la enfermedad y en el desarrollo de futuras complicaciones relacionadas con la edad como los eventos cardiovasculares. Además, nuestra investigación representa un "punto de partida" para entender las posibles interacciones entre el bacterioma y el viroma intestinal en estos pacientes. El completo entendimiento de estas interacciones podría permitir el desarrollo de terapias coadyuvantes basadas en la modulación de la microbiota (prebióticos, probióticos, terapia con fagos, trasplante fecal…) para mejorar la calidad de vida de estos pacientes.

9.PUBLICATIONS AND CONFERENCES

SCIENTIFIC ARTICLES PUBLISHED AND CONFERENCES IN WHICH THE PhD STUDENT HAS PARTICIPATED

Published articles regarding the present Doctoral Thesis

- Villoslada-Blanco Pablo *et al.* (2021) 'Lights and Shadows of Microbiota Modulation and Cardiovascular Risk in HIV Patients', International Journal of Environmental Research and Public Health, 18(13):6837.
- Villoslada-Blanco Pablo *et al.* (2022) 'Integrase Inhibitors Partially Restore Bacterial Translocation, Inflammation and Gut Permeability Induced by HIV Infection: Impact on Gut Microbiota', Infectious Diseases and Therapy, 11(4):1541-1557.
- Villoslada-Blanco Pablo *et al.* (2022) 'Impact of HIV infection and integrase strand transfer inhibitors-based treatment on gut virome', Scientific Reports, In Review.

Published articles carried out in collaboration

- Ochoa-Callejero Laura *et al.* (2021) 'Circulating Levels of Calcitonin Gene-Related Peptide Are Lower in COVID-19 Patients', Journal of Endocrine Society, 5(3):bvaa199.
- Ochoa-Callejero Laura *et al.* (2021) 'Response to Letter to the Editor from Anis Abobaker: Circulating Levels of Calcitonin Gene-Related Peptide Are Lower in COVID-19 Patients', Journal of Endocrine Society, 5(10):bvab053.
- Íñiguez María *et al*. (2021) 'ACE Gene Variants Rise the Risk of Severe COVID-19 in Patients With Hypertension, Dyslipidemia or Diabetes: A Spanish Pilot Study', Frontiers in Endocrinology, 12:688071.
- Íñiguez María *et al*. (2021) 'Corrigendum: ACE Gene Variants Rise the Risk of Severe COVID-19 in Patients With Hypertension, Dyslipidemia or Diabetes: A Spanish Pilot Study', Frontiers in Endocrinology, 12:771445.

Conferences

- Pérez-Matute Patricia *et al.* (2019) 'Autologous fecal transplantation potentiates caloric restriction effects on body weight and adiposity by decreasing energy efficiency and by increasing adipose tissue lipolysis in high-fat fed mice', 42nd Congress of the Spanish Society of Biochemistry and Molecular Biology, SSBMB.

- Íñiguez María *et al.* (2020) 'Influencia de polimorfismos de ACE1 y ACE2 en la severidad de la COVID-19 en La Rioja', I Congreso Nacional COVID, SEIMC.

- Villoslada-Blanco Pablo *et al.* (2022) 'Characterization of gut phages in HIV-infected patients', International Virus Bioinformatics Meeting (ViBioM) 2022, EVBC.

- Pichel José G. *et al.* (2022) 'Serum Levels of IFG System Proteins Change with the Severity of COVID-19', Spanish Symposium on IFGs and Insulin (SSii) 2022: Implications in Physiology and Disease, SSBBM.

- Villoslada-Blanco Pablo *et al.* (2022) 'Los inhibidores de la integrasa restauran la traslocación bacteriana, la inflamación y los cambios en la microbiota intestinal inducidos por la infección por el VIH', XXV Congreso Nacional de la Sociedad Española de Enfermedades Infecciosas y Microbiología Clínica, SEIMC. PREMIO A LA MEJOR COMUNICACIÓN.

- Villoslada-Blanco Pablo *et al.* (2022) 'Primera descripción del impacto de la infección por el VIH y del tratamiento con inhibidores de la integrasa sobre el viroma intestinal', XXV Congreso Nacional de la Sociedad Española de Enfermedades Infecciosas y Microbiología Clínica, SEIMC.

- Pichel José G. *et al.* (2022) 'Serum Levels of IFG System Proteins Change with the Severity of COVID-19', The Biochemistry Global Summit (the IUBMB–FEBS–PABMB Congress 2022), IUBMB–FEBS–PABMB.

- Pichel José G. *et al.* (2022) 'Serum Levels of IFG System Proteins Change with the Severity of COVID-19', 44th Congress of the Spanish Society of Biochemistry and Molecular Biology, SSBMB.

10. REFERENCES

1. Gottlieb MS, Schroff R, Schanker HM, Weisman JD, Fan PT, Wolf RA, et al. Pneumocystis carinii pneumonia and mucosal candidiasis in previously healthy homosexual men: evidence of a new acquired cellular immunodeficiency. N Engl J Med. 1981;305(24):1425–31.

2. Centers for Disease Control [CDC]. Update on acquired immune deficiency syndrome (AIDS)--United States. MMWR Morb Mortal Wkly Rep. 1982;31(37):507–8.

3. Centers for Disease Control [CDC]. A Cluster of Kaposi's Sarcoma and Pneumocystis carinii Pneumonia among Homosexual Male Residents of Los Angeles and range Counties, California. Morb Mortal Wkly Rep. 1982;31(23):305–7.

4. Barré-Sinoussi F, Chermann J-C, Rey F, Nugeyre MT, Chamaret S, Gruest J, et al. Isolation of a T-lymphotropic retrovirus from a patient at risk for acquired immune deficiency syndrome (AIDS). Science (80-). 1983;220(4599):868–71.

5. Gallo RC, Sarin PS, Gelmann EP, Robert-Guroff M, Richardson E, Kalyanaraman VS, et al. Isolation of human T-cell leukemia virus in acquired immune deficiency syndrome (AIDS). Science (80-). 1983;220(4599):865–7.

6. Coffin J, Haase A, Levy JA, Montagnier L, Oroszlan S, Teich N TH, Toyoshima K, Varmus H, Vogt P et al. What to call the AIDS virus? Nature. 1986;321(6065):10.

7. Weiss RA. On Viruses, Discovery, and Recognition. Cell. 2008;135(6):983–6.

8. Clavel F, Guetard D, Brun-Vézinet F, Chamaret S, Rey M-A, Santos-

Ferreira MO, et al. Isolation of a new human retrovirus from West African patients with AIDS. Science (80-). 1986;233(4761):343–6.

9.   Gao F, Bailes E, Robertson DL, Chen Y, Rodenburg CM, Michael SF, et al. Origin of HIV-1 in the chimpanzee Pan troglodytes troglodytes. Nature. 1999;397(6718):436.

10.   Sharp PM, Hahn BH. Origins of HIV and the AIDS pandemic. Cold Spring Harb Perspect Med. 2011;1(1):a006841.

11.   Faria NR, Rambaut A, Suchard MA, Baele G, Bedford T, Ward MJ, et al. The early spread and epidemic ignition of HIV-1 in human populations. Science (80-). 2014;346(6205):56–61.

12.   Luciw PA. Human immunodeficiency viruses and their replication. Fields Virol. 1996;2:1881–952.

13.   German Advisory Committe Blood. Human Immunodeficiency Virus (HIV). Transfus Med Hemother. 2016;43(3):203–22.

14.   Nyamweya S, Hegedus A, Jaye A, Rowland-Jones S, Flanagan KL, Macallan DC. Comparing HIV-1 and HIV-2 infection: Lessons for viral immunopathogenesis. Rev Med Virol. 2013;23(4):221–40.

15.   Popper SJ, Sarr AD, Travers KU, Gueye-Ndiaye A, Mboup S, Essex ME, et al. Lower human immunodeficiency virus (HIV) type 2 viral load reflects the difference in pathogenicity of HIV-1 and HIV-2. J Infect Dis. 1999;180(4):1116–21.

16.   Simon F, Mauclère P, Roques P, Loussert-Ajaka I, Müller-Trutwin MC, Saragosti S, et al. Identification of a new human immunodeficiency virus type 1 distinct from group M and group O. Nat Med. 1998;4(9):1032–7.

17.   Plantier JC, Leoz M, Dickerson JE, De Oliveira F, Cordonnier F, Lemée V, et al. A new human immunodeficiency virus derived from gorillas. Nat Med.

2009;15(8):871–2.

18. Vallari A, Holzmayer V, Harris B, Yamaguchi J, Ngansop C, Makamche F, et al. Confirmation of Putative HIV-1 Group P in Cameroon. J Virol. 2011;85(3):1403–7.

19. Peeters M, Sharp PM. Genetic diversity of HIV-1: The moving target. AIDS. 2000;14(Suppl 3):S129–40.

20. Merson MH, O'Malley J, Serwadda D, Apisuk C. The history and challenge of HIV prevention. Lancet. 2008;372(9637):475–88.

21. WHO HIV data [Internet]. Available from: https://www.who.int/hiv/data/en/

22. WHO facts [Internet]. Available from: https://www.who.int/news-room/fact-sheets/detail/the-top-10-causes-of-death

23. Gelderblom HR. Assembly and morphology of HIV: Potential effect of structure on viral function. AIDS. 1991;5(6):617–37.

24. Niedrig M, Gelderblom HR, Pauli G, Marz J, Bickhard H, Wolf H, et al. Inhibition of infectious human immunodeficiency virus type 1 particle formation by Gag protein-derived peptides. J Gen Virol. 1994;75(6):1469–74.

25. US National Institute of Health (NIH) [Internet]. Available from: https://www.nih.gov/

26. Dean M, Carrington M, Winkler C, Huttley GA, Smith MW, Allikmets R, et al. Genetic restriction of HIV-1 infection and progression to AIDS by a deletion allele of the CKR5 structural gene. Science (80-). 1996;273(5283):1856–62.

27. Feng Y, Broder CC, Kennedy PE, Berger EA. HIV-1 entry cofactor: Functional cDNA cloning of a seven-transmembrane, G protein-coupled receptor. Science (80-). 1996;272(5263):872–7.

28. Archin NM, Sung JM, Garrido C, Soriano-Sarabia N, Margolis DM. Eradicating HIV-1 infection: Seeking to clear a persistent pathogen. Nat Rev Microbiol. 2014;12(11):750–64.

29. Stein BS, Gowda SD, Lifson JD, Penhallow RC, Bensch KG, Engleman EG. pH-independent HIV entry into CD4-positive T cells via virus envelope fusion to the plasma membrane. Cell. 1987;49(5):659–68.

30. Sousa R, Chung YJ, Rose JP, Wang BC. Crystal structure of bacteriophage T7 RNA polymerase at 3.3 Å resolution. Nature. 1993;364(6438):593–9.

31. Pan X, Baldauf HM, Keppler OT, Fackler OT. Restrictions to HIV-1 replication in resting CD4 + T lymphocytes. Cell Res. 2013;23(7):876–85.

32. Perelson AS, Neumann AU, Markowitz M, Leonard JM, Ho DD. HIV-1 dynamics in vivo: Virion clearance rate, infected cell life-span, and viral generation time. Science (80-). 1996;271(5255):1582–886.

33. Zeng M, Southern PJ, Reilly CS, Beilman GJ, Chipman JG, Schacker TW, et al. Lymphoid tissue damage in HIV-1 infection depletes naïve T cells and limits T cell reconstitution after antiretroviral therapy. PLoS Pathog. 2012;8(1):e1002437.

34. Moudgil T, Daar ES. Infectious decay of human immunodeficiency virus type 1 in plasma. J Infect Dis. 1993;167(1):210–2.

35. HIV.gov [Internet]. Available from: hiv.gov

36. Mogensen TH, Melchjorsen J, Larsen CS, Paludan SR. Innate immune recognition and activation during HIV infection. Retrovirology. 2010;7:54.

37. Nasi M, Pinti M, Mussini C, Cossarizza A. Persistent inflammation in HIV infection: established concepts, new perspectives. Immunol Lett. 2014;161(2):184–8.

38. Wu L, KewalRamani VN. Dendritic-cell interactions with HIV: infection and

viral dissemination. Nat Rev Immunol. 2006;6(11):859.

39. Lapenta C, Boirivant M, Marini M, Santini SM, Logozzi M, Viora M, et al. Human intestinal lamina propria lymphocytes are naturally permissive to HIV-1 infection. Eur J Immunol. 1999;29(4):1202–8.

40. Churchill MJ, Deeks SG, Margolis DM, Siliciano RF, Swanstrom R. HIV reservoirs: what, where and how to target them. Nat Rev Microbiol. 2016;14(1):55.

41. Murray AJ, Kwon KJ, Farber DL, Siliciano RF. The latent reservoir for HIV-1: how immunologic memory and clonal expansion contribute to HIV-1 persistence. J Immunol. 2016;197(2):407–17.

42. Brenchley JM, Paiardini M, Knox KS, Asher AI, Cervasi B, Asher TE, et al. Differential Th17 CD4 T-cell depletion in pathogenic and nonpathogenic lentiviral infections. Blood. 2008;112(7):2826–35.

43. ElHed A, Unutmaz D. Th17 cells and HIV infection. Curr Opin HIV AIDS. 2010;5(2):146.

44. An P, Winkler CA. Host genes associated with HIV/AIDS: advances in gene discovery. Trends Genet. 2010;26(3):119–31.

45. Kahn JO, Walker BD. Acute human immunodeficiency virus type 1 infection. N Engl J Med. 1998;339(1):33–9.

46. Fauci AS, Pantaleo G, Stanley S, Weissman D. Immunopathogenic mechanisms of HIV infection. Ann Intern Med. 1996;124(7):654–63.

47. Douek DC. Disrupting T-cell homeostasis: how HIV-1 infection causes disease. AIDS Rev. 2003;5(3):172–7.

48. Okoye AA, Picker LJ. CD 4+ T-cell depletion in HIV infection: mechanisms of immunological failure. Immunol Rev. 2013;254(1):54–64.

49. Deeks SG, Lewin SR, Havlir D V. The end of AIDS: HIV infection as a chronic disease. Lancet. 2013;382(9903):1523–33.

50. Initiation of Antiretroviral Therapy in Early Asymptomatic HIV Infection. N Engl J Med. 2015;373(9):795–807.

51. Kitahata MM, Gange SJ, Abraham AG, Merriman B, Saag MS, Justice AC, et al. Effect of Early versus Deferred Antiretroviral Therapy for HIV on Survival. N Engl J Med. 2009;360(18):1815–26.

52. Samji H, Cescon A, Hogg RS, Modur SP, Althoff KN, Buchacz K, et al. Closing the gap: Increases in life expectancy among treated HIV-positive individuals in the United States and Canada. PLoS One. 2013;8(12):e81355.

53. Cohen MS, Chen YQ, McCauley M, Gamble T, Hosseinipour MC, Kumarasamy N, et al. Antiretroviral Therapy for the Prevention of HIV-1 Transmission. N Engl J Med. 2016;375(9):830–9.

54. McNairy ML, El-Sadr WM. Antiretroviral therapy for the prevention of HIV transmission: What will it take? Clin Infect Dis. 2014;58(7):1003–11.

55. Rodger AJ, Cambiano V, Bruun T, Vernazza P, Collins S, Van Lunzen J, et al. Sexual activity without condoms and risk of HIV transmission in serodifferent couples when the HIV-positive partner is using suppressive antiretroviral therapy. JAMA - J Am Med Assoc. 2016;316(2):171–81.

56. Arts EJ, Hazuda DJ. HIV-1 antiretroviral drug therapy. Cold Spring Harb Perspect Med. 2012;2(4):a007161.

57. Barré-Sinoussi F, Ross AL, Delfraissy J-F. Past, present and future: 30 years of HIV research. Nat Rev Microbiol. 2013;11(12):877.

58. Pau AK, George JM. Antiretroviral therapy: current drugs. Infect Dis Clin. 2014;28(3):371–402.

59. Gandhi M, Gandhi RT. Single-pill combination regimens for treatment of HIV-1 infection. N Engl J Med. 2014;371(3):248–59.

60. SIDA P de expertos de G y PN sobre el. Documento de consenso de GeSIDA/Plan Nacional sobre el SIDA respecto al tratamiento antirretroviral en adultos infectados por el virus de la inmunodeficiencia humana. 2022.

61. Esté JA, Telenti A. HIV entry inhibitors. Lancet. 2007;370(9581):81–8.

62. Kilby JM, Eron JJ. Novel Therapies Based on Mechanisms of HIV-1 Cell Entry. N Engl J Med. 2003;348(22):2228–38.

63. Wilkin TJ, Gulick RM. CCR5 antagonism in HIV Infection: Current concepts and future opportunities. Annu Rev Med. 2012;63:81–93.

64. Food and Drug Administration (FDA) [Internet]. Available from: https://www.fda.gov/

65. European Medicines Agency (EMA) [Internet]. Available from: https://www.ema.europa.eu/en

66. Tilton JC, Doms RW. Entry inhibitors in the treatment of HIV-1 infection. Antiviral Res. 2010;85(1):91–100.

67. Cervia JS, Smith MA. Enfuvirtide (T-20): A Novel Human Immunodeficiency Virus Type 1 Fusion Inhibitor. Clin Infect Dis. 2003;37(8):1102–6.

68. Schauer G, Leuba S, Sluis-Cremer N. Biophysical Insights into the Inhibitory Mechanism of Non-Nucleoside HIV-1 Reverse Transcriptase Inhibitors. Biomolecules. 2013;3(4):889–904.

69. Clavel F, Hance AJ. HIV Drug Resistance. N Engl J Med. 2004;350(10):1023–35.

70. Singh K, Marchand B, Kirby KA, Michailidis E, Sarafianos SG. Structural

aspects of drug resistance and inhibition of HIV-1 reverse transcriptase. Viruses. 2010;2(2):606–38.

71. Grandgenett DP. Multifunctional facets of retrovirus integrase. World J Biol Chem. 2015;6(3):83–94.

72. Ingale KB, Bhatia MS. HIV-1 integrase inhibitors: A review of their chemical development. Antivir Chem Chemother. 2012;22(3):95–105.

73. Alan E, Peter C. Retroviral Integrase Structure and DNA Recombination Mechanism. Microbiol Spectr. 2015;2(6):1–22.

74. Hazuda DJ. HIV integrase as a target for antiretroviral therapy. Curr Opin HIV AIDS. 2012;7(5):38–389.

75. Lataillade M, Kozal MJ. The hunt for HIV-1 integrase inhibitors. AIDS Patient Care STDS. 2006;20(7):489–501.

76. Brooks KM, Sherman EM, Egelund EF, Brotherton A, Durham S, Badowski ME, et al. Integrase Inhibitors: After 10 Years of Experience, Is the Best Yet to Come? Pharmacotherapy. 2019;39(5):576–98.

77. Smith SJ, Zhao XZ, Burke TR, Hughes SH. Efficacies of Cabotegravir and Bictegravir against drug-resistant HIV-1 integrase mutants. Retrovirology. 2018;15(1):37.

78. GESIDA guidelines [Internet]. Available from: https://gesida-seimc.org/category/guias-clinicas/

79. 123rf [Internet]. Available from: https://es.123rf.com/

80. Selleckchem [Internet]. Available from: https://www.selleckchem.com/

81. Bowerman B, Brown PO, Bishop JM, Varmus HE. A nucleoprotein complex mediates the integration of retroviral DNA. Genes Dev. 1989;3(4):469–78.

82. Miller MD, Farnet CM, Bushman FD. Human immunodeficiency virus type 1 preintegration complexes: studies of organization and composition. J Virol. 1997;71(7):5382–90.

83. Wei SQ, Mizuuchi K, Craigie R. A large nucleoprotein assembly at the ends of the viral DNA mediates retroviral DNA integration. EMBO J. 1997;3(4):469–78.

84. Engelman A, Mizuuchi K, Craigie R. HIV-1 DNA integration: Mechanism of viral DNA cleavage and DNA strand transfer. Cell. 1991;67(6):1211–21.

85. Craigie R, Fujiwara T, Bushman F. The IN protein of Moloney murine leukemia virus processes the viral DNA ends and accomplishes their integration in vitro. Cell. 1990;62(4):829–37.

86. Hare S, Maertens GN, Cherepanov P. 3′-Processing and strand transfer catalysed by retroviral integrase in crystallo. EMBO J. 2012;31(13):3020–8.

87. Jóźwik IK, Passos DO, Lyumkis D. Structural Biology of HIV Integrase Strand Transfer Inhibitors. Trends Pharmacol Sci. 2020;41(9):611–26.

88. Hazuda DJ, Felock P, Witmer M, Wolfe A, Stillmock K, Grobler JA, et al. Inhibitors of strand transfer that prevent integration and inhibit HIV-1 replication in cells. Science (80-). 2000;287(5453):646–50.

89. Yang LL, Li Q, Zhou LB, Chen SQ. Meta-analysis and systematic review of the efficacy and resistance for human immunodeficiency virus type 1 integrase strand transfer inhibitors. Int J Antimicrob Agents. 2019;54(5):547–55.

90. Margolis DA, Brinson CC, Smith GHR, de Vente J, Hagins DP, Eron JJ, et al. Cabotegravir plus rilpivirine, once a day, after induction with cabotegravir plus nucleoside reverse transcriptase inhibitors in antiretroviral-naive adults with HIV-1 infection (LATTE): a randomised,

phase 2b, dose-ranging trial. Lancet Infect Dis. 2015 Oct;15(10):1145–55.

91.   Elzi L, Erb S, Furrer H, Cavassini M, Calmy A, Vernazza P, et al. Adverse events of raltegravir and dolutegravir. AIDS. 2017 Aug;31(13):1853–8.

92.   Gallant J, Lazzarin A, Mills A, Orkin C, Podzamczer D, Tebas P, et al. Bictegravir, emtricitabine, and tenofovir alafenamide versus dolutegravir, abacavir, and lamivudine for initial treatment of HIV-1 infection (GS-US-380-1489): a double-blind, multicentre, phase 3, randomised controlled non-inferiority trial. Lancet (London, England). 2017 Nov;390(10107):2063–72.

93.   Pantaleo G, Graziosi C, Butini L, Pizzo PA, Schnittman SM, Kotler DP, et al. Lymphoid organs function as major reservoirs for human immunodeficiency virus. Proc Natl Acad Sci. 1991;88(21):9838–42.

94.   Symons J, Chopra A, Malatinkova E, De Spiegelaere W, Leary S, Cooper D, et al. HIV integration sites in latently infected cell lines: evidence of ongoing replication. Retrovirology. 2017;14(1):1–11.

95.   Appay V, Sauce D. Immune activation and inflammation in HIV-1 infection: causes and consequences. J Pathol A J Pathol Soc Gt Britain Irel. 2008;214(2):231–41.

96.   Rossetti B, Meini G, Bianco C, Lamonica S, Mondi A, Belmonti S, et al. Total cellular HIV-1 DNA decreases after switching to raltegravir-based regimens in patients with suppressed HIV-1 RNA. J Clin Virol. 2017;91:18–24.

97.   Chege D, Kovacs C, la Porte C, Ostrowski M, Raboud J, Su D, et al. Effect of raltegravir intensification on HIV proviral DNA in the blood and gut mucosa of men on long-term therapy: a randomized controlled trial. Aids. 2012;26(2):167–74.

98.   Llibre JM, Buzón MJ, Massanella M, Esteve A, Dahl V, Puertas MC, et al.

Treatment intensification with raltegravir in subjects with sustained HIV-1 viraemia suppression: a randomized 48-week study. Antivir Ther. 2012;17(2):355.

99. Buzón MJ, Massanella M, Llibre JM, Esteve A, Dahl V, Puertas MC, et al. HIV-1 replication and immune dynamics are affected by raltegravir intensification of HAART-suppressed subjects. Nat Med. 2010;16(4):460.

100. Morón-López S, Navarro J, Jimenez M, Rutsaert S, Urrea V, Puertas MC, et al. Switching From a Protease Inhibitor–based Regimen to a Dolutegravir-based Regimen: A Randomized Clinical Trial to Determine the Effect on Peripheral Blood and Ileum Biopsies From Antiretroviral Therapy–suppressed Human Immunodeficiency Virus–infected Indi. Clin Infect Dis. 2019;69(8):1320–8.

101. Flexner C. HIV-protease inhibitors. N Engl J Med. 1998;338(18):1281–93.

102. Adamson CS. Protease-Mediated Maturation of HIV: Inhibitors of Protease and the Maturation Process. Mol Biol Int. 2012;2012:604261.

103. Zeldin RK, Petruschke RA. Pharmacological and therapeutic properties of ritonavir-boosted protease inhibitor therapy in HIV-infected patients. J Antimicrob Chemother. 2004;53(1):4–9.

104. Hair M, Sharpe J. Fast facts about the human microbiome. Center for ecogenetics & Environmental Health. 2015.

105. Jorth P, Turner KH, Gumus P, Nizam N, Buduneli N, Whiteley M. Metatranscriptomics of the human oral microbiome during health and disease. MBio. 2014;5(2):e01012–4.

106. Lynch S V., Pedersen O. The Human Intestinal Microbiome in Health and Disease. N Engl J Med. 2016;375(24):2369–79.

107. Morgan XC, Segata N, Huttenhower C. Biodiversity and functional

genomics in the human microbiome. Trends Genet. 2013;29(1):51–8.

108. Fujimura KE, Slusher NA, Cabana MD, Lynch S V. Role of the gut microbiota in defining human health. Expert Rev Anti Infect Ther. 2010;8(4):435–54.

109. Villanueva-Millán MJ, Pérez-Matute P, Oteo JA. Gut microbiota: a key player in health and disease. A review focused on obesity. J Physiol Biochem. 2015;71(3):509–25.

110. Leviatan S, Shoer S, Rothschild D, Gorodetski M, Segal E. An expanded reference map of the human gut microbiome reveals hundreds of previously unknown species. Nat Commun. 2022 Jul;13(1):3863.

111. O'Hara AM, Shanahan F. The gut flora as a forgotten organ. EMBO Rep. 2006;7(7):688–93.

112. Kim JK, Baker LA, Davarian S, Crimmins E. Oral health problems and mortality. J Dent Sci. 2013;8(2):115–20.

113. Ley RE, Hamady M, Lozupone C, Turnbaugh PJ, Ramey RR, Bircher JS, et al. Evolution of mammals and their gut microbes. Science (80-). 2008;320(5883):1647–51.

114. Dethlefsen L, McFall-Ngai M, Relman DA. An ecological and evolutionary perspective on humang-microbe mutualism and disease. Nature. 2007;449(7164):811–8.

115. Arumugam M, Raes J, Pelletier E, Le Paslier D, Yamada T, Mende DR, et al. Enterotypes of the human gut microbiome. Nature. 2011;473(7346):174.

116. Wu GD, Chen J, Hoffmann C, Bittinger K, Chen Y-Y, Keilbaugh SA, et al. Linking long-term dietary patterns with gut microbial enterotypes. Science (80-). 2011;334(6052):105–8.

117. Costea PI, Hildebrand F, Arumugam M, Bäckhed F, Blaser MJ, Bushman

FD, et al. Enterotypes in the landscape of gut microbial community composition. Nat Microbiol. 2018 Jan;3(1):8–16.

118. Vandeputte D, Kathagen G, D'Hoe K, Vieira-Silva S, Valles-Colomer M, Sabino J, et al. Quantitative microbiome profiling links gut community variation to microbial load. Nature. 2017;551(7681):507–11.

119. DiGiulio DB, Romero R, Amogan HP, Kusanovic JP, Bik EM, Gotsch F, et al. Microbial prevalence, diversity and abundance in amniotic fluid during preterm labor: a molecular and culture-based investigation. PLoS One. 2008 Aug;3(8):e3056.

120. Rautava S, Luoto R, Salminen S, Isolauri E. Microbial contact during pregnancy, intestinal colonization and human disease. Nat Rev Gastroenterol Hepatol. 2012;9(10):565.

121. Wang B, Li L. Who determines the outcomes of HBV exposure? Trends Microbiol. 2015;23(6):328–9.

122. Macpherson AJ, Harris NL. Interactions between commensal intestinal bacteria and the immune system. Nat Rev Immunol. 2004;4(6):478–85.

123. Ottman N, Smidt H, De Vos WM, Belzer C. The function of our microbiota: who is out there and what do they do? Front Cell Infect Microbiol. 2012;2:104.

124. Whitman WB, Coleman DC, Wiebe WJ. Prokaryotes: The unseen majority. Proc Natl Acad Sci U S A. 1998;95(12):6578–83.

125. Liu Q, Duan ZP, Ha DK, Bengmark S, Kurtovic J, Riordan SM. Synbiotic Modulation of Gut Flora: Effect on Minimal Hepatic Encephalopathy in Patients with Cirrhosis. Hepatology. 2004;39(5):1441–9.

126. Scanlan PD, Shanahan F, Clune Y, Collins JK, O'Sullivan GC, O'Riordan M, et al. Culture-independent analysis of the gut microbiota in colorectal

cancer and polyposis. Environ Microbiol. 2008;10(3):789–98.

127. Bäckhed F, Ding H, Wang T, Hooper L V., Gou YK, Nagy A, et al. The gut microbiota as an environmental factor that regulates fat storage. Proc Natl Acad Sci U S A. 2004;101(44):15718–23.

128. Bäckhed F, Ley RE, Sonnenburg JL, Peterson DA, Gordon JI. Host-bacterial mutualism in the human intestine. Science (80-). 2005;307(5717):1915–20.

129. Shen J, Obin MS, Zhao L. The gut microbiota, obesity and insulin resistance. Mol Aspects Med. 2013;34(1):39–58.

130. Martínez I, Wallace G, Zhang C, Legge R, Benson AK, Carr TP, et al. Diet-induced metabolic improvements in a hamster model of hypercholesterolemia are strongly linked to alterations of the gut microbiota. Appl Environ Microbiol. 2009;75(12):4175–84.

131. Brenchley JM, Douek DC. Microbial translocation across the GI tract. Annu Rev Immunol. 2012;30:149–73.

132. Gill SR, Pop M, DeBoy RT, Eckburg PB, Turnbaugh PJ, Samuel BS, et al. Metagenomic analysis of the human distal gut microbiome. Science (80-). 2006;312(5778):1355–9.

133. Wilson ID, Nicholson JK. The role of gut microbiota in drug response. Curr Pharm Des. 2009;15(13):1519–23.

134. Kamada N, Chen GY, Inohara N, Núñez G. Control of pathogens and pathobionts by the gut microbiota. Nat Immunol. 2013;14(7):685.

135. Guarner F, Malagelada J-R. Gut flora in health and disease. Lancet. 2003;361(9356):512–9.

136. Kamada N, Núñez G. Role of the gut microbiota in the development and function of lymphoid cells. J Immunol. 2013;190(4):1389–95.

137. Geuking MB, Cahenzli J, Lawson MAE, Ng DCK, Slack E, Hapfelmeier S, et al. Intestinal bacterial colonization induces mutualistic regulatory T cell responses. Immunity. 2011;34(5):794–806.

138. Medina M, Izquierdo E, Ennahar S, Sanz Y. Differential immunomodulatory properties of Bifidobacterium logum strains: Relevance to probiotic selection and clinical applications. Clin Exp Immunol. 2007;150(3):531–8.

139. Guilloteau P, Martin L, Eeckhaut V, Ducatelle R, Zabielski R, Van Immerseel F. From the gut to the peripheral tissues: the multiple effects of butyrate. Nutr Res Rev. 2010;23(2):366–84.

140. Lyte M. Microbial endocrinology in the microbiome-gut-brain axis: how bacterial production and utilization of neurochemicals influence behavior. PLoS Pathog. 2013;9(11):e1003726.

141. Wang B, Mao Y-K, Diorio C, Pasyk M, Wu RY, Bienenstock J, et al. Luminal administration ex vivo of a live Lactobacillus species moderates mouse jejunal motility within minutes. FASEB J. 2010;24(10):4078–88.

142. Moreno-Arribas M, Bartolomé B, Peñalvo JL, Pérez-Matute P, Motilva MJ. Relationship between Wine Consumption, Diet and Microbiome Modulation in Alzheimer's Disease. Nutrients. 2020;12(10):3082.

143. Matsumoto M, Kibe R, Ooga T, Aiba Y, Sawaki E, Koga Y, et al. Cerebral low-molecular metabolites influenced by intestinal microbiota: a pilot study. Front Syst Neurosci. 2013;7:9.

144. Gómez Eguílaz M, Ramón Trapero JL, Pérez Martínez L, Blanco JR. El eje microbiota-intestino-cerebro y sus grandes proyecciones. Rev Neurol. 2019;68(3):111–7.

145. Evenepoel P, Poesen R, Meijers B. The gut-kidney axis. Pediatr Nephrol. 2017 Nov;32(11):2005–14.

146. Bartolomaeus H, McParland V, Wilck N. [Gut-heart axis : How gut bacteria influence cardiovascular diseases]. Herz. 2020 Apr;45(2):134–41.

147. Marsland BJ, Trompette A, Gollwitzer ES. The Gut-Lung Axis in Respiratory Disease. Ann Am Thorac Soc. 2015 Nov;12 Suppl 2:S150-6.

148. Xu L, Yang CS, Liu Y, Zhang X. Effective Regulation of Gut Microbiota With Probiotics and Prebiotics May Prevent or Alleviate COVID-19 Through the Gut-Lung Axis. Front Pharmacol. 2022;13:895193.

149. Eckburg PB, Bik EM, Bernstein CN, Purdom E, Dethlefsen L, Sargent M, et al. Diversity of the human intestinal microbial flora. Science (80-). 2005;308(5728):1635–8.

150. Berg G, Rybakova D, Fischer D, Cernava T, Vergès M-CC, Charles T, et al. Microbiome definition re-visited: old concepts and new challenges. Microbiome. 2020;8(1):103.

151. Arnold JW, Roach J, Azcarate-Peril MA. Emerging Technologies for Gut Microbiome Research. Trends Microbiol. 2016;24(11):887–901.

152. Andrea Azcarate-Peril M, Foster DM, Cadenas MB, Stone MR, Jacobi SK, Stauffer SH, et al. Acute necrotizing enterocolitis of preterm piglets is characterized by dysbiosis of ileal mucosa-associated bacteria. Gut Microbes. 2011;2(4):234–43.

153. Donskey CJ, Hujer AM, Das SM, Pultz NJ, Bonomo RA, Rice LB. Use of denaturing gradient gel electrophoresis for analysis of the stool microbiota of hospitalized patients. J Microbiol Methods. 2003;54(2):249–56.

154. Stewart CJ, Nelson A, Scribbins D, Marrs ECL, Lanyon C, Perry JD, et al. Bacterial and fungal viability in the preterm gut: NEC and sepsis. Arch Dis Child Fetal Neonatal Ed. 2013;98(4):F298-303.

155. Schuppler M, Mertens F, Schon G, Gobel UB. Molecular characterization

of nocardioform actinomycetes in activated sludge by 165 rRNA analysis. Microbiology. 1995;141(Pt 2):513–21.

156. Blaut M, Collins MD, Welling GW, Doré J, van Loo J, de Vos W. Molecular biological methods for studying the gut microbiota: the EU human gut flora project. Br J Nutr. 2002;87(Suppl 2):S203-211.

157. Rhodes AN, Urbance JW, Youga H, Corlew-Newman H, Reddy CA, Klug MJ, et al. Identification of bacterial isolates obtained from intestinal contents associated with 12,000-year-old mastodon remains. Appl Environ Microbiol. 1998;64(2):651–8.

158. Huse SM, Ye Y, Zhou Y, Fodor AA. A core human microbiome as viewed through 16S rRNA sequence clusters. PLoS One. 2012;7(6):e34342.

159. Hiergeist A, Reischl U, Gessner A, Garzetti D, Stecher B, Gálvez EJC, et al. Multicenter quality assessment of 16S ribosomal DNA-sequencing for microbiome analyses reveals high inter-center variability. Int J Med Microbiol. 2016;306(5):334–42.

160. Smith SE, Huang W, Tiamani K, Unterer M, Khan Mirzaei M, Deng L. Emerging technologies in the study of the virome. Curr Opin Virol. 2022;54:101231.

161. Pusch W, Kostrzewa M. Application of MALDI-TOF Mass Spectrometry in Screening and Diagnostic Research. Curr Pharm Des. 2005;11(20):2577–91.

162. Villas-Bôas SG, Mas S, Åkesson M, Smedsgaard J, Nielsen J. Mass spectrometry in metabolome analysis. Mass Spectrom Rev. 2005;24(5):613–46.

163. Tang J. Microbial Metabolomics. Curr Genomics. 2011;12(6):391–403.

164. Lozupone CA, Stombaugh JI, Gordon JI, Jansson JK, Knight R. Diversity,

stability and resilience of the human gut microbiota. Nature. 2012;489(7415):220–30.

165. DeGruttola AK, Low D, Mizoguchi A, Mizoguchi E. Current understanding of dysbiosis in disease in human and animal models. Inflamm Bowel Dis. 2016;22(5):1137–50.

166. Carding S, Verbeke K, Vipond DT, Corfe BM, Owen LJ. Dysbiosis of the gut microbiota in disease. Microb Ecol Heal Dis. 2015;26(1):26191.

167. Potgieter M, Bester J, Kell DB, Pretorius E. The dormant blood microbiome in chronic, inflammatory diseases. FEMS Microbiol Rev. 2015 Jul;39(4):567–91.

168. Hansen J, Gulati A, Sartor RB. The role of mucosal immunity and host genetics in defining intestinal commensal bacteria. Curr Opin Gastroenterol. 2010;26(6):564–71.

169. Frank DN, St. Amand AL, Feldman RA, Boedeker EC, Harpaz N, Pace NR. Molecular-phylogenetic characterization of microbial community imbalances in human inflammatory bowel diseases. Proc Natl Acad Sci U S A. 2007;104(34):13780–5.

170. Sokol H, Pigneur B, Watterlot L, Lakhdari O, Bermúdez-Humarán LG, Gratadoux JJ, et al. Faecalibacterium prausnitzii is an anti-inflammatory commensal bacterium identified by gut microbiota analysis of Crohn disease patients. Proc Natl Acad Sci U S A. 2008;105(43):16731–6.

171. Carroll IM, Chang YH, Park J, Sartor RB, Ringel Y. Luminal and mucosal-associated intestinal microbiota in patients with diarrhea-predominant irritable bowel syndrome. Gut Pathog. 2010;2(1):19.

172. Krogius-Kurikka L, Lyra A, Malinen E, Aarnikunnas J, Tuimala J, Paulin L, et al. Microbial community analysis reveals high level phylogenetic alterations in the overall gastrointestinal microbiota of diarrhoea-

predominant irritable bowel syndrome sufferers. BMC Gastroenterol. 2009;9:95.

173. De Palma G, Nadal I, Medina M, Donat E, Ribes-Koninckx C, Calabuig M, et al. Intestinal dysbiosis and reduced immunoglobulin-coated bacteria associated with coeliac disease in children. BMC Microbiol. 2010;10:63.

174. Shen XJ, Rawls JF, Randall T, Burcal L, Mpande CN, Jenkins N, et al. Molecular characterization of mucosal adherent bacteria and associations with colorectal adenomas. Gut Microbes. 2010;1(3):138–47.

175. Wirbel J, Pyl PT, Kartal E, Zych K, Kashani A, Milanese A, et al. Meta-analysis of fecal metagenomes reveals global microbial signatures that are specific for colorectal cancer. Nat Med. 2019 Apr;25(4):679–89.

176. Mathur R, Barlow GM. Obesity and the microbiome. Expert Rev Gastroenterol Hepatol. 2015;9(8):1087–99.

177. Turnbaugh PJ, Hamady M, Yatsunenko T, Cantarel BL, Duncan A, Ley RE, et al. A core gut microbiome in obese and lean twins. Nature. 2009;457(7228):480–4.

178. Turnbaugh PJ, Ley RE, Mahowald MA, Magrini V, Mardis ER, Gordon JI. An obesity-associated gut microbiome with increased capacity for energy harvest. Nature. 2006;444(7122):1027–31.

179. Bäckhed F, Manchester JK, Semenkovich CF, Gordon JI. Mechanisms underlying the resistance to diet-induced obesity in germ-free mice. Proc Natl Acad Sci U S A. 2007;104(3):979–84.

180. Ridaura VK, Faith JJ, Rey FE, Cheng J, Duncan AE, Kau AL, et al. Gut microbiota from twins discordant for obesity modulate metabolism in mice. Science (80-). 2013;341(6150):1241214.

181. Olivares M, Neef A, Castillejo G, De Palma G, Varea V, Capilla A, et al.

The HLA-DQ2 genotype selects for early intestinal microbiota composition in infants at high risk of developing coeliac disease. Gut. 2015;64(3):406–17.

182. Cámara RJA, Ziegler R, Begré S, Schoepfer AM, Von Känel R. The role of psychological stress in inflammatory bowel disease: Quality assessment of methods of 18 prospective studies and suggestions for future research. Digestion. 2009;80(2):129–39.

183. Mawdsley JE, Rampton DS. Psychological stress in IBD: New insights into pathogenic and therapeutic implications. Gut. 2005;54(10):1481–91.

184. Reyes A, Semenkovich NP, Whiteson K, Rohwer F, Gordon JI. Going viral: next-generation sequencing applied to phage populations in the human gut. Nat Rev Microbiol. 2012;10(9):607–17.

185. Furlan M, Whiteson KL, Auro R, Barr JJ, Stotland A, Wolkowicz R, et al. Bacteriophage adhering to mucus provide a non-host-derived immunity. Proc Natl Acad Sci. 2013;110(26):10771–6.

186. Liang G, Bushman FD. The human virome: assembly, composition and host interactions. Nat Rev Microbiol. 2021 Aug;19(8):514–27.

187. Sinha A, Li Y, Mirzaei MK, Shamash M, Samadfam R, King IL, et al. Transplantation of bacteriophages from ulcerative colitis patients shifts the gut bacteriome and exacerbates the severity of DSS colitis. Microbiome. 2022 Jul;10(1):105.

188. Zuo T, Wong SH, Lam K, Lui R, Cheung K, Tang W, et al. Bacteriophage transfer during faecal microbiota transplantation in Clostridium difficile infection is associated with treatment outcome. Gut. 2018;67(4):634–43.

189. Yang K, Niu J, Zuo T, Sun Y, Xu Z, Tang W, et al. Alterations in the Gut Virome in Obesity and Type 2 Diabetes Mellitus. Gastroenterology. 2021 Oct;161(4):1257-1269.e13.

190. Liang W, Feng Z, Rao S, Xiao C, Xue X, Lin Z, et al. Diarrhoea may be underestimated: a missing link in 2019 novel coronavirus. Gut. 2020 Jun;69(6):1141–3.

191. Zuo T, Zhan H, Zhang F, Liu Q, Tso EYK, Lui GCY, et al. Alterations in Fecal Fungal Microbiome of Patients With COVID-19 During Time of Hospitalization until Discharge. Gastroenterology. 2020 Oct;159(4):1302-1310.e5.

192. Jiang L, Lang S, Duan Y, Zhang X, Gao B, Chopyk J, et al. Intestinal Virome in Patients With Alcoholic Hepatitis. Hepatology. 2020 Dec;72(6):2182–96.

193. Khan Mirzaei M, Khan MAA, Ghosh P, Taranu ZE, Taguer M, Ru J, et al. Bacteriophages Isolated from Stunted Children Can Regulate Gut Bacterial Communities in an Age-Specific Manner. Cell Host Microbe. 2020 Feb;27(2):199-212.e5.

194. Ott SJ, Waetzig GH, Rehman A, Moltzau-Anderson J, Bharti R, Grasis JA, et al. Efficacy of Sterile Fecal Filtrate Transfer for Treating Patients With Clostridium difficile Infection. Gastroenterology. 2017;152(4):799-811.e7.

195. Duan Y, Llorente C, Lang S, Brandl K, Chu H, Jiang L, et al. Bacteriophage targeting of gut bacterium attenuates alcoholic liver disease. Nature. 2019 Nov;575(7783):505–11.

196. Minot S, Bryson A, Chehoud C, Wu GD, Lewis JD, Bushman FD. Rapid evolution of the human gut virome. Proc Natl Acad Sci [Internet]. 2013;110(30):12450–5. Available from: http://www.pnas.org/cgi/doi/10.1073/pnas.1300833110

197. Mukhopadhya I, Segal JP, Carding SR, Hart AL, Hold GL. The gut virome: the 'missing link' between gut bacteria and host immunity? Therap Adv Gastroenterol. 2019;12:1756284819836620.

198. Hunter P. The secret garden's gardeners: research increasingly

appreciates the crucial role of gut viruses for human health and disease. EMBO Rep. 2013;14(8):683–5.

199. Pfeiffer JK, Virgin HW. Viral immunity: Transkingdom control of viral infection and immunity in the mammalian intestine. Science (80-). 2016;351(6270):10.1126/science.aad5872 aad5872.

200. Dalmasso M, Hill C, Ross RP. Exploiting gut bacteriophages for human health. Trends Microbiol. 2014;22(7):399–405.

201. Weinbauer MG. Ecology of prokaryotic viruses. FEMS Microbiol Rev. 2004;28(2):127–81.

202. Saint Girons I, Bourhy P, Ottone C, Picardeau M, Yelton D, Hendrix RW, et al. The LE1 bacteriophage replicates as a plasmid within Leptospira biflexa: construction of an L. biflexa-Escherichia coli shuttle vector. J Bacteriol. 2000;182(20):5700–5.

203. Guerin E, Shkoporov A, Stockdale SR, Clooney AG, Ryan FJ, Sutton TDS, et al. Biology and taxonomy of crAss-like bacteriophages, the most abundant virus in the human gut. Cell Host Microbe. 2018;24(5):653–64.

204. Vander Elst N, Meyer E. Potential therapeutic application of bacteriophages and phage-derived endolysins as alternative treatment of bovine mastitis. Vlaams Diergeneeskd Tijdschr. 2018;87(4):181–7.

205. Breitbart M, Haynes M, Kelley S, Angly F, Edwards RA, Felts B, et al. Viral diversity and dynamics in an infant gut. Res Microbiol. 2008;159(5):367–73.

206. Lim ES, Zhou Y, Zhao G, Bauer IK, Droit L, Ndao IM, et al. Early life dynamics of the human gut virome and bacterial microbiome in infants. Nat Med. 2015;21(10):1228.

207. Kapusinszky B, Minor P, Delwart E. Nearly constant shedding of diverse

enteric viruses by two healthy infants. J Clin Microbiol. 2012;50(11):3427–34.

208. Reyes A, Blanton L V, Cao S, Zhao G, Manary M, Trehan I, et al. Gut DNA viromes of Malawian twins discordant for severe acute malnutrition. Proc Natl Acad Sci. 2015;112(38):11941–6.

209. Norman JM, Handley SA, Baldridge MT, Droit L, Liu CY, Keller BC, et al. Disease-specific alterations in the enteric virome in inflammatory bowel disease. Cell. 2015;160(3):447–60.

210. Minot S, Sinha R, Chen J, Li H, Keilbaugh SA, Wu GD, et al. The human gut virome: inter-individual variation and dynamic response to diet. Genome Res. 2011;21(10):1616–25.

211. Holtz LR, Cao S, Zhao G, Bauer IK, Denno DM, Klein EJ, et al. Geographic variation in the eukaryotic virome of human diarrhea. Virology. 2014;468:556–64.

212. Modi SR, Lee HH, Spina CS, Collins JJ. Antibiotic treatment expands the resistance reservoir and ecological network of the phage metagenome. Nature. 2013;499(7457):219–22.

213. Reyes A, Wu M, McNulty NP, Rohwer FL, Gordon JI. Gnotobiotic mouse model of phage-bacterial host dynamics in the human gut. Proc Natl Acad Sci [Internet]. 2013;110(50):20236–41. Available from: http://www.pnas.org/cgi/doi/10.1073/pnas.1319470110

214. Mills S, Shanahan F, Stanton C, Hill C, Coffey A, Ross RP. Movers and shakers: influence of bacteriophages in shaping the mammalian gut microbiota. Gut Microbes. 2013;4(1):4–16.

215. Nascimento MM. Chapter 9 - The Oral Microbiome. In: Microbiome and Metabolome in Diagnosis, Therapy, and other Strategic Applications. 2019. p. 91–100.

216. Segata N, Haake SK, Mannon P, Lemon KP, Waldron L, Gevers D, et al. Composition of the adult digestive tract bacterial microbiome based on seven mouth surfaces, tonsils, throat and stool samples. Genome Biol. 2012 Jun;13(6):R42.

217. Belstrøm D, Holmstrup P, Bardow A, Kokaras A, Fiehn N-E, Paster BJ. Temporal Stability of the Salivary Microbiota in Oral Health. PLoS One. 2016;11(1):e0147472.

218. Cameron SJS, Huws SA, Hegarty MJ, Smith DPM, Mur LAJ. The human salivary microbiome exhibits temporal stability in bacterial diversity. FEMS Microbiol Ecol. 2015 Sep;91(9):fiv091.

219. Schafer CA, Schafer JJ, Yakob M, Lima P, Camargo P, Wong DTW. Saliva diagnostics: utilizing oral fluids to determine health status. Monogr Oral Sci. 2014;24:88–98.

220. Yakob M, Fuentes L, Wang MB, Abemayor E, Wong DTW. Salivary biomarkers for detection of oral squamous cell carcinoma - current state and recent advances. Curr oral Heal reports. 2014 Jun;1(2):133–41.

221. Yoshizawa JM, Schafer CA, Schafer JJ, Farrell JJ, Paster BJ, Wong DTW. Salivary biomarkers: toward future clinical and diagnostic utilities. Clin Microbiol Rev. 2013 Oct;26(4):781–91.

222. Giannobile W V, McDevitt JT, Niedbala RS, Malamud D. Translational and clinical applications of salivary diagnostics. Adv Dent Res. 2011 Oct;23(4):375–80.

223. Miller CS, Foley JD, Bailey AL, Campell CL, Humphries RL, Christodoulides N, et al. Current developments in salivary diagnostics. Biomark Med. 2010 Feb;4(1):171–89.

224. Dewhirst FE, Chen T, Izard J, Paster BJ, Tanner ACR, Yu W-H, et al. The human oral microbiome. J Bacteriol. 2010;192(19):5002–17.

225. Ghannoum MA, Jurevic RJ, Mukherjee PK, Cui F, Sikaroodi M, Naqvi A, et al. Characterization of the oral fungal microbiome (mycobiome) in healthy individuals. PLoS Pathog. 2010;6(1):e1000713.

226. Pride DT, Salzman J, Haynes M, Rohwer F, Davis-Long C, White RA, et al. Evidence of a robust resident bacteriophage population revealed through analysis of the human salivary virome. ISME J. 2012;6(5):915–26.

227. Richards VP, Alvarez AJ, Luce AR, Bedenbaugh M, Mitchell ML, Burne RA, et al. Microbiomes of site-specific dental plaques from children with different caries status. Infect Immun. 2017;85(8):e00106-17.

228. Chen T, Yu W-H, Izard J, Baranova O V, Lakshmanan A, Dewhirst FE. The Human Oral Microbiome Database: a web accessible resource for investigating oral microbe taxonomic and genomic information. Vol. 2010, Database. Oxford Academic; 2010.

229. Griffen AL, Beall CJ, Firestone ND, Gross EL, DiFranco JM, Hardman JH, et al. CORE: a phylogenetically-curated 16S rDNA database of the core oral microbiome. PLoS One. 2011;6(4):e19051.

230. Gevers D, Knight R, Petrosino JF, Huang K, McGuire AL, Birren BW, et al. The Human Microbiome Project: a community resource for the healthy human microbiome. 2012;10(8):e1001377.

231. Finlayson TL, Gupta A, Ramos-Gomez FJ. Prenatal maternal factors, intergenerational transmission of disease, and child oral health outcomes. Dent Clin. 2017;61(3):483–518.

232. Lif Holgerson P, Harnevik L, Hernell O, Tanner ACR, Johansson I. Mode of birth delivery affects oral microbiota in infants. J Dent Res. 2011;90(10):1183–8.

233. Aagaard K, Ma J, Antony KM, Ganu R, Petrosino J, Versalovic J. The placenta harbors a unique microbiome. Sci Transl Med.

2014;6(237):237ra65-237ra65.

234. Lif Holgerson P, Öhman C, Rönnlund A, Johansson I. Maturation of oral microbiota in children with or without dental caries. PLoS One. 2015;10(5):e0128534.

235. Burne RA, Zeng L, Ahn SJ, Palmer SR, Liu Y, Lefebure T, et al. Progress dissecting the oral microbiome in caries and health. Adv Dent Res. 2012;24(2):77–80.

236. Marsh PD. Ecological events in oral health and disease: new opportunities for prevention and disease control. J Calif Dent Assoc. 2017;45(10):525–37.

237. Frencken JE, Sharma P, Stenhouse L, Green D, Laverty D, Dietrich T. Global epidemiology of dental caries and severe periodontitis–a comprehensive review. J Clin Periodontol. 2017;44:S94–105.

238. Cahill TJ, Harrison JL, Jewell P, Onakpoya I, Chambers JB, Dayer M, et al. Antibiotic prophylaxis for infective endocarditis: a systematic review and meta-analysis. Heart. 2017;103(12):937–44.

239. Jungbauer G, Stähli A, Zhu X, Auber Alberi L, Sculean A, Eick S. Periodontal microorganisms and Alzheimer disease - A causative relationship? Periodontol 2000. 2022 Jun;89(1):59–82.

240. Schmidt TSB, Hayward MR, Coelho LP, Li SS, Costea PI, Voigt AY, et al. Extensive transmission of microbes along the gastrointestinal tract. Elife. 2019;8:e42693.

241. Atarashi K, Suda W, Luo C, Kawaguchi T, Motoo I, Narushima S, et al. Ectopic colonization of oral bacteria in the intestine drives TH1 cell induction and inflammation. Science (80-). 2017;358(6361):359–65.

242. Arimatsu K, Yamada H, Miyazawa H, Minagawa T, Nakajima M, Ryder MI,

et al. Oral pathobiont induces systemic inflammation and metabolic changes associated with alteration of gut microbiota. Sci Rep. 2014;4(1):1–9.

243. Kato T, Yamazaki K, Nakajima M, Date Y, Kikuchi J, Hase K, et al. Oral administration of Porphyromonas gingivalis alters the gut microbiome and serum metabolome. Msphere. 2018;3(5):e00460-18.

244. Gevers D, Kugathasan S, Denson LA, Vázquez-Baeza Y, Van Treuren W, Ren B, et al. The treatment-naive microbiome in new-onset Crohn's disease. Cell Host Microbe. 2014;15(3):382–92.

245. Zhang X, Zhang D, Jia H, Feng Q, Wang D, Liang D, et al. The oral and gut microbiomes are perturbed in rheumatoid arthritis and partly normalized after treatment. Nat Med. 2015;21(8):895–905.

246. Qin N, Yang F, Li A, Prifti E, Chen Y, Shao L, et al. Alterations of the human gut microbiome in liver cirrhosis. Nature. 2014;513(7516):59–64.

247. Lozupone CA, Li M, Campbell TB, Flores SC, Linderman D, Gebert MJ, et al. Alterations in the gut microbiota associated with HIV-1 infection. Cell Host Microbe. 2013;14(3):329–39.

248. Vujkovic-Cvijin I, Dunham RM, Iwai S, Maher MC, Albright RG, Broadhurst MJ, et al. Dysbiosis of the gut microbiota is associated with HIV disease progression and tryptophan catabolism. Sci Transl Med. 2013;5(193):193ra91.

249. Desai SN, Landay AL. HIV and aging: Role of the microbiome. Curr Opin HIV AIDS. 2018;13(1):22–7.

250. Desai SN, Landay AL. Early immune senescence in HIV disease. Curr HIV/AIDS Rep. 2010;7(1):4–10.

251. Triant VA, Lee H, Hadigan C, Grinspoon SK. Increased acute myocardial

infarction rates and cardiovascular risk factors among patients with human immunodeficiency virus disease. J Clin Endocrinol Metab. 2007;92(7):2506–12.

252. Smith RL, de Boer R, Brul S, Budovskaya Y V, van der Spek H. Premature and accelerated aging: HIV or HAART? Front Genet. 2013;3:328.

253. Negredo E, Back D, Blanco JR, Blanco J, Erlandson KM, Garolera M, et al. Aging in HIV-Infected Subjects: A New Scenario and a New View. Biomed Res Int. 2017;2017:58972.

254. Desquilbet L, Jacobson LP, Fried LP, Phair JP, Jamieson BD, Holloway M, et al. HIV-1 infection is associated with an earlier occurrence of a phenotype related to frailty. Journals Gerontol - Ser A Biol Sci Med Sci. 2007;62(11):1279–86.

255. Deeks SG, Verdin E, McCune JM. Immunosenescence and HIV. Curr Opin Immunol. 2012;24(4):501–6.

256. Choi AI, Shlipak MG, Hunt PW, Martin JN, Deeks SG. HIV-infected persons continue to lose kidney function despite successful antiretroviral therapy. AIDS. 2009;23(16):2143–9.

257. Alejos B, Hernando V, López-Aldeguer J, Segura F, Antonio Oteo J, Rubio R, et al. Overall and cause-specific mortality in HIV-positive subjects compared to the general population. J Int AIDS Soc. 2014;17(4 Suppl 3):19711.

258. Klatt NR, Silvestri G. CD4+ T cells and HIV: a paradoxical Pas de Deux. Sci Transl Med. 2012;4(123):123ps4-123ps4.

259. Ribeiro RM, Mohri H, Ho DD, Perelson AS. In vivo dynamics of T cell activation, proliferation, and death in HIV-1 infection: why are CD4+ but not CD8+ T cells depleted? Proc Natl Acad Sci. 2002;99(24):15572–7.

260. Paiardini M, Cervasi B, Dunham R, Sumpter B, Radziewicz H, Silvestri G. Cell-cycle dysregulation in the immunopathogenesis of AIDS. Immunol Res. 2004;29(1–3):253–67.

261. Moir S, Fauci AS. B cells in HIV infection and disease. Nat Rev Immunol. 2009;9(4):235–45.

262. Klatt NR, Estes JD, Sun X, Ortiz AM, Barber JS, Harris LD, et al. Loss of mucosal CD103+ DCs and IL-17+ and IL-22+ lymphocytes is associated with mucosal damage in SIV infection. Mucosal Immunol. 2012;5(6):646–57.

263. Kwa S, Kannanganat S, Nigam P, Siddiqui M, Shetty RD, Armstrong W, et al. Plasmacytoid dendritic cells are recruited to the colorectum and contribute to immune activation during pathogenic SIV infection in rhesus macaques. Blood, J Am Soc Hematol. 2011;118(10):2763–73.

264. Reeves RK, Evans TI, Gillis J, Wong FE, Kang G, Li Q, et al. SIV infection induces accumulation of plasmacytoid dendritic cells in the gut mucosa. J Infect Dis. 2012;206(9):1462–8.

265. Estes JD, Harris LD, Klatt NR, Tabb B, Pittaluga S, Paiardini M, et al. Damaged intestinal epithelial integrity linked to microbial translocation in pathogenic simian immunodeficiency virus infections. PLoS Pathog. 2010;6(8):e1001052.

266. Wallet MA, Rodriguez CA, Yin L, Saporta S, Chinratanapisit S, Hou W, et al. Microbial translocation induces persistent macrophage activation unrelated to HIV-1 levels or T cell activation following therapy. AIDS. 2010;24(9):1281.

267. Nazli A, Chan O, Dobson-Belaire WN, Ouellet M, Tremblay MJ, Gray-Owen SD, et al. Exposure to HIV-1 directly impairs mucosal epithelial barrier integrity allowing microbial translocation. PLoS Pathog. 2010;6(4):e1000852.

268. Mohan M, Kaushal D, Aye PP, Alvarez X, Veazey RS, Lackner AA. Focused examination of the intestinal lamina propria yields greater molecular insight into mechanisms underlying SIV induced immune dysfunction. PLoS One. 2012;7(4):e34561.

269. Sharpstone D, Neild P, Crane R, Taylor C, Hodgson C, Sherwood R, et al. Small intestinal transit, absorption, and permeability in patients with AIDS with and without diarrhoea. Gut. 1999;45(1):70–6.

270. Villanueva-Millán MJ, Pérez-Matute P, Recio-Fernández E, Rosales JML, Oteo JA. Differential effects of antiretrovirals on microbial translocation and gut microbiota composition of HIV-infected patients. J Int AIDS Soc. 2017;20(1):21526.

271. Lichtfuss GF, Hoy J, Rajasuriar R, Kramski M, Crowe SM, Lewin SR. Biomarkers of immune dysfunction following combination antiretroviral therapy for HIV infection. Biomark Med. 2011;5(2):171–86.

272. Brenchley JM, Price DA, Schacker TW, Asher TE, Silvestri G, Rao S, et al. Microbial translocation is a cause of systemic immune activation in chronic HIV infection. Nat Med. 2006;12(12):1365–71.

273. Ancuta P, Kamat A, Kunstman KJ, Kim E-Y, Autissier P, Wurcel A, et al. Microbial translocation is associated with increased monocyte activation and dementia in AIDS patients. PLoS One. 2008;3(6):e2516.

274. Balagopal A, Philp FH, Astemborski J, Block TM, Mehta A, Long R, et al. Human immunodeficiency virus-related microbial translocation and progression of hepatitis C. Gastroenterology. 2008;135(1):226–33.

275. Marchetti G, Bellistrì GM, Borghi E, Tincati C, Ferramosca S, La Francesca M, et al. Microbial translocation is associated with sustained failure in CD4+ T-cell reconstitution in HIV-infected patients on long-term highly active antiretroviral therapy. Aids. 2008;22(15):2035–8.

276. Jiang W, Lederman MM, Hunt P, Sieg SF, Haley K, Rodriguez B, et al. Plasma Levels of Bacterial DNA Correlate with Immune Activation and the Magnitude of Immune Restoration in Persons with Antiretroviral-Treated HIV Infection. J Infect Dis. 2009;199(8):1177–85.

277. Cassol E, Malfeld S, Mahasha P, van der Merwe S, Cassol S, Seebregts C, et al. Persistent Microbial Translocation and Immune Activation in HIV-1–Infected South Africans Receiving Combination Antiretroviral Therapy. J Infect Dis. 2010;202(5):723–33.

278. Ciccone EJ, Read SW, Mannon PJ, Yao MD, Hodge JN, Dewar R, et al. Cycling of gut mucosal CD4+ T cells decreases after prolonged anti-retroviral therapy and is associated with plasma LPS levels. Mucosal Immunol. 2010;3(2):172–81.

279. Favre D, Mold J, Hunt PW, Kanwar B, Loke P, Seu L, et al. Tryptophan catabolism by indoleamine 2, 3-dioxygenase 1 alters the balance of TH17 to regulatory T cells in HIV disease. Sci Transl Med. 2010;2(32):32ra36.

280. Funderburg NT, Mayne E, Sieg SF, Asaad R, Jiang W, Kalinowska M, et al. Increased tissue factor expression on circulating monocytes in chronic HIV infection: relationship to in vivo coagulation and immune activation. Blood. 2010;115(2):161–7.

281. Gordon SN, Cervasi B, Odorizzi P, Silverman R, Aberra F, Ginsberg G, et al. Disruption of Intestinal CD4+ T Cell Homeostasis Is a Key Marker of Systemic CD4+ T Cell Activation in HIV-Infected Individuals. J Immunol. 2010;185(9):5169–79.

282. Leinert C, Stahl-Hennig C, Ecker A, Schneider T, Fuchs D, Sauermann U, et al. Microbial translocation in simian immunodeficiency virus (SIV)-infected rhesus monkeys (Macaca mulatta). J Med Primatol. 2010;39(4):243–51.

283. Nowroozalizadeh S, Månsson F, Da Silva Z, Repits J, Dabo B, Pereira C, et al. Microbial translocation correlates with the severity of both HIV-1 and HIV-2 infections. J Infect Dis. 2010;201(8):1150–4.

284. Chege D, Sheth PM, Kain T, Kim CJ, Kovacs C, Loutfy M, et al. Sigmoid Th17 populations, the HIV latent reservoir, and microbial translocation in men on long-term antiretroviral therapy. AIDS. 2011;25(6):741–9.

285. d'Ettorre G, Paiardini M, Zaffiri L, Andreotti M, Ceccarelli G, Rizza C, et al. HIV persistence in the gut mucosa of HIV-infected subjects undergoing antiretroviral therapy correlates with immune activation and increased levels of LPS. Curr HIV Res. 2011;9(3):148–53.

286. Marchetti G, Cozzi-Lepri A, Merlini E, Bellistrì GM, Castagna A, Galli M, et al. Microbial translocation predicts disease progression of HIV-infected antiretroviral-naive patients with high CD4+ cell count. Aids. 2011;25(11):1385–94.

287. Merlini E, Bai F, Bellistrì GM, Tincati C, d'Arminio Monforte A, Marchetti G. Evidence for polymicrobic flora translocating in peripheral blood of HIV-infected patients with poor immune response to antiretroviral therapy. PLoS One. 2011;6(4):e18580.

288. Sandler NG, Wand H, Roque A, Law M, Nason MC, Nixon DE, et al. Plasma levels of soluble CD14 independently predict mortality in HIV infection. J Infect Dis. 2011;203(6):780–90.

289. Pandrea I, Cornell E, Wilson C, Ribeiro RM, Ma D, Kristoff J, et al. Coagulation biomarkers predict disease progression in SIV-infected nonhuman primates. Blood, J Am Soc Hematol. 2012;120(7):1357–66.

290. Pilakka-Kanthikeel S, Huang S, Fenton T, Borkowsky W, Cunningham CK, Pahwa S. Increased gut microbial translocation in HIV-infected children persists in virologic responders and virologic failures after antiretroviral therapy. Pediatr Infect Dis J. 2012;31(6):583–91.

291. Harris LD, Klatt NR, Vinton C, Briant JA, Tabb B, Ladell K, et al. Mechanisms underlying γδ T-cell subset perturbations in SIV-infected Asian rhesus macaques. Blood, J Am Soc Hematol. 2010;116(20):4148–57.

292. Chaoul N, Burelout C, Peruchon S, van Buu BN, Laurent P, Proust A, et al. Default in plasma and intestinal IgA responses during acute infection by simian immunodeficiency virus. Retrovirology. 2012;9(1):43.

293. Shetty RD, Velu V, Titanji K, Bosinger SE, Freeman GJ, Silvestri G, et al. PD-1 blockade during chronic SIV infection reduces hyperimmune activation and microbial translocation in rhesus macaques. J Clin Invest. 2012;122(5):1712–6.

294. Klatt NR, Brenchley JM. Th17 cell dynamics in HIV infection. Curr Opin HIV AIDS. 2010;5(2):135.

295. Zevin AS, McKinnon L, Burgener A, Klatt NR. Microbial translocation and microbiome dysbiosis in HIV-associated immune activation. Curr Opin HIV AIDS. 2016;11(2):182–90.

296. Paiardini M, Pandrea I, Apetrei C, Silvestri G. Lessons learned from the natural hosts of HIV-related viruses. Annu Rev Med. 2009;60:485–95.

297. Pandrea I, Gaufin T, Brenchley JM, Gautam R, Monjure C, Gautam A, et al. Cutting edge: experimentally induced immune activation in natural hosts of simian immunodeficiency virus induces significant increases in viral replication and CD4+ T cell depletion. J Immunol. 2008;181(10):6687–91.

298. Pérez-Matute P, Íñiguez M, Villanueva-Millán MJ, Oteo JA. Chapter 32 - The Oral, Genital and Gut Microbiome in HIV Infection. In: Microbiome and Metabolome in Diagnosis, Therapy, and other Strategic Applications. Academic Press; 2019. p. 307–23.

299. Meier A, Altfeld M. Toll-like receptor signaling in HIV-1 infection: A potential

target for therapy? Expert Review of Anti-Infective Therapy. 2007;5(3):323–6.

300. Gribar SC, Anand RJ, Sodhi CP, Hackam DJ. The role of epithelial Toll-like receptor signaling in the pathogenesis of intestinal inflammation. J Leukoc Biol. 2008;83(3):493–8.

301. Kitchens RL, Thompson PA. Modulatory effects of sCD14 and LBP on LPS-host cell interactions. J Endotoxin Res. 2005;11(4):225–9.

302. Thomsen HH, Møller HJ, Trolle C, Groth KA, Skakkebæk A, Bojesen A, et al. The macrophage low-grade inflammation marker sCD163 is modulated by exogenous sex steroids. Endocr Connect. 2013;2(4):216–24.

303. Hanna DB, Lin J, Post WS, Hodis HN, Xue X, Anastos K, et al. Association of macrophage inflammation biomarkers with progression of subclinical carotid artery atherosclerosis in HIV-infected women and men. J Infect Dis. 2017;215(9):1352–61.

304. Connolly NC, Riddler SA, Rinaldo CR. Proinflammatory cytokines in HIV disease-a review and rationale for new therapeutic approaches. AIDS Rev. 2005;7(3):168–80.

305. Giorgi J V., Hultin LE, McKeating JA, Johnson TD, Owens B, Jacobson LP, et al. Shorter Survival in Advanced Human Immunodeficiency Virus Type 1 Infection Is More Closely Associated with T Lymphocyte Activation than with Plasma Virus Burden or Virus Chemokine Coreceptor Usage. J Infect Dis. 1999;179(4):859–70.

306. Salazar-Gonzalez JF, Martinez-Maza O, Nishanian P, Aziz N, Shen L-P, Grosser S, et al. Increased immune activation precedes the inflection point of CD4 T cells and the increased serum virus load in human immunodeficiency virus infection. J Infect Dis. 1998;178(2):423–30.

307. Hunt PW, Brenchley J, Sinclair E, McCune JM, Roland M, Page-Shafer K,

et al. Relationship between T Cell Activation and CD4 + T Cell Count in HIV-Seropositive Individuals with Undetectable Plasma HIV RNA Levels in the Absence of Therapy. J Infect Dis. 2008;197(1):126–33.

308. Kuller LH, Tracy R, Belloso W, De Wit S, Drummond F, Lane HC, et al. Inflammatory and coagulation biomarkers and mortality in patients with HIV infection. PLoS Med. 2008;5(10):1496–508.

309. Rodger AJ, Fox Z, Lundgren JD, Kuller LH, Boesecke C, Gey D, et al. Activation and coagulation biomarkers are independent predictors of the development of opportunistic disease in patients with HIV infection. J Infect Dis. 2009;200(6):973–83.

310. Sodora DL, Silvestri G. Immune activation and AIDS pathogenesis. Aids. 2008;22(4):439–46.

311. Stubbs JR, House JA, Ocque AJ, Zhang S, Johnson C, Kimber C, et al. Serum Trimethylamine-N-Oxide is Elevated in CKD and Correlates with Coronary Atherosclerosis Burden. J Am Soc Nephrol. 2016;27(1):305–13.

312. Tang WHW, Wang Z, Levison BS, Koeth RA, Britt EB, Fu X, et al. Intestinal Microbial Metabolism of Phosphatidylcholine and Cardiovascular Risk. N Engl J Med. 2013;368(17):1575–84.

313. Trøseid M, Ueland T, Hov JR, Svardal A, Gregersen I, Dahl CP, et al. Microbiota-dependent metabolite trimethylamine-N-oxide is associated with disease severity and survival of patients with chronic heart failure. J Intern Med. 2015;277(6):717–26.

314. Wang Z, Klipfell E, Bennett BJ, Koeth R, Levison BS, Dugar B, et al. Gut flora metabolism of phosphatidylcholine promotes cardiovascular disease. Nature. 2011;472(7341):57–65.

315. Koeth RA, Wang Z, Levison BS, Buffa JA, Org E, Sheehy BT, et al. Intestinal microbiota metabolism of l-carnitine, a nutrient in red meat,

promotes atherosclerosis. Nat Med. 2013;19(5):576–85.

316. Tang WHW, Wang Z, Shrestha K, Borowski AG, Wu Y, Troughton RW, et al. Intestinal microbiota-dependent phosphatidylcholine metabolites, diastolic dysfunction, and adverse clinical outcomes in chronic systolic heart failure. J Card Fail. 2015;21(2):91–6.

317. Wang Z, Tang WHW, Buffa JA, Fu X, Britt EB, Koeth RA, et al. Prognostic value of choline and betaine depends on intestinal microbiota-generated metabolite trimethylamine-N-oxide. Eur Heart J. 2014;35(14):904–10.

318. Suzuki T, Heaney LM, Bhandari SS, Jones DJL, Ng LL. Trimethylamine N-oxide and prognosis in acute heart failure. Heart. 2016;102(11):841–8.

319. Fu Q, Zhao M, Wang D, Hu H, Guo C, Chen W, et al. Coronary Plaque Characterization Assessed by Optical Coherence Tomography and Plasma Trimethylamine-N-oxide Levels in Patients With Coronary Artery Disease. Am J Cardiol. 2016;118(9):1311–5.

320. Suzuki T, Heaney LM, Jones DJL, Ng LL. Trimethylamine N-oxide and risk stratification after acute myocardial infarction. Clin Chem. 2017;63(1):420–8.

321. Haissman JM, Knudsen A, Hoel H, Kjær A, Kristoffersen US, Berge RK, et al. Microbiota-Dependent Marker TMAO Is Elevated in Silent Ischemia but Is Not Associated with First-Time Myocardial Infarction in HIV Infection. J Acquir Immune Defic Syndr. 2016;71(2):130–6.

322. Srinivasa S, Fitch K V., Lo J, Kadar H, Knight R, Wong K, et al. Plaque burden in HIV-infected patients is associated with serum intestinal microbiota-generated trimethylamine. AIDS. 2015;29(4):443–52.

323. Elliott Miller P, Haberlen SA, Brown TT, Margolick JB, DiDonato JA, Hazen SL, et al. Intestinal microbiota-produced trimethylamine-N-oxide and its association with coronary stenosis and HIV serostatus. J Acquir Immune

Defic Syndr. 2016;72(1):114–8.

324. Shan Z, Clish CB, Hua S, Scott JM, Hanna DB, Burk RD, et al. Gut microbial-related choline metabolite trimethylamine-N-oxide is associated with progression of carotid artery atherosclerosis in HIV infection. J Infect Dis. 2018;218(9):1474–9.

325. Montrucchio C, De Nicolò A, D'Ettorre G, D'Ascenzo F, Lazzaro A, Tettoni M, et al. Serum Trimethylamine-N-oxide Concentrations in People Living with HIV and the Effect of Probiotics Supplementation. Int J Antimicrob Agents. 2020;55(4):105908.

326. Haissman JM, Haugaard AK, Ostrowski SR, Berge RK, Hov JR, Trøseid M, et al. Microbiota-dependent metabolite and cardiovascular disease marker trimethylamine-N-oxide (TMAO) is associated with monocyte activation but not platelet function in untreated HIV infection. BMC Infect Dis. 2017;17(1):445.

327. Missailidis C, Neogi U, Stenvinkel P, Trøseid M, Nowak P, Bergman P. The microbial metabolite trimethylamine-N-oxide in association with inflammation and microbial dysregulation in three HIV cohorts at various disease stages. AIDS. 2018;32(12):1589–98.

328. McHardy IH, Li X, Tong M, Ruegger P, Jacobs J, Borneman J, et al. HIV Infection is associated with compositional and functional shifts in the rectal mucosal microbiota. Microbiome. 2013;1(1):26.

329. Mutlu EA, Keshavarzian A, Losurdo J, Swanson G, Siewe B, Forsyth C, et al. A compositional look at the human gastrointestinal microbiome and immune activation parameters in HIV infected subjects. PLoS Pathog. 2014;10(2):e1003829.

330. Nowak P, Troseid M, Avershina E, Barqasho B, Neogi U, Holm K, et al. Gut microbiota diversity predicts immune status in HIV-1 infection. Aids. 2015;29(18):2409–18.

331. Dillon SM, Lee EJ, Kotter C V, Austin GL, Dong Z, Hecht DK, et al. An altered intestinal mucosal microbiome in HIV-1 infection is associated with mucosal and systemic immune activation and endotoxemia. Mucosal Immunol. 2014;7(4):983–94.

332. Dinh DM, Volpe GE, Duffalo C, Bhalchandra S, Tai AK, Kane A V., et al. Intestinal Microbiota, microbial translocation, and systemic inflammation in chronic HIV infection. J Infect Dis. 2015;211(1):19–27.

333. Ling Z, Jin C, Xie T, Cheng Y, Li L, Wu N. Alterations in the fecal microbiota of patients with HIV-1 infection: an observational study in a Chinese population. Sci Rep. 2016;6:30673.

334. Dubourg G, Surenaud M, Lévy Y, Hüe S, Raoult D. Microbiome of HIV-infected people. Microb Pathog. 2017;106:85–93.

335. Paquin-Proulx D, Ching C, Vujkovic-Cvijin I, Fadrosh D, Loh L, Huang Y, et al. Bacteroides are associated with GALT iNKT cell function and reduction of microbial translocation in HIV-1 infection. Mucosal Immunol. 2017;10(1):69.

336. Gori A, Tincati C, Rizzardini G, Torti C, Quirino T, Haarman M, et al. Early impairment of gut function and gut flora supporting a role for alteration of gastrointestinal mucosa in human immunodeficiency virus pathogenesis. J Clin Microbiol. 2008;46(2):757–8.

337. Noguera-Julian M, Rocafort M, Guillén Y, Rivera J, Casadellà M, Nowak P, et al. Gut Microbiota Linked to Sexual Preference and HIV Infection. EBioMedicine. 2016;5:135–46.

338. Volpe GE, Ward H, Mwamburi M, Dinh D, Bhalchandra S, Wanke C, et al. Associations of cocaine use and HIV infection with the intestinal microbiota, microbial translocation, and inflammation. J Stud Alcohol Drugs. 2014;75(2):347–57.

339. Yu G, Fadrosh D, Ma B, Ravel J, Goedert JJ. Anal microbiota profiles in HIV-positive and HIV-negative MSM. Aids. 2014;28(5):753–60.

340. Li S-K, Leung RKK, Guo H-X, Wei J-F, Wang J-H, Kwong K-T, et al. Detection and identification of plasma bacterial and viral elements in HIV/AIDS patients in comparison to healthy adults. Clin Microbiol Infect. 2012;18(11):1126–33.

341. Belshaw R, Katzourakis A, Paces J, Burt A, Tristem M. High copy number in human endogenous retrovirus families is associated with copying mechanisms in addition to reinfection. Mol Biol Evol. 2005;22(4):814–7.

342. Ormsby CE, SenGupta D, Tandon R, Deeks SG, Martin JN, Jones RB, et al. Human endogenous retrovirus expression is inversely associated with chronic immune activation in HIV-1 infection. PLoS One. 2012;7(8):e41021.

343. van der Kuyl AC. HIV infection and HERV expression: a review. Retrovirology. 2012;9(1):1–10.

344. Contreras-Galindo R, González M, Almodovar-Camacho S, González-Ramírez S, Lorenzo E, Yamamura Y. A new Real-Time-RT-PCR for quantitation of human endogenous retroviruses type K (HERV-K) RNA load in plasma samples: increased HERV-K RNA titers in HIV-1 patients with HAART non-suppressive regimens. J Virol Methods. 2006;136(1–2):51–7.

345. Contreras-Galindo R, Kaplan MH, He S, Contreras-Galindo AC, Gonzalez-Hernandez MJ, Kappes F, et al. HIV infection reveals widespread expansion of novel centromeric human endogenous retroviruses. Genome Res. 2013;23(9):1505–13.

346. Contreras-Galindo R, Kaplan MH, Markovitz DM, Lorenzo E, Yamamura Y. Detection of HERV-K (HML-2) viral RNA in plasma of HIV type 1-infected individuals. AIDS Res Hum Retroviruses. 2006;22(10):979–84.

347. Zhang X, Boyce M, Bhattacharya B, Zhang X, Schein S, Roy P, et al. Bluetongue virus coat protein VP2 contains sialic acid-binding domains, and VP5 resembles enveloped virus fusion proteins. Proc Natl Acad Sci. 2010;107(14):6292–7.

348. Maclachlan NJ, Guthrie AJ. Re-emergence of bluetongue, African horse sickness, and other orbivirus diseases. Vet Res. 2010;41(6):35.

349. Li L, Deng X, Linsuwanon P, Bangsberg D, Bwana MB, Hunt P, et al. AIDS alters the commensal plasma virome. J Virol. 2013;87(19):10912–5.

350. Schwarze-Zander C, Blackard JT, Rockstroh JK. Role of GB virus C in modulating HIV disease. Expert Rev Anti Infect Ther. 2012;10(5):563–72.

351. Zhang W, Chaloner K, Tillmann HL, Williams CF, Stapleton JT. Effect of early and late GB virus C viraemia on survival of HIV-infected individuals: a meta-analysis. HIV Med. 2006;7(3):173–80.

352. Zur Hausen H, De Villiers E-M. TT viruses: oncogenic or tumor-suppressive properties? TT Viruses. 2009;331:109–16.

353. Li L, Deng X, Da Costa AC, Bruhn R, Deeks SG, Delwart E. Virome analysis of antiretroviral-treated HIV patients shows no correlation between T-cell activation and anelloviruses levels. J Clin Virol. 2015;72:106–13.

354. Liu K, Li Y, Xu R, Zhang Y, Zheng C, Wan Z, et al. HIV-1 Infection Alters the Viral Composition of Plasma in Men Who Have Sex with Men. Msphere. 2021;6(3):e00081-21.

355. Li Y, Altan E, Pilcher C, Hartogensis W, Hecht FM, Deng X, et al. Semen virome of men with HIV on or off antiretroviral treatment. AIDS. 2020 May;34(6):827–32.

356. Siqueira JD, Curty G, Xutao D, Hofer CB, Machado ES, Seuánez HN, et al. Composite Analysis of the Virome and Bacteriome of HIV/HPV Co-

Infected Women Reveals Proxies for Immunodeficiency. Viruses. 2019;11(5):422.

357. Guo Y, Huang X, Sun X, Yu Y, Wang Y, Zhang B, et al. The Underrated Salivary Virome of Men Who Have Sex With Men Infected With HIV. Front Immunol. 2021;12:759253.

358. Monaco CL, Gootenberg DB, Zhao G, Handley SA, Ghebremichael MS, Lim ES, et al. Altered Virome and Bacterial Microbiome in Human Immunodeficiency Virus-Associated Acquired Immunodeficiency Syndrome. Cell Host Microbe. 2016;19(3):311–22.

359. Li Y, Saxena D, Chen Z, Liu G, Abrams WR, Phelan JA, et al. HIV infection and microbial diversity in saliva. J Clin Microbiol. 2014;52(5):1400–11.

360. Leigh JE, Shetty K, Fidel Jr PL. Oral opportunistic infections in HIV-positive individuals: review and role of mucosal immunity. AIDS Patient Care STDS. 2004;18(8):443–56.

361. Ghannoum MA, Mukherjee PK, Jurevic RJ, Retuerto M, Brown RE, Sikaroodi M, et al. Metabolomics reveals differential levels of oral metabolites in HIV-infected patients: toward novel diagnostic targets. Omi a J Integr Biol. 2013;17(1):5–15.

362. Shiboski CH, Patton LL, Webster-Cyriaque JY, Greenspan D, Traboulsi RS, Ghannoum M, et al. The Oral HIV/AIDS Research Alliance: updated case definitions of oral disease endpoints. J oral Pathol Med. 2009;38(6):481–8.

363. Hodgson TA, Greenspan D, Greenspan JS. Oral lesions of HIV disease and HAART in industrialized countries. Adv Dent Res. 2006;19(1):57–62.

364. Mitchell D, Israr M, Alam S, Dinello D, Kishel J, Jia R, et al. HIV nucleoside reverse transcriptase inhibitors efavirenz and tenofovir change the growth and differentiation of primary gingival epithelium. HIV Med.

2014;15(4):196–202.

365. Ghosh SK, McCormick TS, Eapen BL, Yohannes E, Chance MR, Weinberg A. Comparison of epigenetic profiles of human oral epithelial cells from HIV-positive (on HAART) and HIV-negative subjects. Epigenetics. 2013;8(7):703–9.

366. Lu D, Zhang J-B, Wang Y-X, Geng S-T, Zhang Z, Xu Y, et al. Association between CD4+ T cell counts and gut microbiota and serum cytokines levels in HIV-infected immunological non-responders. BMC Infect Dis. 2021;21(1):1–11.

367. Presti RM, Handley S, Droit L, Ghannoum M, Jacobson M, Shiboski CH, et al. Alterations in the oral microbiome in HIV-infected participants after ART administration are influenced by immune status. AIDS. 2018;32(10):1279–87.

368. Beck JM, Schloss PD, Venkataraman A, Twigg III H, Jablonski KA, Bushman FD, et al. Multicenter comparison of lung and oral microbiomes of HIV-infected and HIV-uninfected individuals. Am J Respir Crit Care Med. 2015;192(11):1335–44.

369. Imahashi M, Ode H, Kobayashi A, Nemoto M, Matsuda M, Hashiba C, et al. Impact of long-term antiretroviral therapy on gut and oral microbiotas in HIV-1-infected patients. Sci Rep. 2021;11(1):1–10.

370. Afdhal NH. Fibroscan (transient elastography) for the measurement of liver fibrosis. Gastroenterol Hepatol (N Y). 2012;8(9):605.

371. Pérez-Matute P, Íñiguez M, Villanueva-Millán MJ, Recio-Fernández E, Vázquez AM, Sánchez SC, et al. Short-term effects of direct-acting antiviral agents on inflammation and gut microbiota in hepatitis C-infected patients. Eur J Intern Med. 2019 Sep;67:47–58.

372. Caparrós-Martín JA, Lareu RR, Ramsay JP, Peplies J, Reen FJ, Headlam

HA, et al. Statin therapy causes gut dysbiosis in mice through a PXR-dependent mechanism. Microbiome. 2017;5(1):95.

373. Nolan JA, Skuse PH, Govindarajan K, Patterson E, Konstantinidou N, Casey PG, et al. The influence of rosuvastatin upon the gastrointestinal microbiota and host gene expression profiles. Am J Physiol Circ Physiol. 2017;312(5):G488–97.

374. Abeles SR, Ly M, Santiago-Rodriguez TM, Pride DT. Effects of long term antibiotic therapy on human oral and fecal viromes. PLoS One. 2015;10(8):e0134941.

375. Villanueva-Millán MJ. Effects of different antiretroviral treatments on gut microbiota of HIV-infected patients. Universidad de La Rioja; 2018.

376. Sigma-Aldrich. Sandwich ELISA [Internet]. Available from: https://www.sigmaaldrich.com/ES/es/technical-documents/technical-article/protein-biology/elisa/conferma-sandwich-elisas#References

377. Matthews DR, Hosker JP, Rudenski AS, Naylor BA, Treacher DF, Turner RC. Homeostasis model assessment: insulin resistance and β-cell function from fasting plasma glucose and insulin concentrations in man. Diabetologia. 1985;28(7):412–9.

378. R&D. Luminex Assay [Internet]. Available from: https://www.rndsystems.com/resources/technical/luminex-assay-principle

379. Qiime2. Qiime2 [Internet]. Available from: https://qiime2.org/

380. SILVA [Internet]. Available from: https://www.arb-silva.de/

381. Mandal S, Van Treuren W, White RA, Eggesbø M, Knight R, Peddada SD. Analysis of composition of microbiomes: a novel method for studying microbial composition. Microb Ecol Health Dis. 2015;26(1):27663.

382. Conceição-Neto N, Yinda KC, Van Ranst M, Matthijnssens J. NetoVIR:

Modular approach to customize sample preparation procedures for viral metagenomics. In: Methods in Molecular Biology. 2018. p. 85–95.

383. Conceição-Neto N, Zeller M, Lefrère H, De Bruyn P, Beller L, Deboutte W, et al. Modular approach to customise sample preparation procedures for viral metagenomics: a reproducible protocol for virome analysis. Sci Rep. 2015;5:16532.

384. ViPER [Internet]. Available from: https://github.com/Matthijnssenslab/ViPER

385. Bolger AM, Lohse M, Usadel B. Trimmomatic: a flexible trimmer for Illumina sequence data. Bioinformatics. 2014;30(15):2114–20.

386. Langmead B, Trapnell C, Pop M, Salzberg SL. Ultrafast and memory-efficient alignment of short DNA sequences to the human genome. Genome Biol. 2009;10(3):1–10.

387. Bankevich A, Nurk S, Antipov D, Gurevich AA, Dvorkin M, Kulikov AS, et al. SPAdes: a new genome assembly algorithm and its applications to single-cell sequencing. J Comput Biol. 2012;19(5):455–77.

388. Nayfach S, Camargo AP, Schulz F, Eloe-Fadrosh E, Roux S, Kyrpides NC. CheckV assesses the quality and completeness of metagenome-assembled viral genomes. Nat Biotechnol. 2021;39(5):578–85.

389. Houtgast EJ, Sima V-M, Bertels K, Al-Ars Z. Hardware acceleration of BWA-MEM genomic short read mapping for longer read lengths. Comput Biol Chem. 2018;75:54–64.

390. McGinnis S, Madden TL. BLAST: at the core of a powerful and diverse set of sequence analysis tools. Nucleic Acids Res. 2004;32(Web Server issue):W20–5.

391. Buchfink B, Xie C, Huson DH. Fast and sensitive protein alignment using

DIAMOND. Nat Methods. 2015;12(1):59–60.

392. Cambuy DD, Coutinho FH, Dutilh BE. Contig annotation tool CAT robustly classifies assembled metagenomic contigs and long sequences. BioRxiv. 2016;72868.

393. Ondov BD, Bergman NH, Phillippy AM. Interactive metagenomic visualization in a Web browser. BMC Bioinformatics. 2011;12(1):1–10.

394. Guo J, Bolduc B, Zayed AA, Varsani A, Dominguez-Huerta G, Delmont TO, et al. VirSorter2: a multi-classifier, expert-guided approach to detect diverse DNA and RNA viruses. Microbiome. 2021;9(1):1–13.

395. Tisza MJ, Belford AK, Dominguez-Huerta G, Bolduc B, Buck CB. Cenote-Taker 2 democratizes virus discovery and sequence annotation. Virus Evol. 2021;7(1):veaa100.

396. Coutinho FH, Zaragoza-Solas A, López-Pérez M, Barylski J, Zielezinski A, Dutilh BE, et al. RaFAH: Host prediction for viruses of Bacteria and Archaea based on protein content. Patterns. 2021;2(7):100274.

397. Yutin N, Makarova KS, Gussow AB, Krupovic M, Segall A, Edwards RA, et al. Discovery of an expansive bacteriophage family that includes the most abundant viruses from the human gut. Nat Microbiol. 2018;3(1):38–46.

398. McMurdie PJ, Holmes S. Phyloseq: An R Package for Reproducible Interactive Analysis and Graphics of Microbiome Census Data. PLoS One. 2013;8(4).

399. EEUU HIV guidelines [Internet]. Available from: https://clinicalinfo.hiv.gov/en/guidelines

400. EACS guidelines [Internet]. Available from: https://eacs.sanfordguide.com/

401. Richter E, Bornemann L, Korencak M, Alter G, Schuster M, Esser S, et al. Reduction of CD8 T cell functionality but not inhibitory capacity by integrase

inhibitors. J Virol. 2022;96(5):e0173021.

402. Burdo TH, Lo J, Abbara S, Wei J, DeLelys ME, Preffer F, et al. Soluble CD163, a novel marker of activated macrophages, is elevated and associated with noncalcified coronary plaque in HIV-infected patients. J Infect Dis. 2011;204(8):1227–36.

403. Quiros-Roldan E, Castelli F, Bonito A, Vezzoli M, Calza S, Biasiotto G, et al. The impact of integrase inhibitor-based regimens on markers of inflammation among HIV naïve patients. Cytokine. 2020;126:154884.

404. O'Halloran JA, Sahrmann J, Butler AM, Olsen MA, Powderly WG. Brief Report: Integrase Strand Transfer Inhibitors Are Associated With Lower Risk of Incident Cardiovascular Disease in People Living With HIV. J Acquir Immune Defic Syndr. 2020 Aug;84(4):396–9.

405. Ricciuto A, Griffiths AM. Clinical value of fecal calprotectin. Crit Rev Clin Lab Sci. 2019 Aug;56(5):307–20.

406. Eckard AR, Hughes HY, Hagood NL, O'Riordan MA, Labbato D, Kosco JC, et al. Fecal Calprotectin Is Elevated in HIV and Related to Systemic Inflammation. J Acquir Immune Defic Syndr. 2021 Feb;86(2):231–9.

407. Ancona G, Merlini E, Tincati C, Barassi A, Calcagno A, Augello M, et al. Long-Term Suppressive cART Is Not Sufficient to Restore Intestinal Permeability and Gut Microbiota Compositional Changes. Front Immunol. 2021;12:459.

408. Tuddenham SA, Koay WLA, Zhao N, White JR, Ghanem KG, Sears CL. The impact of human immunodeficiency virus infection on gut microbiota α-diversity: an individual-level meta-analysis. Clin Infect Dis. 2020;70(4):615–27.

409. Clay PG, Crutchley RD. Noninfectious diarrhea in HIV seropositive individuals: a review of prevalence rates, etiology, and management in the

era of combination antiretroviral therapy. Infect Dis Ther. 2014;3(2):103–22.

410. Archin NM, Margolis DM. Emerging strategies to deplete the HIV reservoir. Curr Opin Infect Dis. 2014;27(1):29.

411. Hill A, Balkin A. Risk factors for gastrointestinal adverse events in HIV treated and untreated patients. AIDS Rev. 2009;11(1):30–8.

412. Johnson MO, Neilands TB. Coping with HIV treatment side effects: conceptualization, measurement, and linkages. AIDS Behav. 2007;11(4):575–85.

413. Larsen JM. The immune response to Prevotella bacteria in chronic inflammatory disease. Immunology. 2017;151(4):363–74.

414. Ouyang J, Lin J, Isnard S, Fombuena B, Peng X, Marette A, et al. The Bacterium Akkermansia muciniphila: A Sentinel for Gut Permeability and Its Relevance to HIV-Related Inflammation. Front Immunol. 2020;11:645.

415. Mahmoud YI, Abd El-Ghffar EA. Spirulina ameliorates aspirin-induced gastric ulcer in albino mice by alleviating oxidative stress and inflammation. Biomed Pharmacother. 2019;109:314–21.

416. Schaeffer DJ, Krylov VS. Anti-HIV activity of extracts and compounds from algae and cyanobacteria. Ecotoxicol Environ Saf. 2000 Mar;45(3):208–27.

417. Wexler HM. Bacteroides: the good, the bad, and the nitty-gritty. Clin Microbiol Rev. 2007;20(4):593–621.

418. Qin P, Zou Y, Dai Y, Luo G, Zhang X, Xiao L. Characterization a Novel Butyric Acid-Producing Bacterium Collinsella aerofaciens Subsp. Shenzhenensis Subsp. Nov. Microorganisms. 2019 Mar;7(3):78.

419. O'Callaghan A, van Sinderen D. Bifidobacteria and Their Role as Members of the Human Gut Microbiota. Front Microbiol. 2016 Jun 15;7:925.

420. Sivaprakasam S, Prasad PD, Singh N. Benefits of short-chain fatty acids and their receptors in inflammation and carcinogenesis. Pharmacol Ther. 2016/04/23. 2016 Aug;164:144–51.

421. Maslowski KM, Vieira AT, Ng A, Kranich J, Sierro F, Yu D, et al. Regulation of inflammatory responses by gut microbiota and chemoattractant receptor GPR43. Nature. 2009;461(7268):1282–6.

422. Clarke JM, Young GP, Topping DL, Bird AR, Cobiac L, Scherer BL, et al. Butyrate delivered by butyrylated starch increases distal colonic epithelial apoptosis in carcinogen-treated rats. Carcinogenesis. 2012;33(1):197–202.

423. Saresella M, Marventano I, Barone M, La Rosa F, Piancone F, Mendozzi L, et al. Alterations in Circulating Fatty Acid Are Associated With Gut Microbiota Dysbiosis and Inflammation in Multiple Sclerosis. Front Immunol. 2020 Jul 7;11:1390.

424. Van Immerseel F, De Buck J, Boyen F, Bohez L, Pasmans F, Volf J, et al. Medium-chain fatty acids decrease colonization and invasion through hilA suppression shortly after infection of chickens with Salmonella enterica serovar Enteritidis. Appl Environ Microbiol. 2004 Jun;70(6):3582–7.

425. Gregory AC, Zablocki O, Howell A, Bolduc B, Sullivan MB. The human gut virome database. BioRxiv. 2019;655910.

426. Zuo T, Ng SC. The Gut Microbiota in the Pathogenesis and Therapeutics of Inflammatory Bowel Disease. Front Microbiol. 2018 Sep 25;9:2247.

427. Villoslada-Blanco P, Pérez-Matute P, Íñiguez M, Recio-Fernández E, Blanco-Navarrete P, Metola L, et al. Integrase Inhibitors Partially Restore Bacterial Translocation, Inflammation and Gut Permeability Induced by HIV Infection: Impact on Gut Microbiota. Infect Dis Ther. 2022 May;11(4):1541–57.

428. Li S, Zhu J, Su B, Wei H, Chen F, Liu H, et al. Alteration in Oral Microbiome Among Men Who Have Sex With Men With Acute and Chronic HIV Infection on Antiretroviral Therapy. Front Cell Infect Microbiol. 2021;11:695515.